Supporting Information

Trioxatrianguleniums ($TOTA^+$) as a Robust Carbon-based Lewis Acid in Frustrated Lewis Pair Chemistry

Aslam C. Shaikh,[a] José M. Veleta,[a] Jules Moutet,[a] and Thomas L. Gianetti*[a]

[a]Department of Chemistry and Biochemistry, University of Arizona, Tucson, AZ, United States.* E-mail:tgianetti@email.arizona.edu.

Table of Contents

I. General Information S2

II. Experimental Section S4

II.1 Synthesis of 1-X S4

II.2 Syntheses of Lewis adduct and frustrated Lewis pair S8

II.3 Frustrated Lewis pair mediated disulfide bond cleavage S35

II.4 Frustrated Lewis pair mediated dehydrogenation of cyclohexadiene S60

II.5 Frustrated Lewis pair mediated cleavage of C-Br bond in alkyl halide S64

II.6 Frustrated Lewis pair mediated fixation of formaldehyde S66

II.7 Frustrated Lewis pair mediated fixation of Staudinger reaction intermediate S69

II.8 The reaction of I*t*Bu with 1-[X] S72

III. Single crystal X-ray Diffraction S88

IV. Computational Details S100

V. References S107

I. General Information

Unless otherwise stated, the syntheses were carried out in oven-dried vials or reaction vessels loaded with magnetic stirring bars inside an N_2 filled glove box. Dried solvents and liquid reagents were transferred by oven-dried or hypodermic syringes. Experiments were monitored by analytical thin-layer chromatography (TLC) on pre-coated silica gel plates. After elution, plates were revealed under UV light (254 nm wavelength). Melting points are reported uncorrected and were recorded using a digital Buchi Melting Point Apparatus B-540. All the chemicals and solvents were purchased from Sigma Aldrich, Fisher Scientific, or VWR and used without further purification. Organic solvents used were dried by using a solvent purification system. Compound S1 was prepared according to the Laursen report.[1]

NMR spectroscopy. NMR spectra and were recorded on Bruker AVII 400, DRX-500, and NEO-500 spectrometers in deuterated solvents using TMS as internal standard, or the solvent residue signals as secondary standards, and the chemical shifts are shown in δ scales. Deuterated solvents were degassed by three freeze-pump-thaw cycles then dried by storing over molecular sieves (3 or 4 Å) for at least one day before using. Multiplicities of the ^{1}H NMR signals are denoted by s(singlet), d (doublet), dd (doublet of doublet), dt (doublet of the triplet), t (triplet), quin (quintet), m (multiplet), br.s (broad singlet)… etc. Compounds were drawn using ChemDraw and the assignments of NMR spectra were done on MestReNova.

Mass spectrometry. HRMS (ESI) was performed via LTQ Orbitrap Velos ETD mass-spectrometer (ThermoFisher Scientific, Bremen, Germany).

X-ray crystallography. Single-crystal X-ray diffraction data were collected on either a Bruker Kappa APEX II CCD diffractometer using Mo Ka radiation (l = 0.71073Å) radiation, or a Bruker AXS single-crystal system equipped with an Excillum METALJET liquid gallium X-ray source, kappa goniometer, Oxford 800 series cryo stream set to 100 K, and Photon III detector. Image collection, data reduction, and scaling were performed with Bruker AXS APEX3 software.

UV-vis spectroscopy. Data were recorded on ThermoScientific Evolution 220 UV-Visible spectrophotometer (Agilent Technologies).

EPR Spectroscopy. The EPR measurements were performed at room temperature using the University of Arizona EPR Facility, on the X-band EPR spectrometer Elexsys E500 (Bruker Biospin) equipped with the electron-nuclear double resonance (ENDOR) system and variable temperature nitrogen flow system (from Bruker BioSpin GmbH, Karlsruhe, Germany).

II. Experimental Section

II.1 Synthesis of 1-X

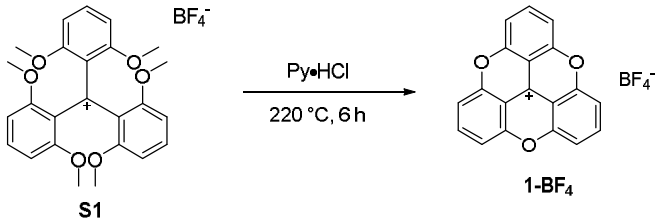

Compound 1, 1-BF_4^- was prepared according to a slightly modified previous report:[2] To a solid mixture of tris(2,6-dimethoxyphenyl)carbenium tetrafluoroborate salt (1.53 g, 3 mmol, 1.0 eq) and pyridine hydrochloride (6.49 g, 56.2 mmol, 19 eq) under vigorous stirring, a small amount of pure pyridine (5 mL) was added. The deep purple reaction mixture was heated to 220 °C for 6 h and slowly turned deep brick red. During the reaction, MeOH and pyridine produced were collected through by a distillation apparatus. The reaction was let return to room temperature, and the slurry red residue was extracted by HCl (0.5M, 300mL) to obtain a deep yellow filtrate. The remaining pad was washed with 3 x 50mL of distilled water. The aqueous solution was basified by pouring NaOH solution until pH 14 under vigorous stirring. The off-white precipitate formed was filtered through a frit and washed with 3 x 30mL of 0.5 M NaOH solution. Then the off-white compound was extracted by 3 x 35 mL of Et_2O and 10 ml of CH_2Cl_2:Et_2O (1:4) to obtain a clear pale-yellow solution. A yellow precipitate appeared instantly after HBF_4 (48 wt%, 3 mL, 7.6 mmol, 7 eq.) was added. This was filtrated, intensively washed with Et_2O, and is finally recovered by dissolution in CH_3CN followed by evaporation and vacuum drying to obtain deep yellow needles (67% yield).

^{1}H NMR (400 MHz, CD_3CN) δ = 8.46 (t, *J* = 8.5 Hz, 3H), 7.79 (d, *J* = 8.5 Hz, 6H).

^{13}C NMR (101 MHz, CD_3CN) δ = 154.63, 146.57, 144.60, 113.55, 107.23.

^{19}F NMR (376 MHz, CD_3CN) δ = -151.92.

^{11}B NMR (160 MHz, CD_3CN) δ = -1.28.

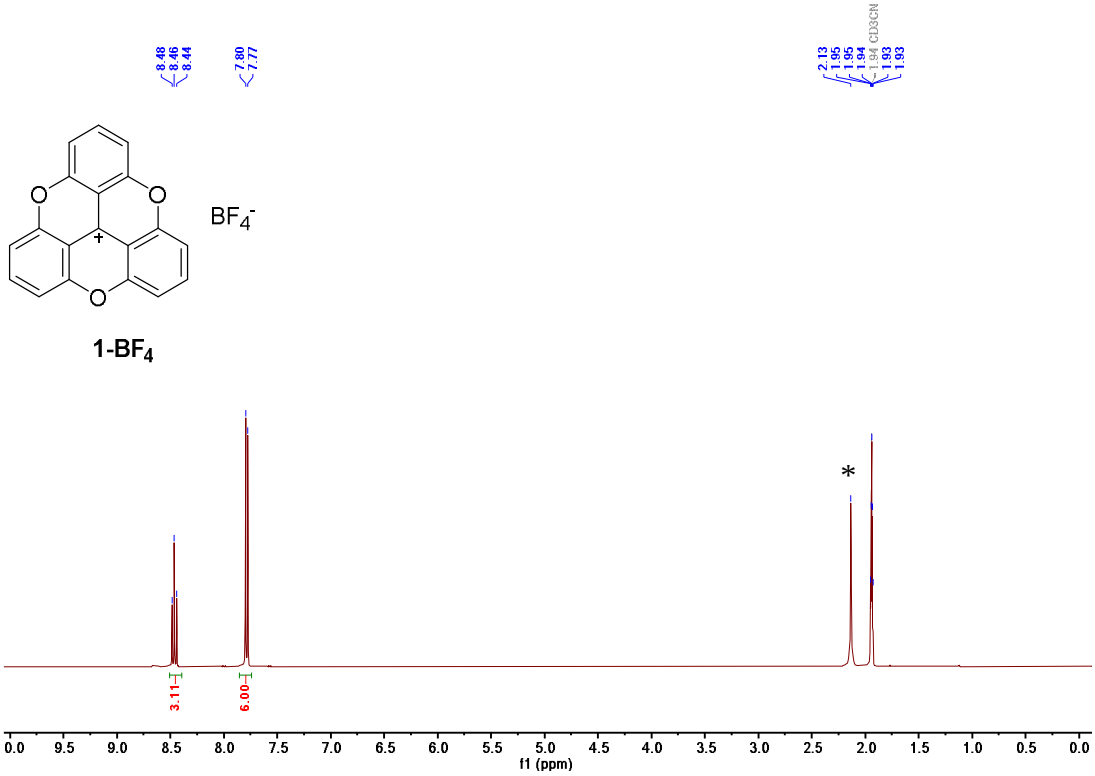

Figure S1: ^{1}H NMR spectrum of 1-BF_4 in CD_3CN (* indicates residual water)

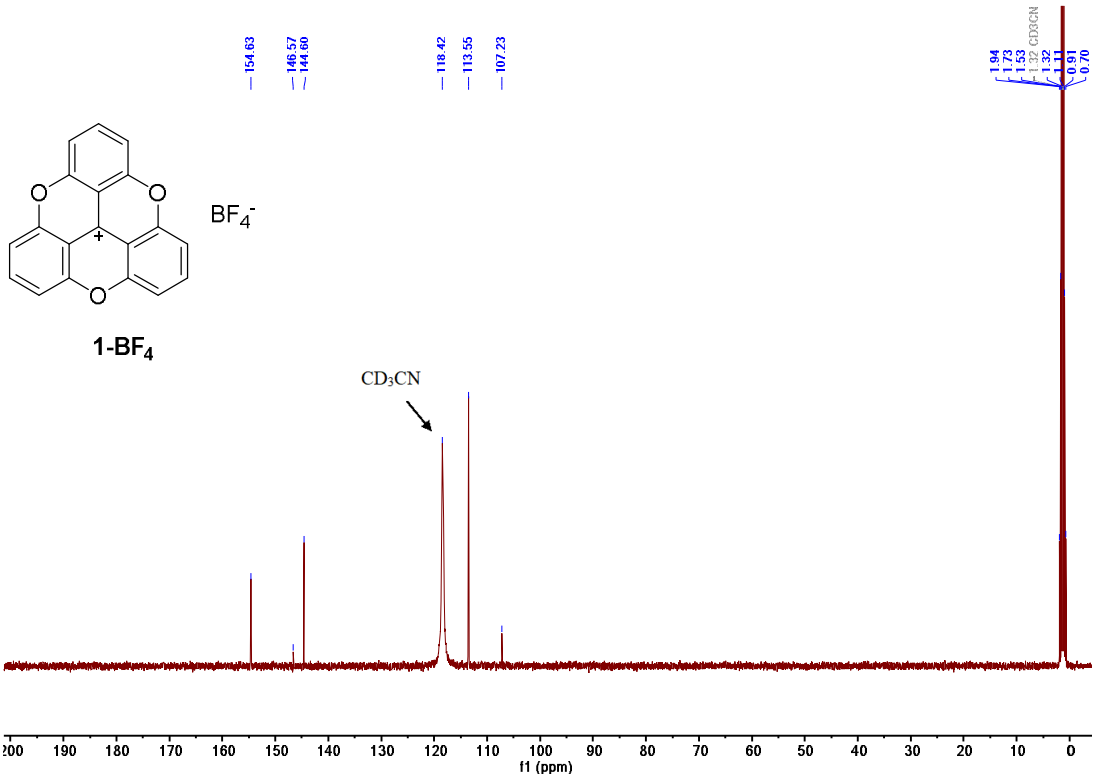

Figure S2: ^{13}C NMR spectrum of 1-BF_4 in CD_3CN

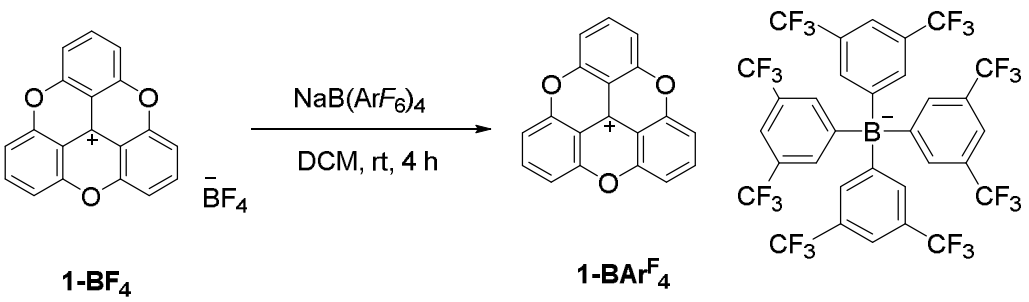

Compound 1, 1-BAr$^{F}_{4}$ was prepared according to slightly modified previous report Procedure:[3] **1-BF$_4$** (372 mg, 1.00 mmol) and sodium tetrakis[3,5-bis(trifluoromethyl)phenyl]borate (0.88 g, 1.20 mmol) were suspended in dichloromethane (250 mL) and stirred at room temperature for 6 h. The mixture was filtered and the solution was washed with water (3 × 150 mL) and dried over sodium sulfate. The solvent was removed under reduced pressure and the crude product was recrystallized from CH_2Cl_2 and pentane at room temperature. Filtration gave 1.2 g (90% yield) of a yellow solid.

^{1}H NMR (400 MHz, CD_2Cl_2) δ = 8.27 (t, *J* = 8.5 Hz, 3H), 7.75 – 7.65 (m, 8H), 7.59 (d, *J* = 8.5 Hz, 6H), 7.46 (s, 4H).

^{13}C NMR (100 MHz, CD_2Cl_2) δ = 162.17 (dd, *J* = 99.8, 49.7 Hz), 153.79, 145.29, 144.22, 135.21, 130.83 – 127.86 (m), 126.34, 123.63, 120.92, 117.87 (d, *J* = 4.4 Hz), 113.44, 106.02.

^{19}F NMR (376 MHz, CD_2Cl_2) δ = -62.46.

^{11}B NMR (160 MHz, CD_2Cl_2) δ = -6.63 (dt, *J* = 5.4, 2.8 Hz).

Assessment of Lewis acidity of TOTA$^+$: The Gutmann-Beckett method was used to determine Lewis acidity.[4] (AN = Acceptor Number, see Figure 5)

^{31}P{1H} NMR: $Et_3P{=}O$ (δ = 51.15)*;

^{31}P{1H} NMR: $(Et_3P{=}O)\cdot TOTA^+$ (δ = 51.44 ppm);
Δδ/ppm = 0.29 ppm

$AN = (\delta_{(sample)} - 41.0) \times \{100/(86.14 - 41.0)\}$

AN for TOTA+ = (51.44 - 41.0) × {100/(86.14 - 41.0)}
= 23.1
Note: * The value obtained for $Et_3P{=}O$ in CD_2Cl_2

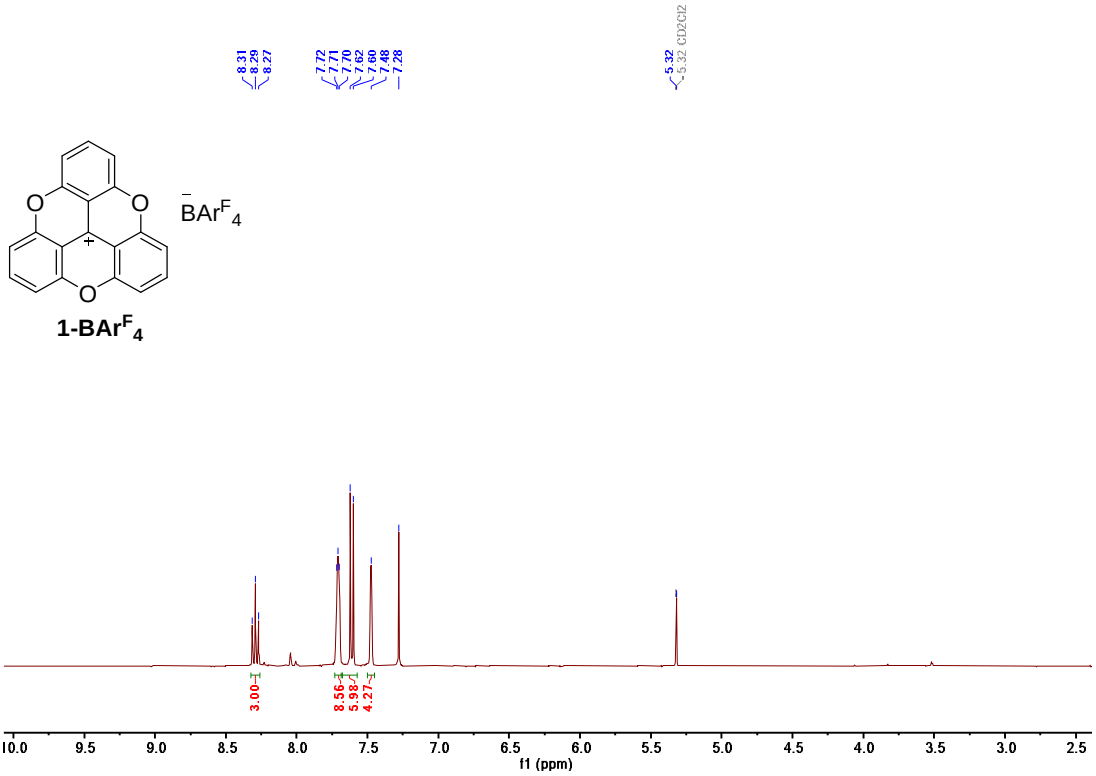

Figure S3: ^{1}H NMR spectrum of 1-BAr$^F_4$ in CD_2Cl_2

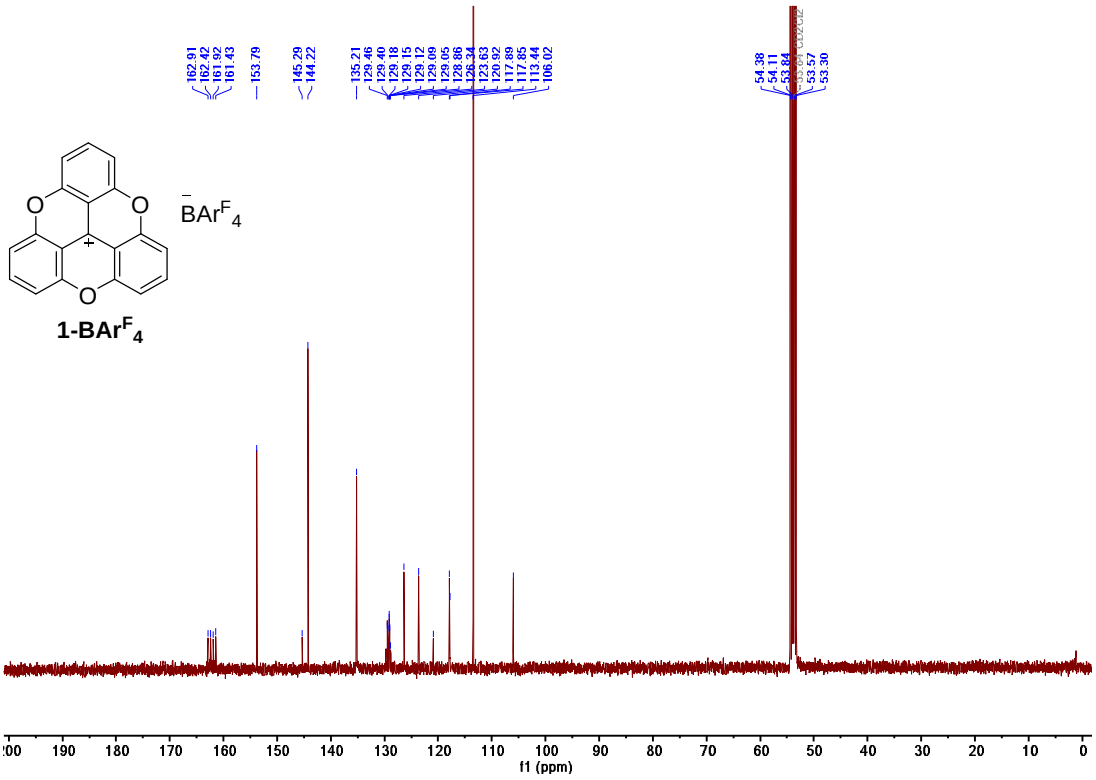

Figure S4: ^{13}C NMR spectrum of 1-BAr$^F_4$ in CD_2Cl_2

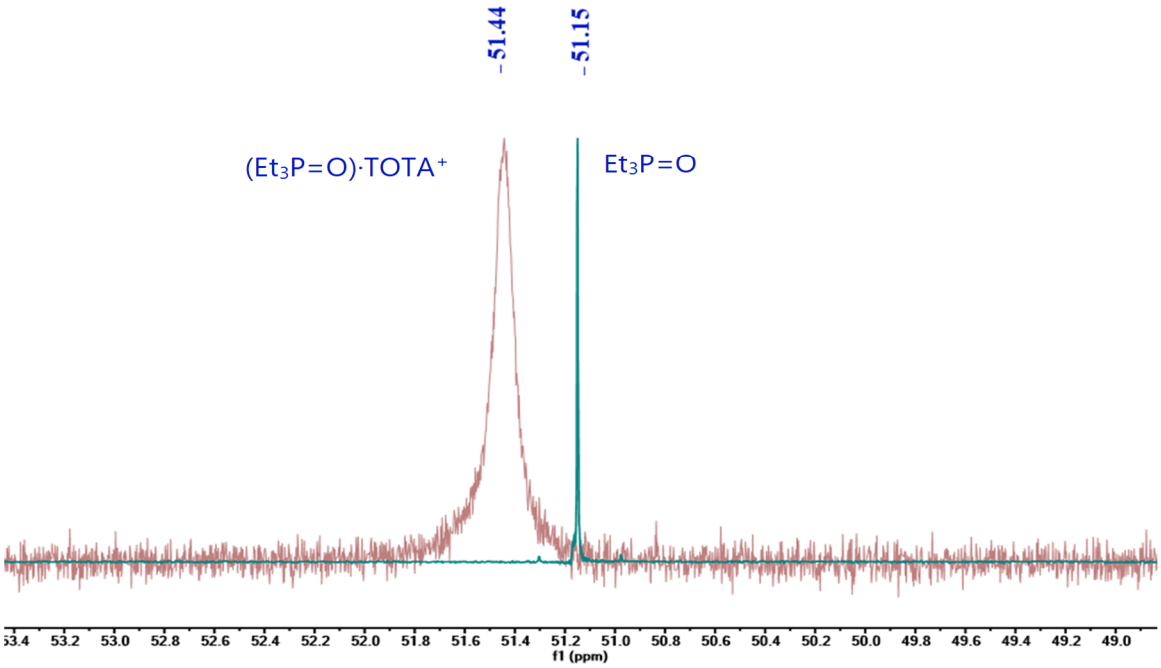

Figure S5: Stacked ^{31}P NMR spectrum for $Et_3P{=}O$ and $Et_3P{=}O)\cdot TOTA^+$ in CD_2Cl_2

II.2 Syntheses of Lewis adduct and frustrated Lewis pair

II.2a The reaction between 1-BF_4 and PMe_3:

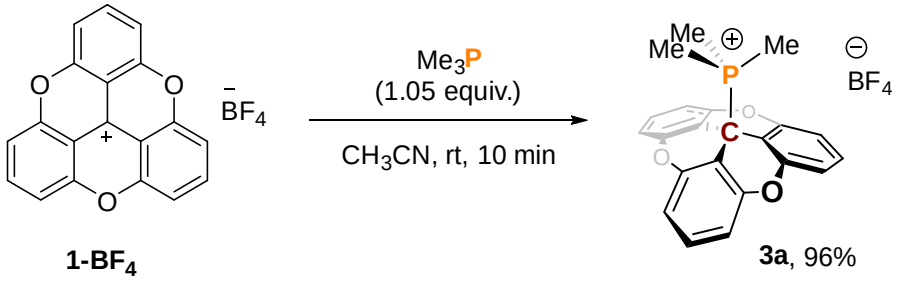

1-BF_4 **3a**, 96%

Procedure: In a glove box, trimethyl phosphine (11 µl, 0.1 mmol, 1.05 equiv.) was added to a stirred solution of **1-BF_4** (37.2 mg, 0.1 mmol, 1.0 equiv.) in CH_3CN (3 mL). After the addition of the phosphine, the reaction mixture immediately changed from yellow to colorless. The solution was stirred at ambient temperature for 5 min. The solvent was removed under vacuum. The crude product was precipitated by the addition of hexanes, filtered, and washed with hexanes and Et_2O. Finally, it was precipitated by adding twofold of hexane to the CH_2Cl_2

solution, and further crystallized by slow diffusion of a hexane layer into a CH_2Cl_2 solution containing the product, yielding **3a** as a colourless microcrystalline powder (46 mg, 96% yield).

(3a^2*H*-4,8,12-trioxadibenzo[*cd,mn*]pyren-3a^2-yl)trimethylphosphonium tetrafluoroborate (3a):

Colorless solid; **MP =** 182-184 ºC (decomposition)

^{1}H NMR (400 MHz, CD_3CN) δ = 7.53 (td, *J* = 8.3, 1.8 Hz, 3H), 7.12 (dd, *J* = 8.4, 0.7 Hz, 6H), 1.67 (d, *J* = 13.5 Hz, 9H).

^{13}C NMR (101 MHz, CD_3CN) δ = 153.62 (d, *J* = 3.4 Hz), 133.15 (d, *J* = 3.3 Hz), 114.06 (d, *J* = 2.8 Hz), 104.01 (d, *J* = 1.8 Hz), 33.70 (d, *J* = 60.8 Hz), 4.71 (d, *J* = 48.1 Hz).

^{31}P NMR (162 MHz, CD_3CN) δ = 44.37 (dh, *J* = 27.1, 13.4 Hz).

^{19}F NMR (376 MHz, CD_3CN) δ = -151.55.

^{11}B NMR (160 MHz, CD_3CN) δ = -1.28.

HRMS (ESI) m/z: [M^+] Calcd. for $C_{22}H_{18}O_3P$ 361.0988; Found: 361.0987.

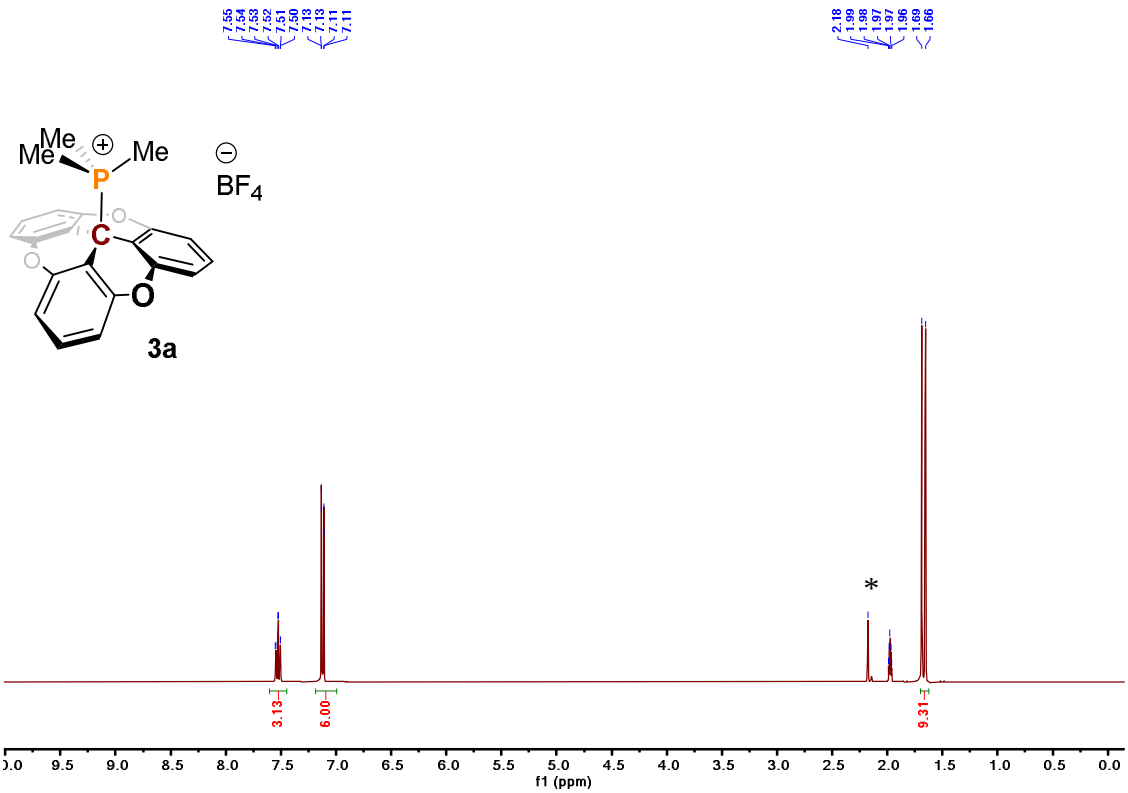

Figure S6: ^{1}H NMR spectrum of 3a in CD_3CN (* indicates residual water)

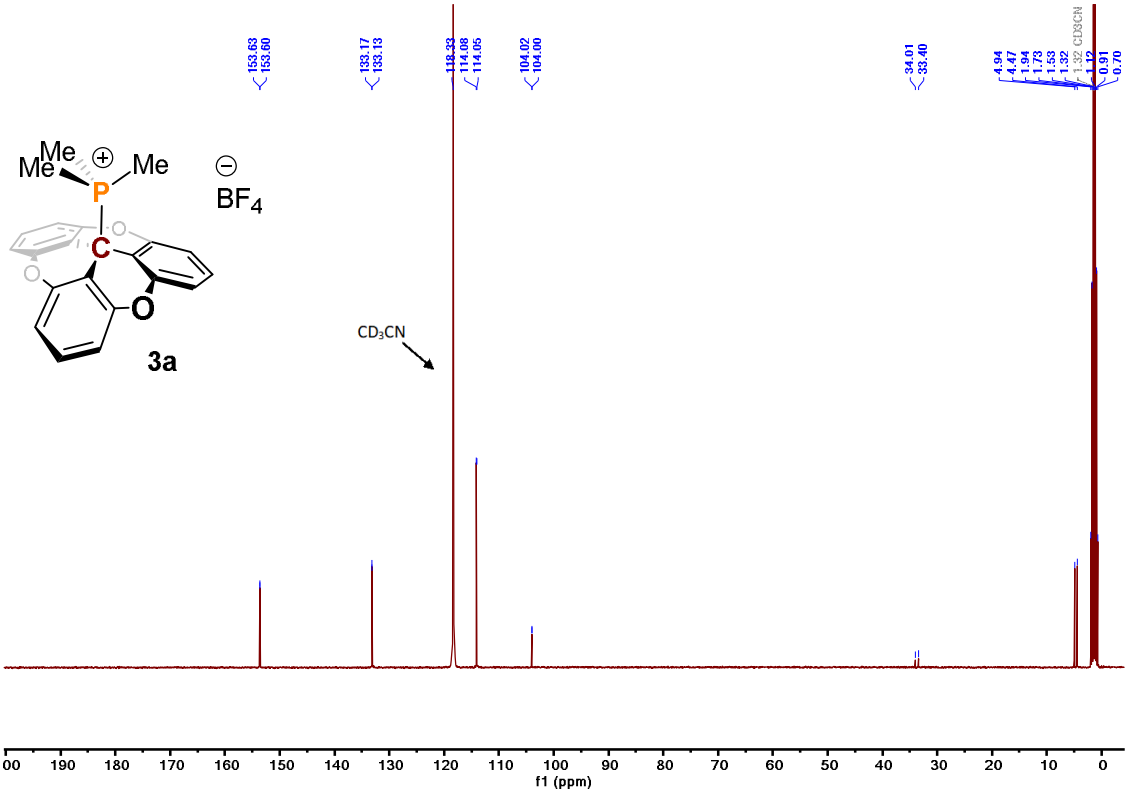

Figure S7: ^{13}C NMR spectrum of 3a in CD_3CN

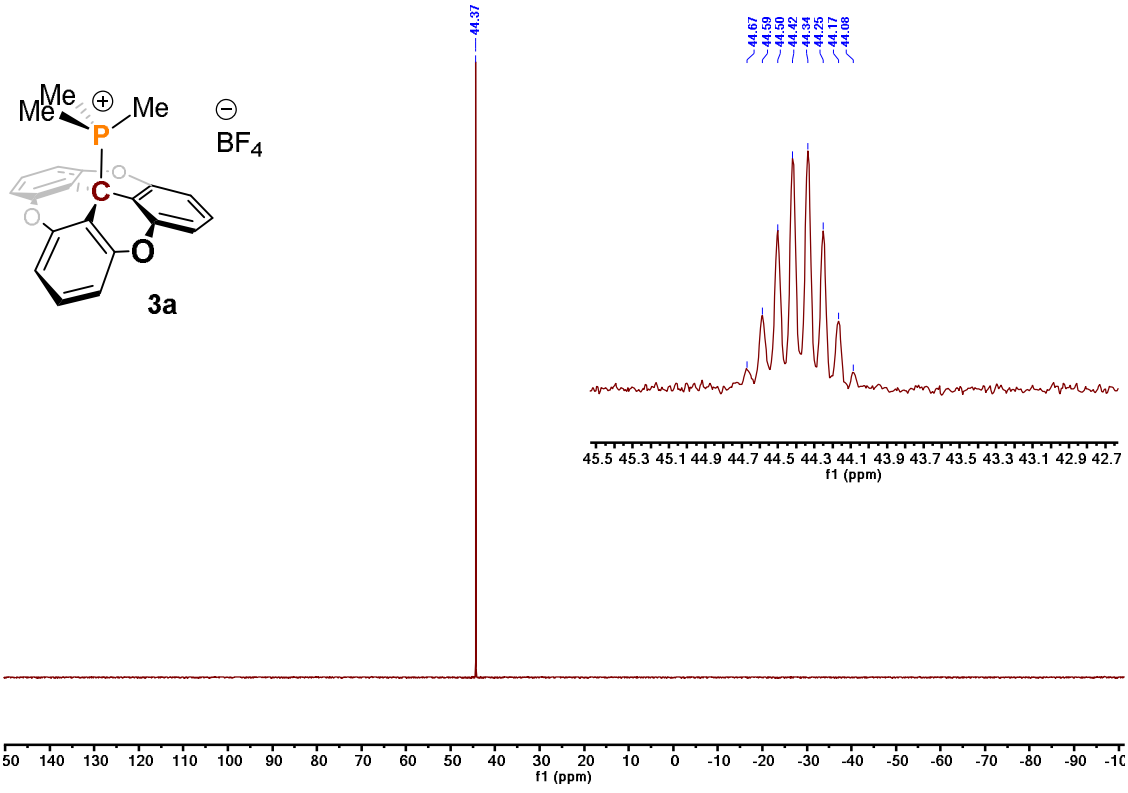

Figure S8: ^{31}P NMR spectrum of 3a in CD_3CN

*

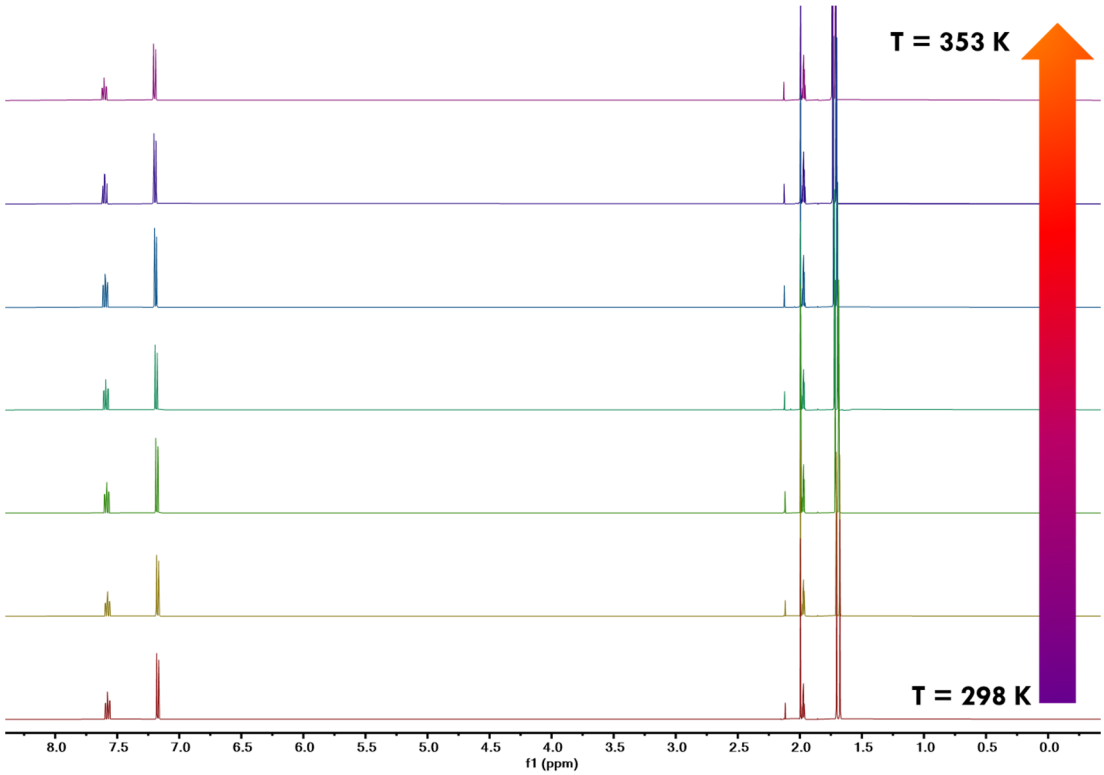

Figure S9: Variable-temperature ^{1}H NMR of 3a in CD_3CN (* indicates residual water)

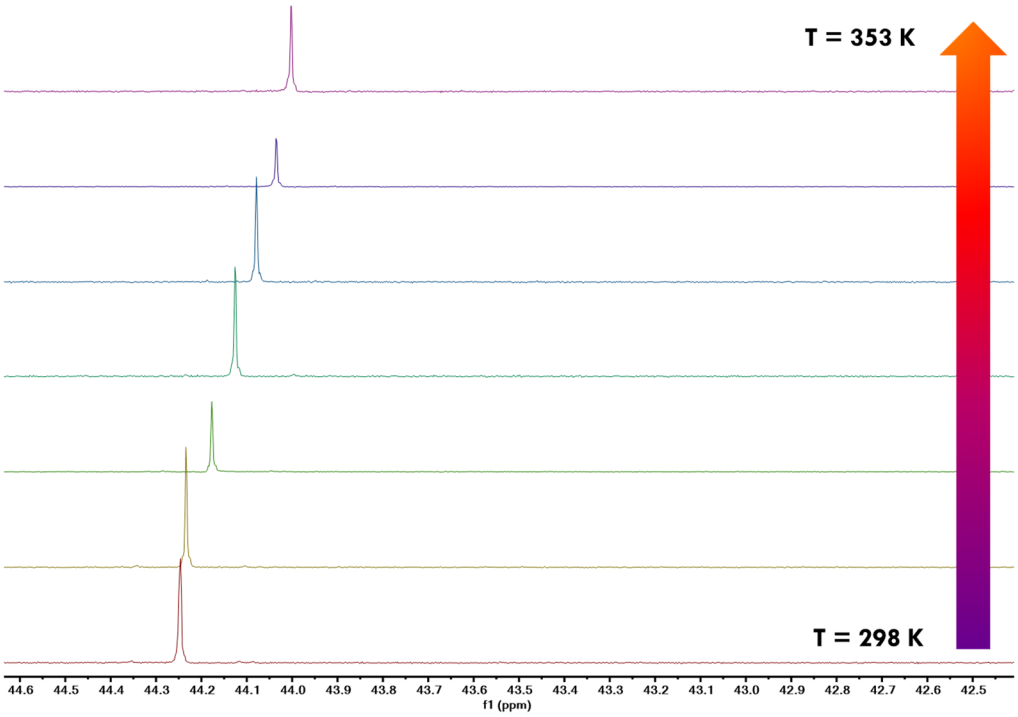

Figure S10: Variable-temperature ^{31}P NMR of 3a in CD_3CN

II.2b Reaction between 1-BF_4 and $PPhMe_2$:

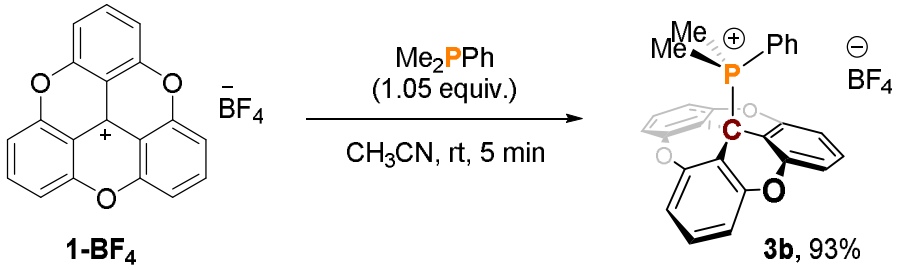

1-BF_4 **3b**, 93%

Following the representative procedure in **II.2a** by using **1-BF_4** (37.2 mg, 0.1 mmol) and dimethyl phenyl phosphine (15 μl, 0.1 mmol) as starting materials.

(3a^2*H*-4,8,12-trioxadibenzo[*cd,mn*]pyren-3a^2-yl)dimethyl(phenyl)phosphonium tetrafluoroborate (3b):

Light yellow solid, 51 mg, 93%; **MP** = 202-204 ºC (decomposition)

^{1}H NMR (400 MHz, CD_3CN) δ = 7.82 (tt, *J* = 6.2, 1.1 Hz, 1H), 7.47 (qd, *J* = 8.3, 2.7 Hz, 5H), 7.12 (ddd, *J* = 11.8, 8.4, 1.3 Hz, 2H), 6.99 (d, *J* = 8.3 Hz, 6H), 2.01 (d, *J* = 13.2 Hz, 6H).

^{13}C NMR (101 MHz, CD_3CN) δ = 153.70 (d, *J* = 3.6 Hz), 136.78 (d, *J* = 3.2 Hz), 133.49 (d, *J* = 9.2 Hz), 133.15 (d, *J* = 3.3 Hz), 130.38 (d, *J* = 12.0 Hz), 116.68 (d, *J* = 77.0 Hz), 113.76 (d, *J* = 2.8 Hz), 103.54 (d, *J* = 2.0 Hz), 36.63 (d, *J* = 57.0 Hz), 3.08 (d, *J* = 49.6 Hz).

^{31}P NMR (162 MHz, CD_3CN) δ = 34.90.

^{19}F NMR (376 MHz, CD_3CN) δ = -151.86.

^{11}B NMR (160 MHz, CD_3CN) δ = -1.28.

MALDI-TOF m/z: [M^+] Calcd. for $C_{27}H_{20}O_3P$ 423.1144; Found: 423.1159. In **HRMS (ESI) m/z**; major fragmentation for TOTA$^+$ [M^+-$C_8H_{11}P$]$^+$ at 285.0544 noted.

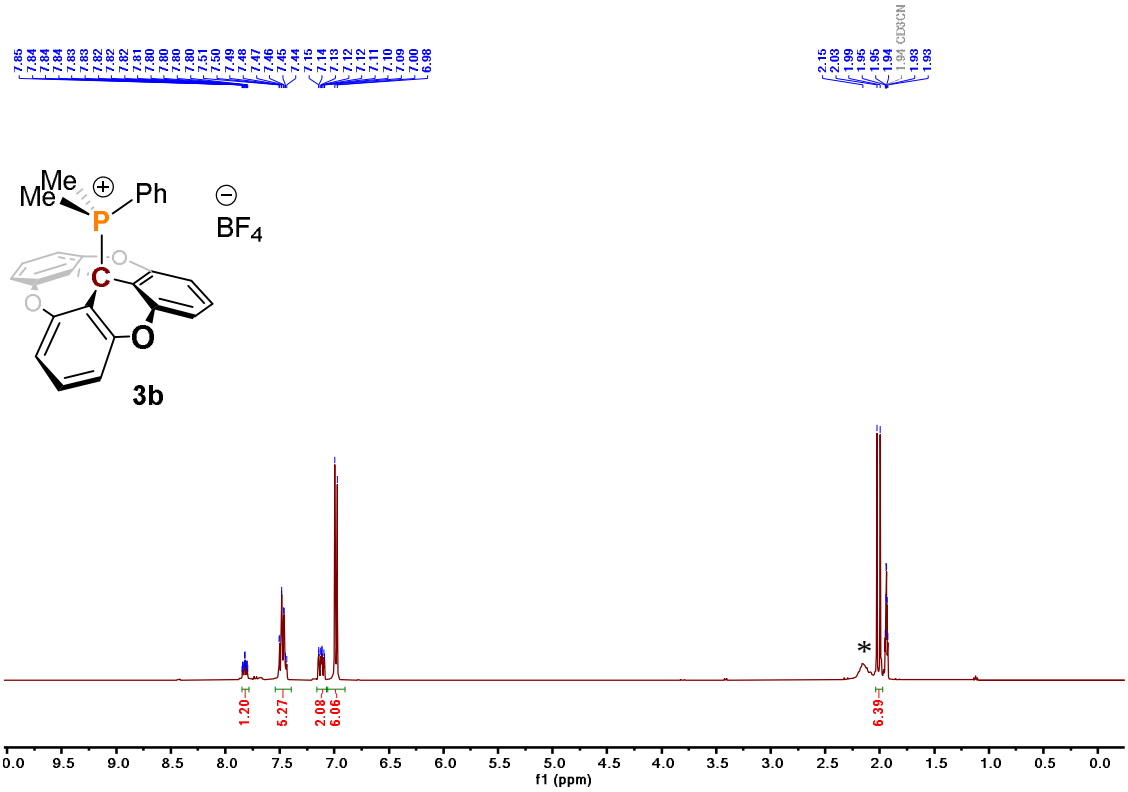

Figure S11: ^{1}H NMR spectrum of 3b in CD_3CN (* indicates residual water)

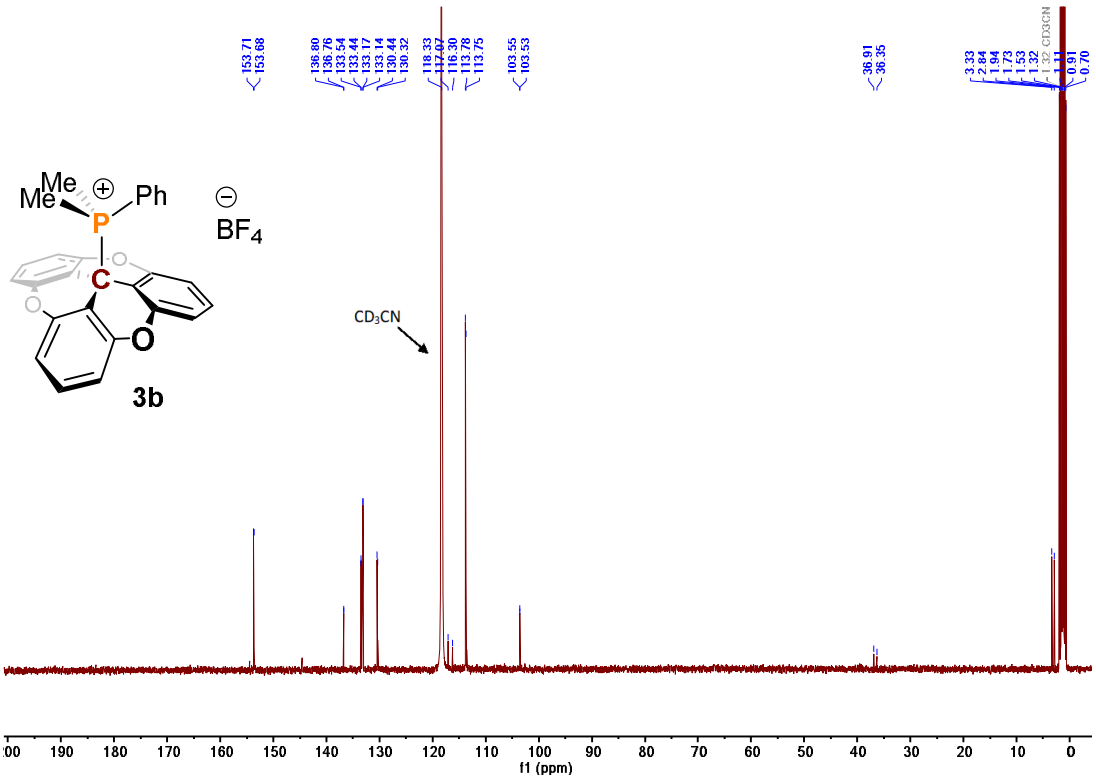

Figure S12: ^{13}C NMR spectrum of 3b in CD_3CN

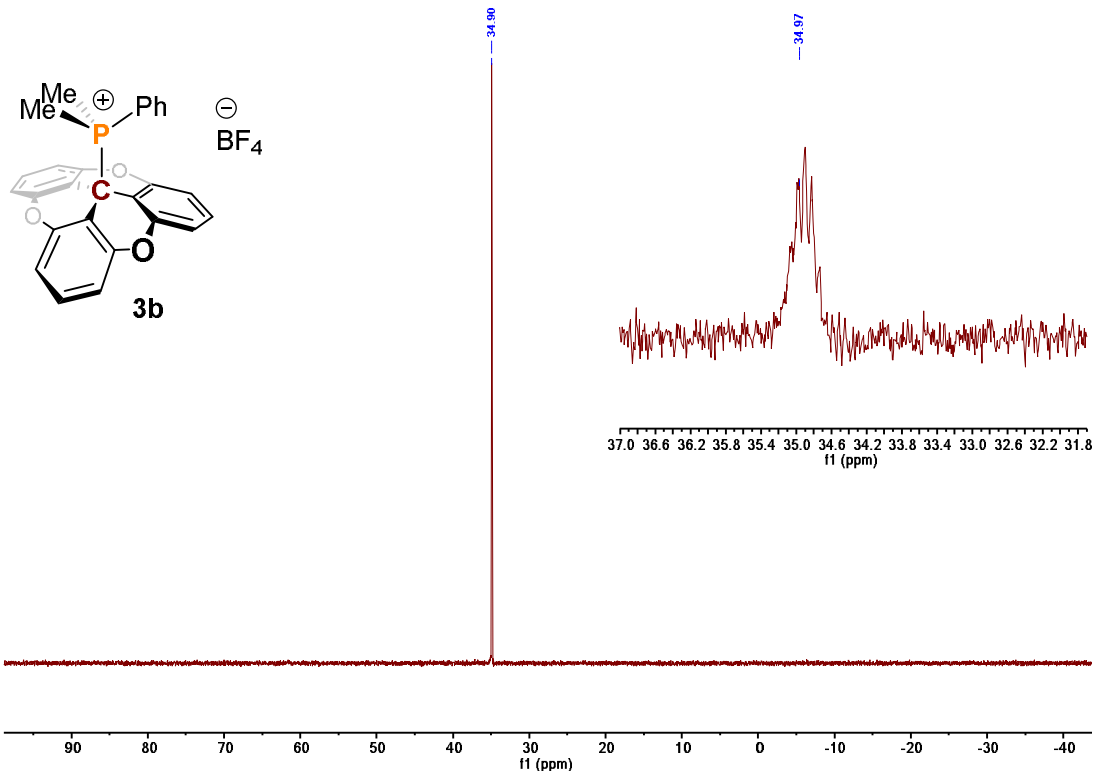

Figure S13: ^{31}P NMR spectrum of 3b in CD_3CN

II.2c. Reaction between 1-BF_4 and ^{n}Pr_3P:

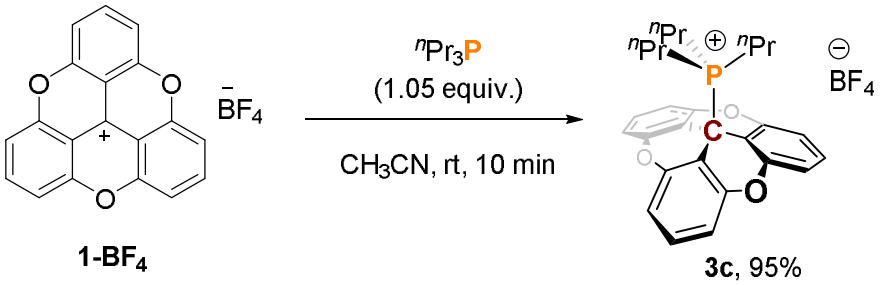

Following the representative procedure in **II.2a** by using **1-BF_4** (37.2 mg, 0.1 mmol) and tri(n-propyl) phosphine (19 µl, 0.1 mmol) as starting materials.

(3a^2*H*-4,8,12-trioxadibenzo[*cd,mn*]pyren-3a^2-yl)tripropylphosphonium tetrafluoroborate (3c):

Light yellow solid; 50 mg, 95 % yield; **MP** = 238-240 ºC (decomposition)

^{1}H NMR (400 MHz, CD_3CN) δ = 7.51 (td, *J* = 8.3, 1.7 Hz, 3H), 7.28 – 6.76 (m, 6H), 2.08 – 1.96 (m, 6H), 1.31 – 1.00 (m, 6H), 0.89 (td, *J* = 7.1, 2.0 Hz, 9H).

^{13}C NMR (101 MHz, CD_3CN) δ = 154.46, 153.80 (d, *J* = 3.2 Hz), 144.60, 133.18 (d, *J* = 3.1 Hz), 114.17 (d, *J* = 2.5 Hz), 113.56, 107.02, 105.13 (d, *J* = 1.9 Hz), 34.80 (d, *J* = 53.0 Hz), 19.16 (d, *J* = 37.8 Hz), 16.31 (d, *J* = 5.2 Hz), 15.82 (d, *J* = 15.8 Hz).

^{31}P NMR (162 MHz, CD_3CN) δ = 49.87.

^{19}F NMR (376 MHz, CD_3CN) δ = -148.37.

^{11}B NMR (160 MHz, CD_3CN) δ = -1.28.

MALDI-TOF m/z: [M^+] Calcd. for $C_{28}H_{30}O_3P$ 445.1927; Found: 445.1938. In **HRMS (ESI) m/z**; only fragmentation for TOTA$^+$ [M^+-$C_9H_{21}P$]$^+$ at 285.0544 noted.

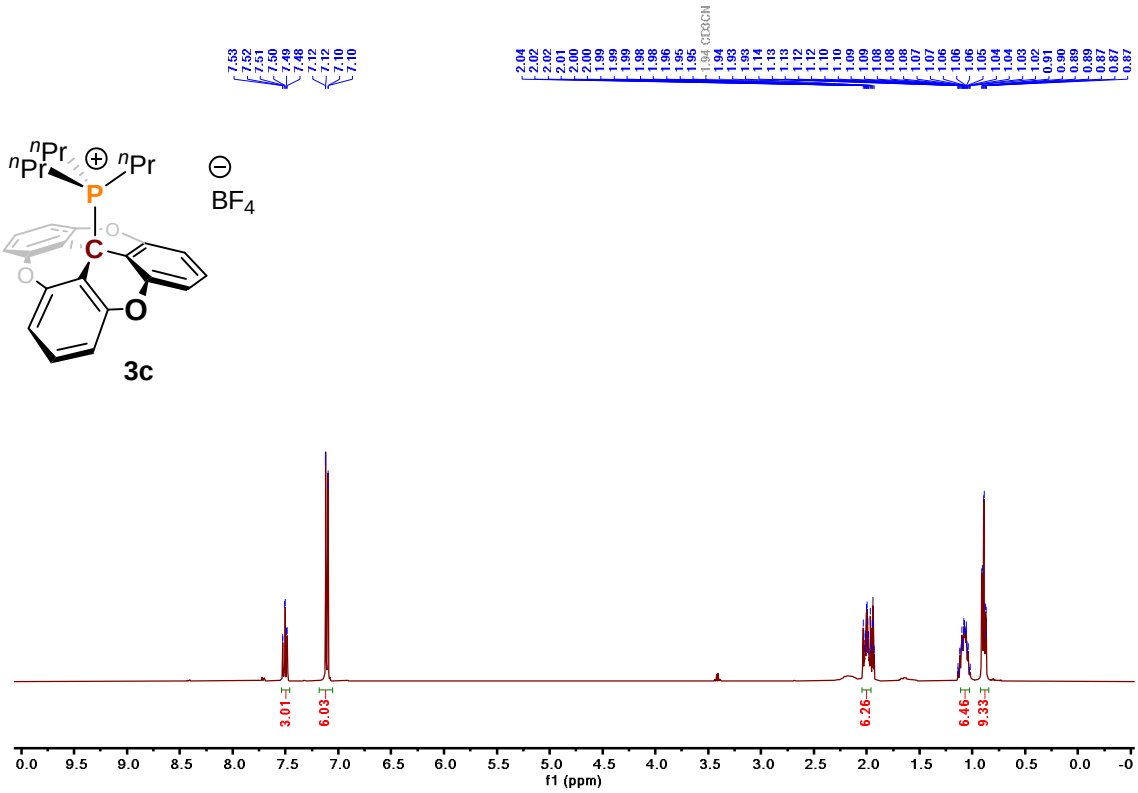

Figure S14: ^{1}H NMR spectrum of 3c in CD_3CN

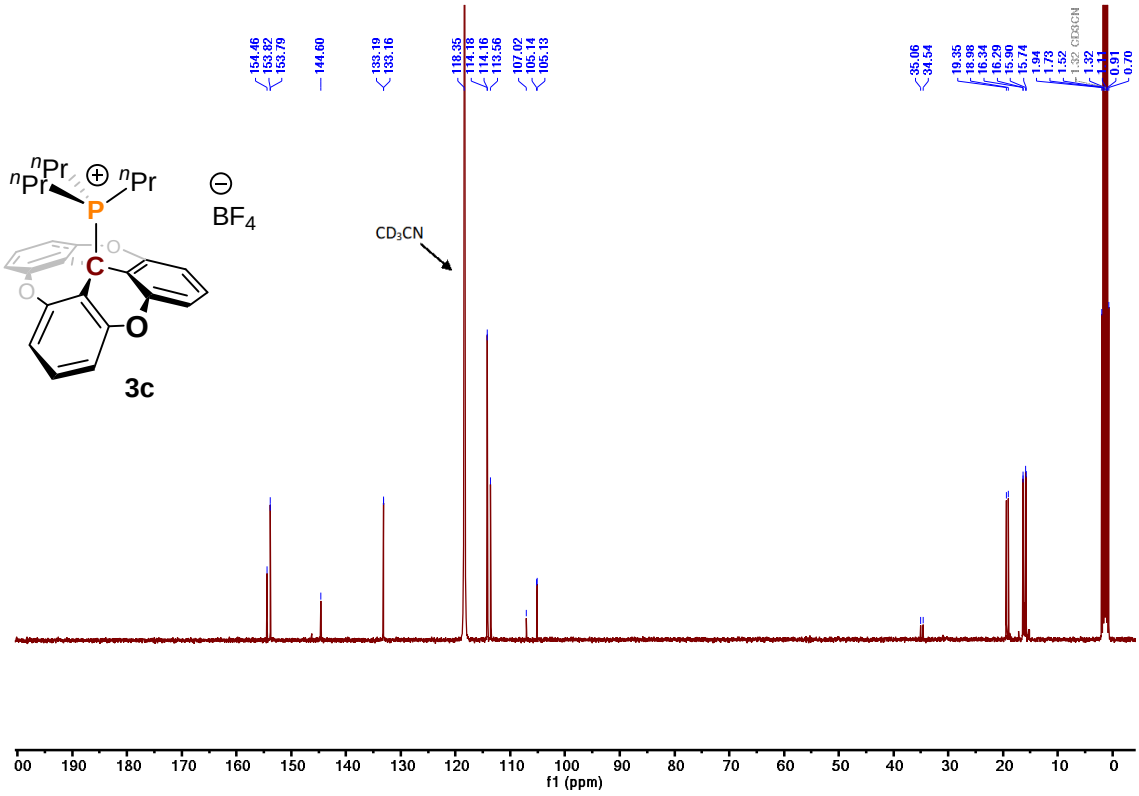

Figure S15: ^{13}C NMR spectrum of 3c in CD_3CN

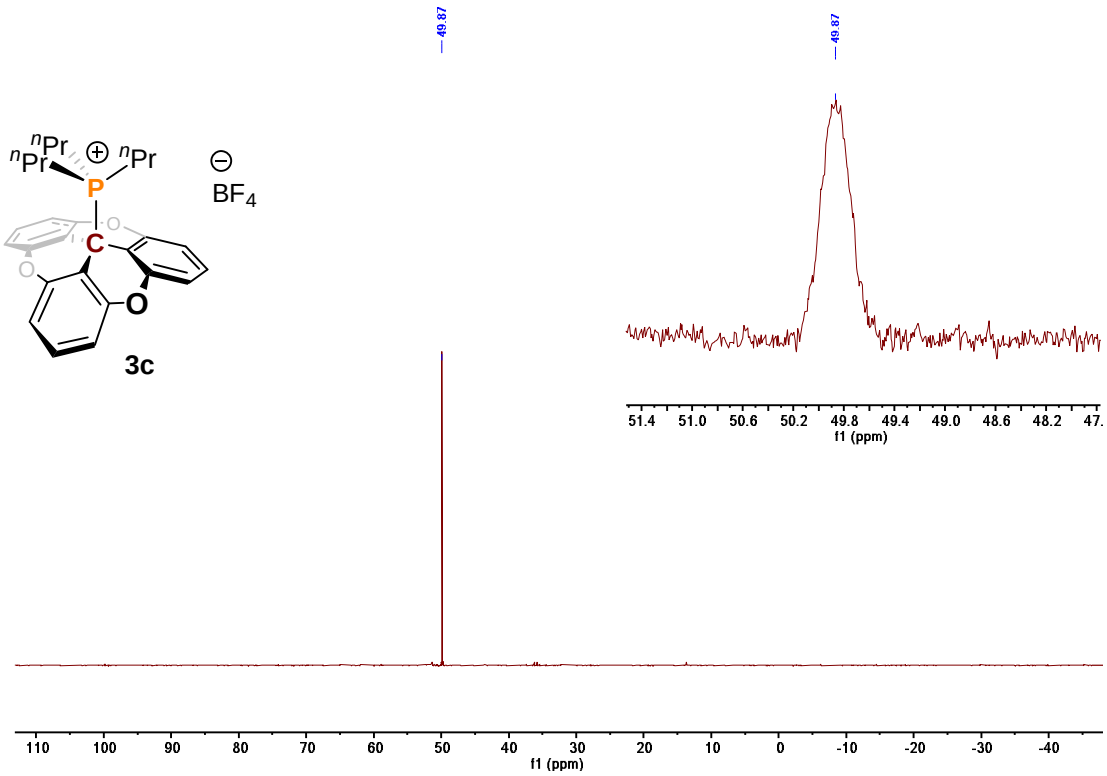

Figure S16: ^{31}P NMR spectrum of 3c in CD_3CN

II.2d Reaction between 1-BF_4 and $^nBu_3P$:

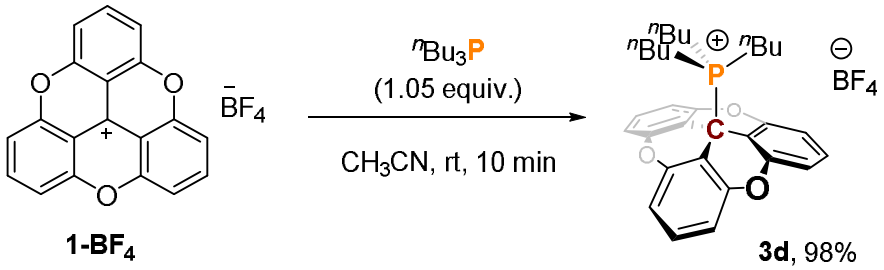

Following the representative procedure in **II.2a** by using **1-BF_4** (37.2 mg, 0.1 mmol) and tributylphosphine (24 µl, 0.1 mmol) as starting materials.

(3a^2*H*-4,8,12-trioxadibenzo[*cd,mn*]pyren-3a^2-yl)tributylphosphonium tetrafluoroborate (3d):

Off white solid; 56 mg, 98 % yield; **MP** = 160 ºC (decomposition of adduct noted)

^{1}H NMR (400 MHz, CD_3CN) δ = 7.50 (td, *J* = 8.3, 1.7 Hz, 3H), 7.10 (d, *J* = 8.3 Hz, 6H), 2.07 – 1.97 (m, 6H), 1.27 (h, *J* = 7.4 Hz, 6H), 0.97 (hept, *J* = 6.9, 6.4 Hz, 6H), 0.78 (t, *J* = 7.3 Hz, 9H).

^{13}C NMR (101 MHz, CD_3CN) δ = 152.85 (d, *J* = 3.2 Hz), 132.12 (d, *J* = 3.0 Hz), 113.17 (d, *J* = 2.5 Hz), 104.25 (d, *J* = 1.8 Hz), 33.81 (d, *J* = 52.7 Hz), 23.81 (d, *J* = 15.0 Hz), 23.07 (d, *J* = 5.5 Hz), 16.40 (d, *J* = 38.2 Hz), 12.30 (d, *J* = 1.2 Hz).

^{31}P NMR (162 MHz, CD_3CN) δ = 47.29.

^{19}F NMR (376 MHz, CD_3CN) δ = -151.77 (d, *J* = 20.1 Hz).

^{11}B NMR (160 MHz, CD_3CN) δ = -1.28.

HRMS (ESI) m/z: [M^+] Calcd. for $C_{31}H_{36}O_3P$ 487.2396; found 487.2400.

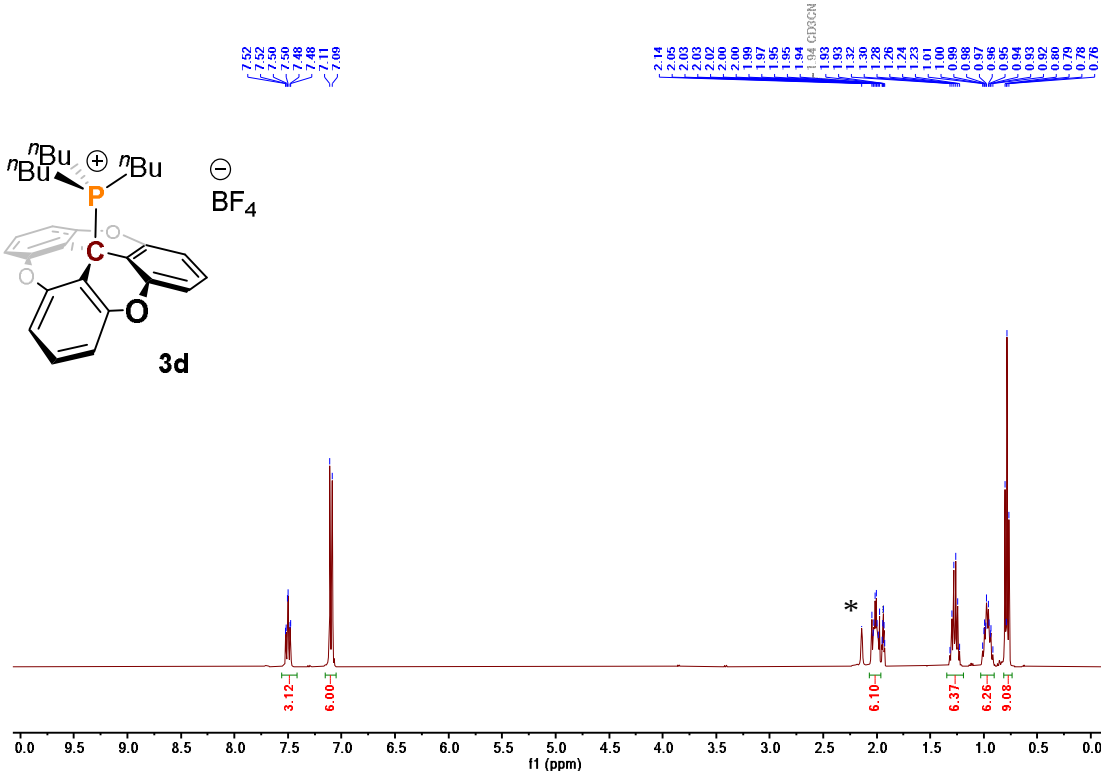

Figure S17: ^{1}H NMR spectrum of 3d in CD_3CN (* indicates residual water)

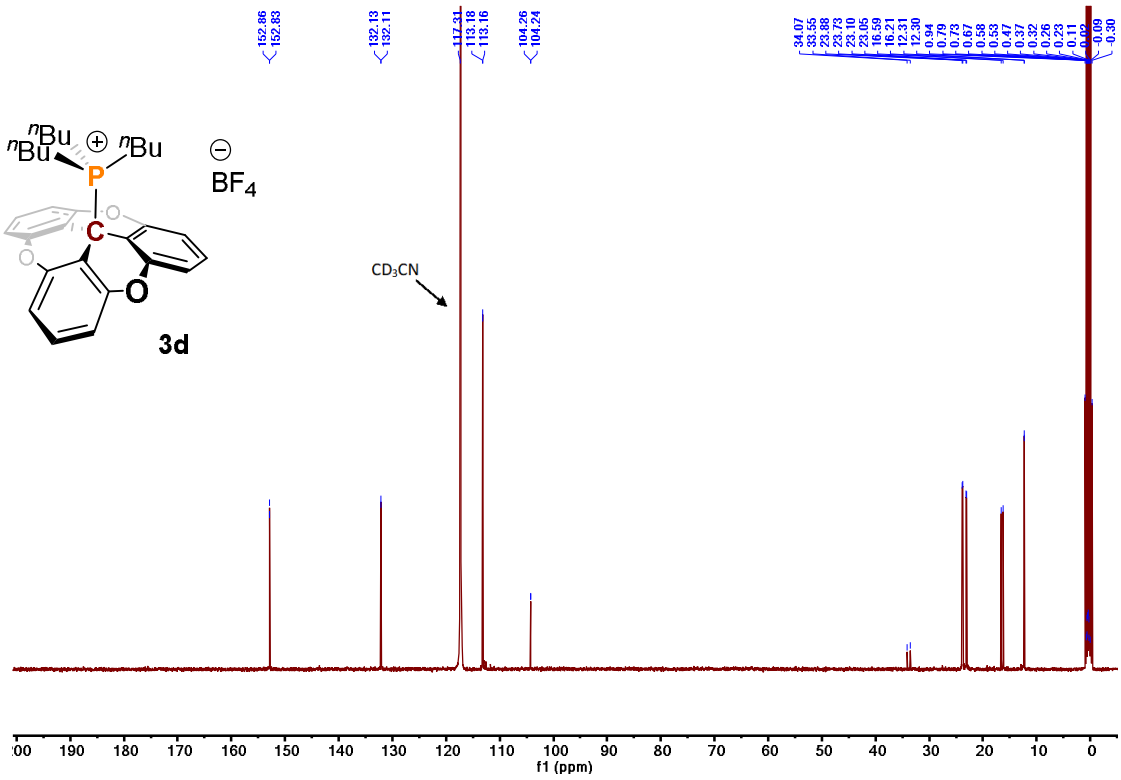

Figure S18: ^{13}C NMR spectrum of 3d in CD_3CN

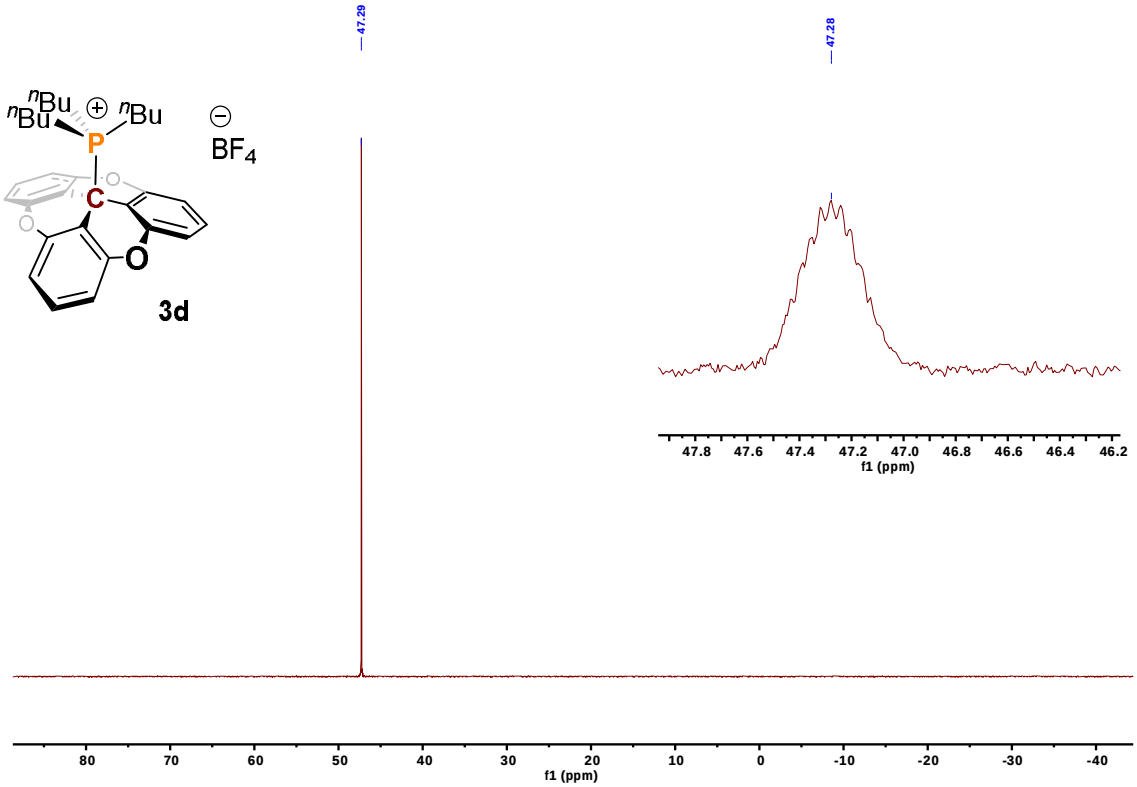

Figure S19: ^{31}P NMR spectrum of 3d in CD_3CN

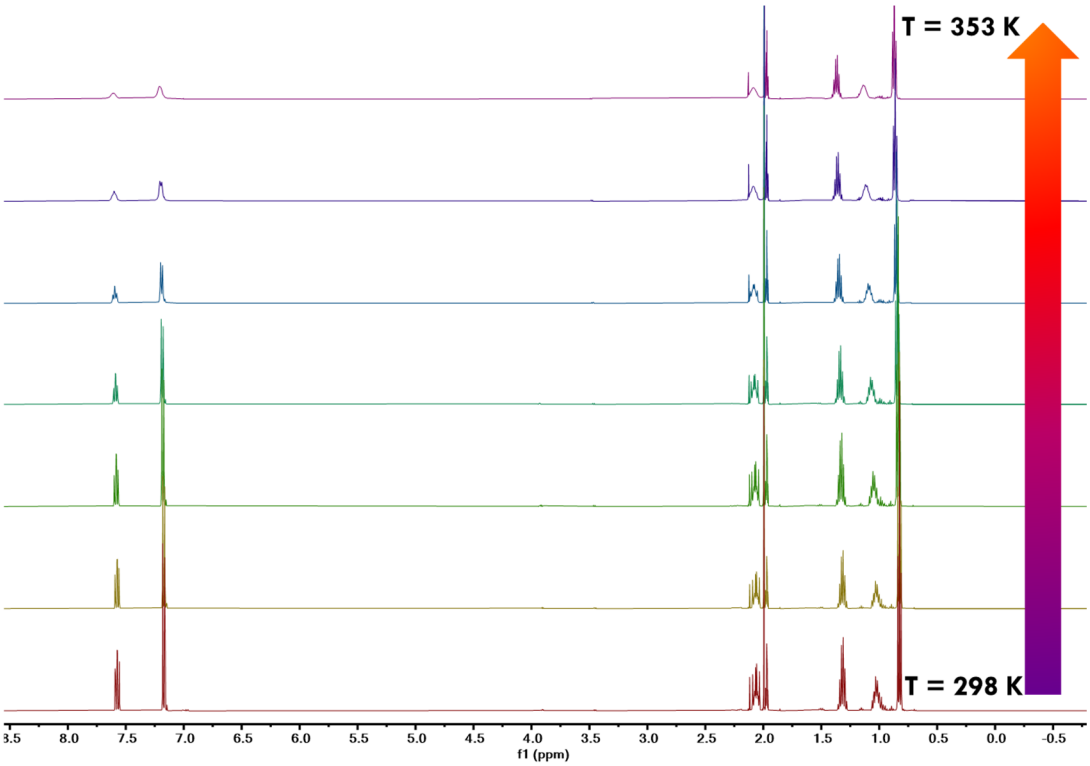

Figure S20: Variable-temperature ^{1}H NMR of 3d in CD_3CN

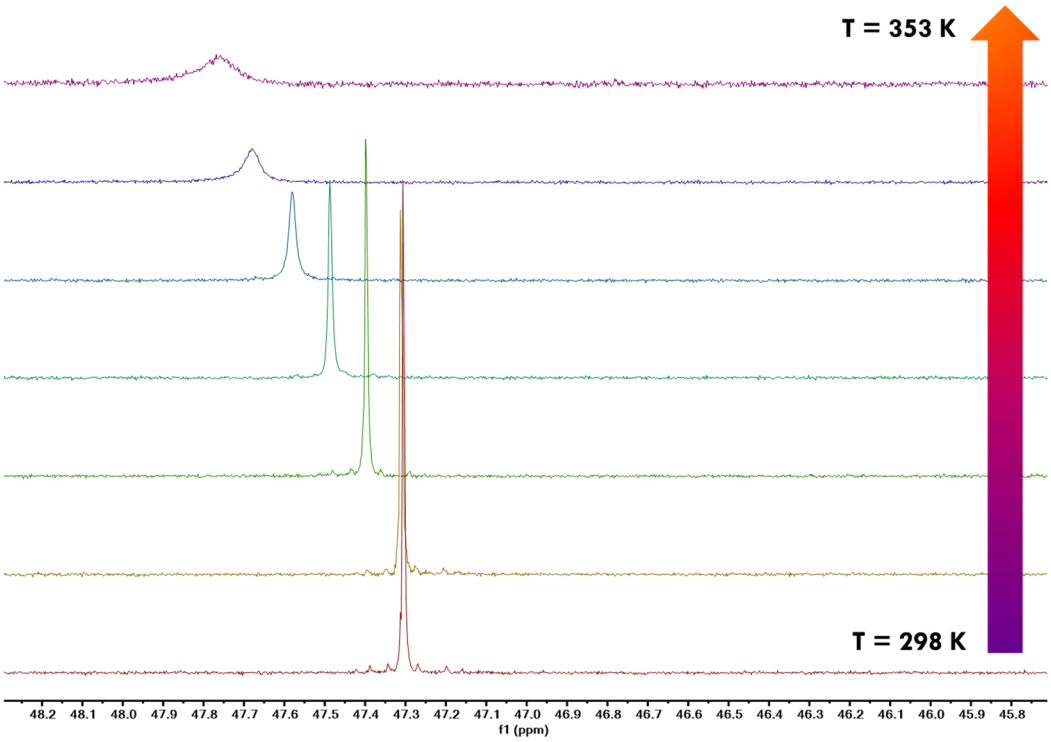

Figure S21: Variable-temperature ^{31}P NMR of 3d in CD_3CN

II.2e Reaction between 1-BAr^F_4 and $PMePh_2$:

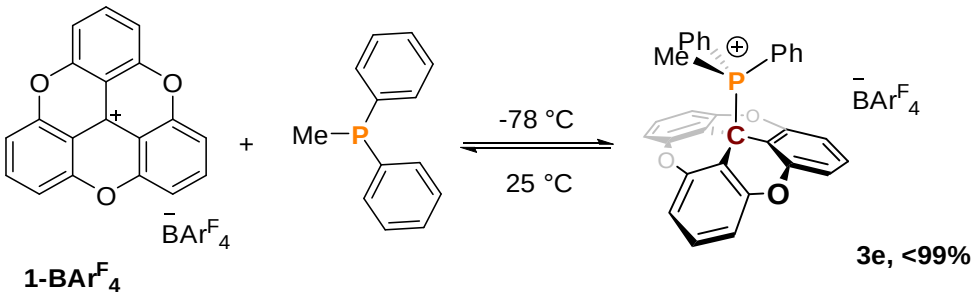

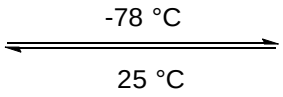

Procedure: In the glove box, a J. Young NMR tube was charged with **1-BAr^F_4** (12 mg, 0.010 mmol), an excess of $PMePh_2$ (4.2 mg, 0.020 mmol) and CD_2Cl_2 (0.5 mL). ^{1}H, ^{19}F, and ^{31}P NMR spectra were recorded at 25˚C followed by lowering the temperature to -60˚C, with NMR spectroscopy measurements were conducted every 10 ˚C. After that, the reaction mixture was warmed back to 30 ˚C, and NMR measurements were conducted again. The results are shown

in Figure S21-S22. When the solution is cooled to -40 ˚C, the NMR spectra show the formation of the corresponding Lewis acid-base adducts **3e**. The ^{13}C NMR spectrum of **3e** at -60˚C shows a typical doublet ($^{2}J_{P,C}$ =52.5 Hz) at 38.99 ppm for the central quaternary carbon and $^{31}P\{^{1}H\}$ NMR show a resonance at 18.24 ppm (vs. free phosphine signal at -28.9 ppm) supporting the formation of the Lewis adduct.

Further, the characterization of non-isolable Lewis acid-base adduct **3e** were carried at -60˚C with stoichiometric amount of **1-BAr$^{F}_{4}$** (12 mg, 0.010 mmol), $PMePh_2$ (2.1 mg, 0.010 mmol) and CD_2Cl_2 (0.5 mL). At room temperature, the dark yellow color of the mixture of **1-BAr$^{F}_{4}$** and $PMePh_2$ indicates the there is no interaction between both species as well as no adduct formation. However, fading of yellow color was observed when cooling at -78 ˚C which indicates the adduct formation between both species.

(3a^{2}*H*-4,8,12-trioxadibenzo[*cd,mn*]pyren-3a^{2}-yl)(methyl)diphenylphosphonium tetrakis(3,5-bis(trifluoromethyl)phenyl)borate (3e):

^{1}H NMR (500 MHz, CD_2Cl_2) δ = 7.78 (tdd, *J* = 7.6, 2.0, 1.1 Hz, 2H), 7.74 (p, *J* = 2.1 Hz, 8H, Ar-H of $BArF_{24}$), 7.53 (s, 4H, Ar-H of $BArF_{24}$), 7.50 – 7.43 (m, 4H), 7.40 (td, *J* = 8.3, 2.0 Hz, 3H), 7.07 (ddd, *J* = 11.2, 8.4, 1.3 Hz, 4H), 6.88 (dd, *J* = 8.3, 0.7 Hz, 6H), 2.21 (d, *J* = 12.2 Hz, 3H).

^{13}C NMR (126 MHz, CD_2Cl_2) δ = 161.65 (dd, *J* = 99.4, 49.8 Hz), 152.65 (d, *J* = 3.4 Hz), 136.05 (d, *J* = 3.2 Hz), 134.48, 133.23 (d, *J* = 8.5 Hz), 132.27 (d, *J* = 3.5 Hz), 129.80, 129.70, 128.44 (q, *J* = 29.8, 28.0 Hz), 127.50, 125.33, 123.16, 120.99, 117.36, 112.63 (d, *J* = 2.9 Hz), 112.57 (d, *J* = 74.6 Hz), 101.91 (d, *J* = 2.6 Hz), 38.99 (d, *J* = 52.5 Hz), 3.36 (d, *J* = 53.0 Hz).

^{31}P NMR (202 MHz, CD_2Cl_2) δ = 18.24.

^{19}F NMR (376 MHz, CD_2Cl_2) δ = -62.86.

^{11}B NMR (160 MHz, CD_2Cl_2) δ = -6.76 (hept, *J* = 2.9 Hz).

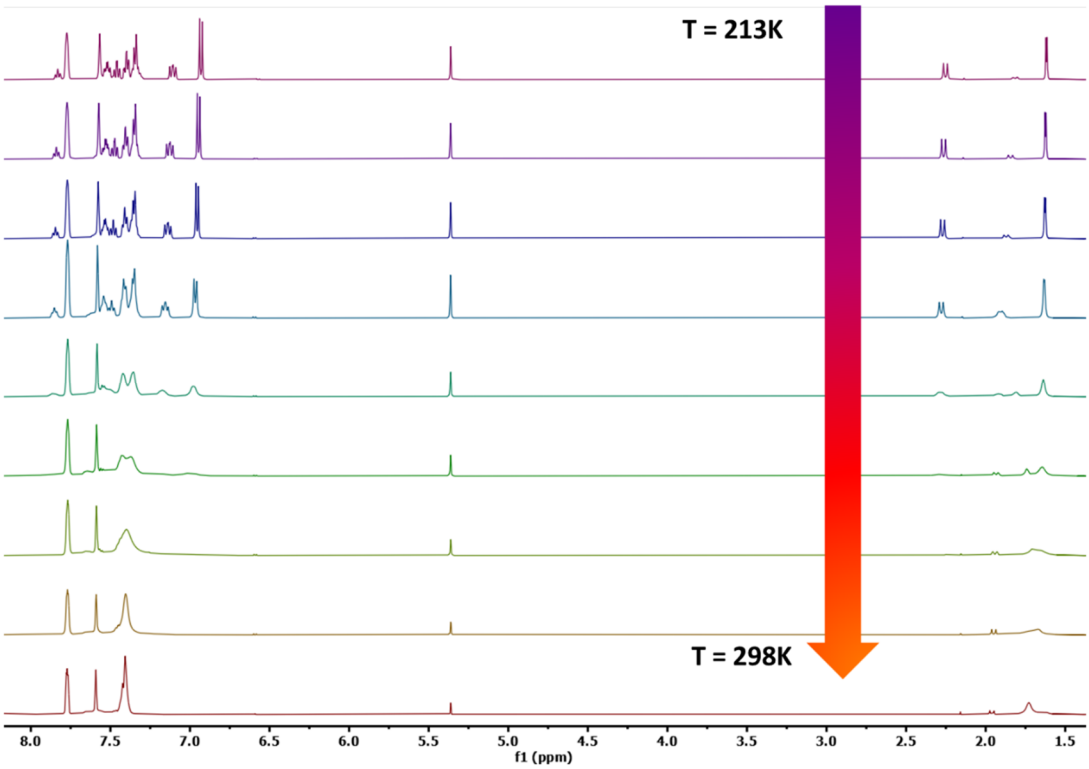

Figure S22: Variable-temperature ^{1}H NMR using 1-BAr$^{F}_{4}$ and 2e in CD_2Cl_2

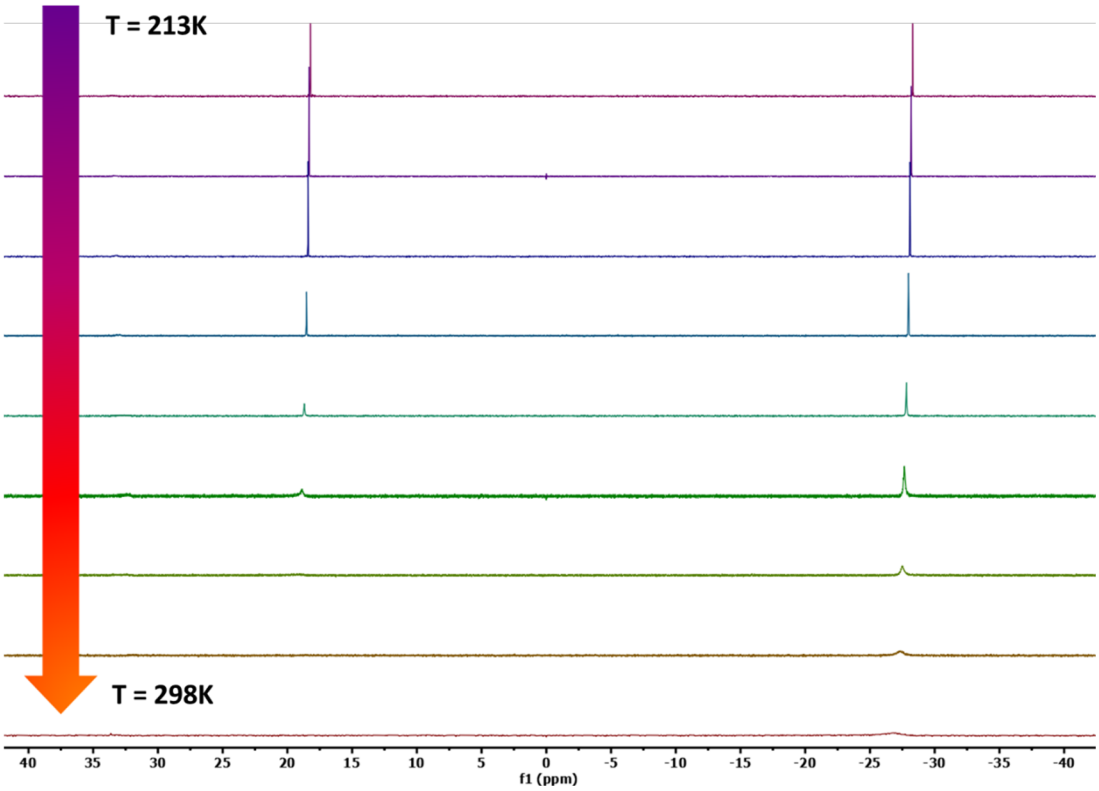

Figure S23: Variable-temperature ^{31}P{^{1}H} NMR using 1-BAr$^{F}_{4}$ and 2e in CD_2Cl_2

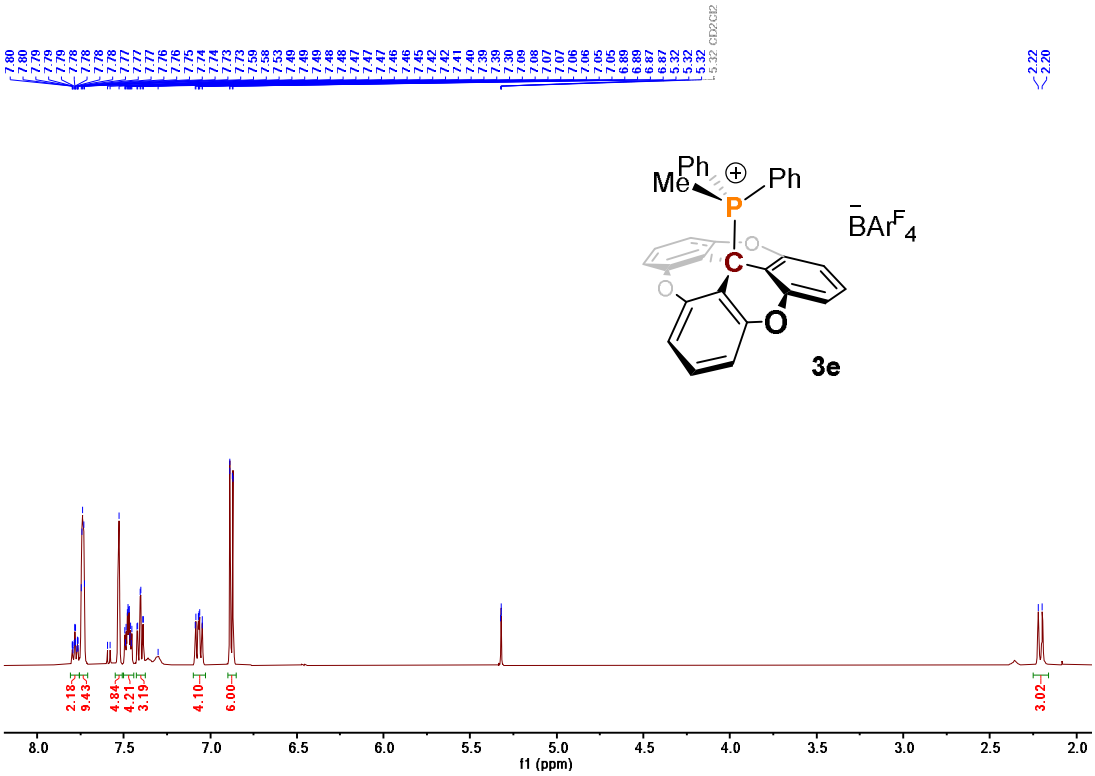

Figure S24: ^{1}H NMR spectrum of 3e in CD_2Cl_2 at -60 ºC

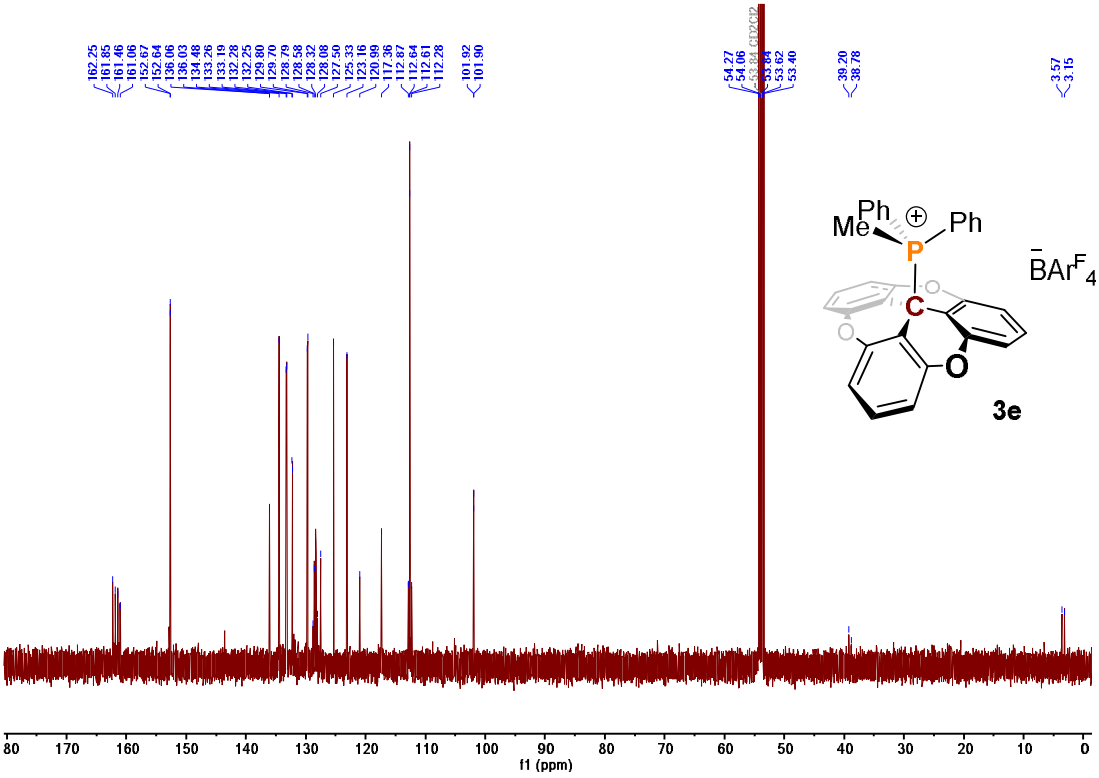

Figure S25: ^{13}C NMR spectrum of 3e in CD_2Cl_2 at -60 ºC

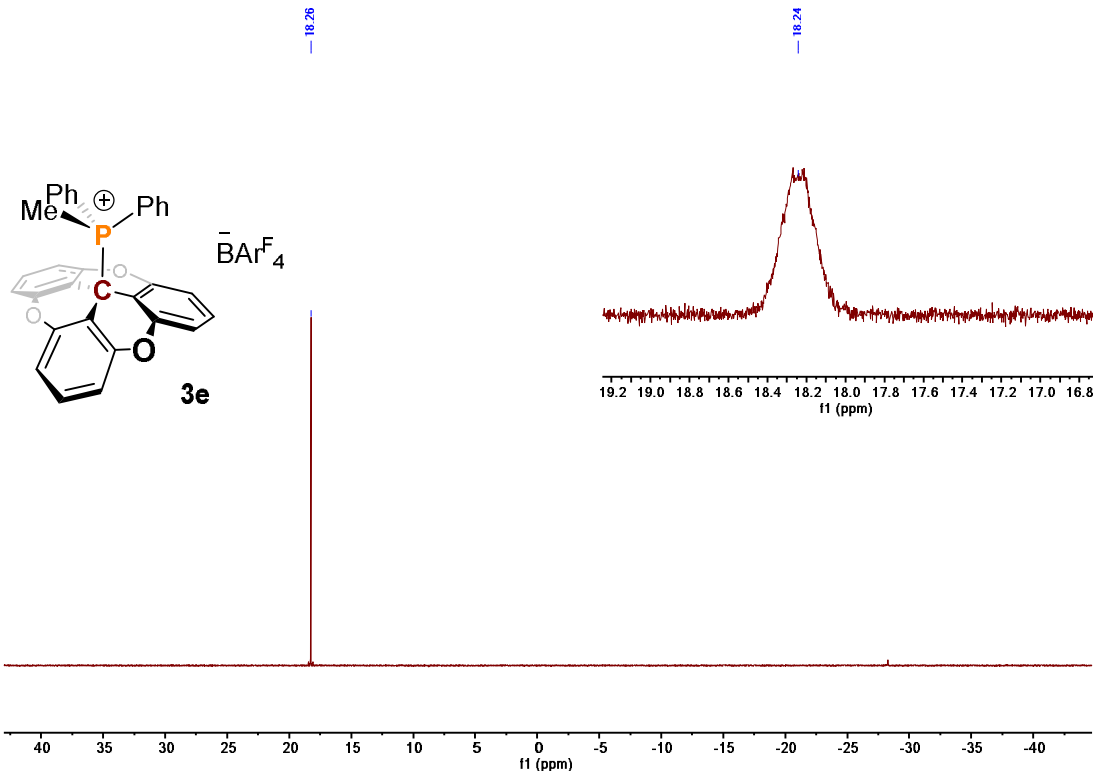

Figure S26: ^{31}P NMR spectrum of 3e in CD_2Cl_2 at -60 ºC

II.2f The reaction between 1-BAr$^F_4$ and Ph_3P:

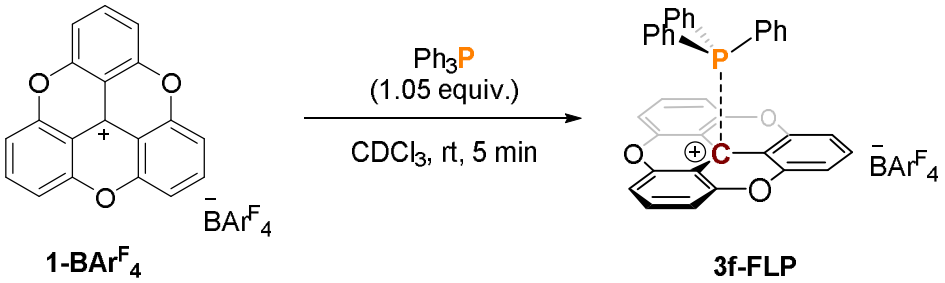

Procedure: In the glove box, a J. Young NMR tube was charged with **1-BAr$^F_4$** (12 mg, 0.010 mmol), PPh_3 (2.7 mg, 0.010 mmol), and $CDCl_3$ (0.5 mL) or CD_3CN (0.5 mL). Then, ^{1}H, ^{19}F, and ^{31}P NMR were recorded at 25˚C followed by lowering the temperature to -40˚C. The broadening of NMR signals noted indicates the $TOTA^+$ and PPh_3 exit as frustrated Lewis pair. No additional peak in ^{31}P NMR is detected, indicates that there is no covalent adduct formation even at a lower temperature. Similarly, VT-experiment for **3f**-FLP was performed in CD3CN.

A mixture of **1-BAr$^F_4$** and PPh_3 in CD_3CN was subjected to ^{1}H-Diffusion Ordered Spectroscopy (DOSY). The data revealed that both **1-BAr$^F_4$** and PPh_3 have almost identical

diffusion constants, supporting the intermolecular interaction between these two species in solution (See Figure S31-32). Semiquantitative spectra were recorded using a 1 s relaxation delay and 800 ms mixing time. Changes in diffusion coefficient noted with mixing excess of either Lewis acid or base.

The values of Diffusion Coefficient (***D***) for the separate components are
1-BAr$^{F}_{4}$ = ~1.42 x 10^{-9} m^2 s^{-1}
PPh_3 = ~1.88 x 10^{-9} m^2 s^{-1}

The values of Diffusion Coefficient (***D***) for upon combination of two species (1-BAr$^{F}_{4}$: PPh_3 = 5:1) are **1-BAr$^{F}_{4}$** = ~1.31 x 10^{-9} m^2 s^{-1}; **PPh_3** = ~1.41 x 10^{-9} m^2 s^{-1}
The values of Diffusion Coefficient (***D***) for upon combination of two species (1-BAr$^{F}_{4}$: PPh_3 = 1:5) are **1-BAr$^{F}_{4}$** = ~1.51 x 10^{-9} m^2 s^{-1} ; **PPh_3** = ~1.52 x 10^{-9} m^2 s^{-1}

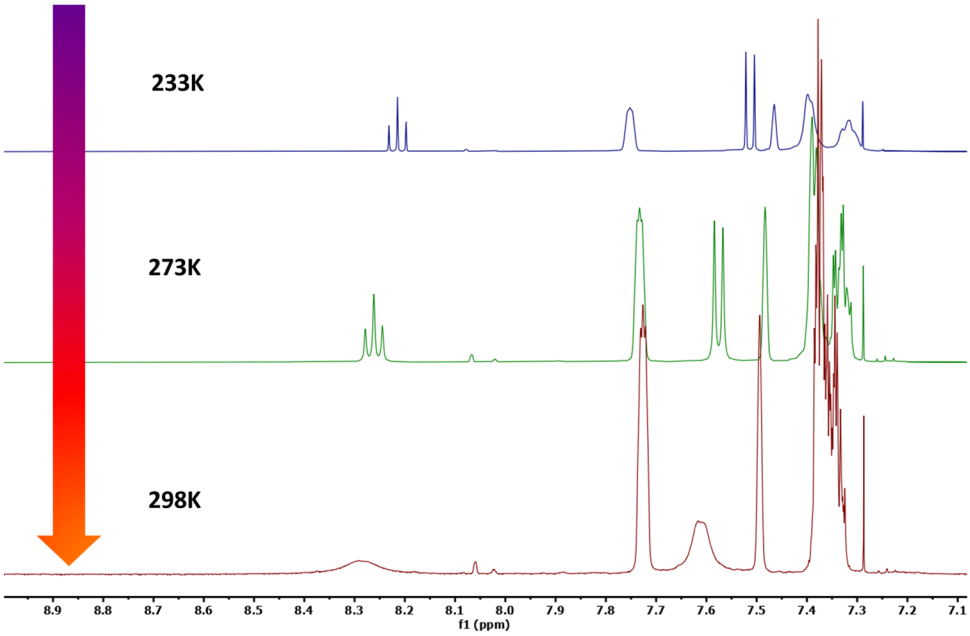

Figure S27. Variable-temperature ^{1}H NMR using 1-BAr$^{F}_{4}$ and 2f in $CDCl_3$

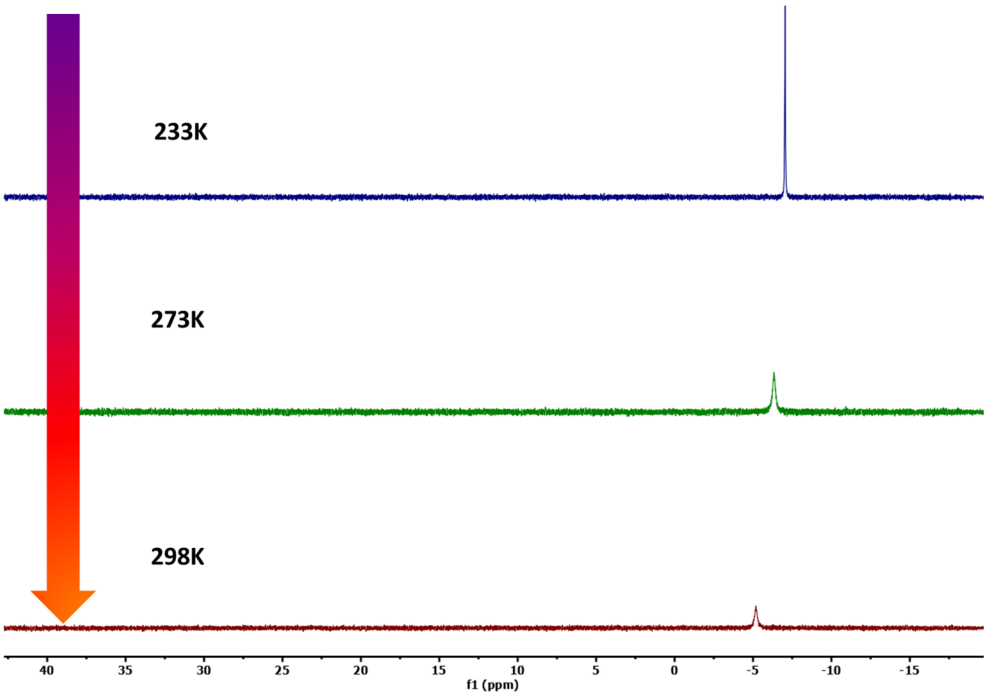

Figure S28. Variable-temperature ^{31}P NMR using 1-BAr$^{F}_{4}$ and 2f in $CDCl_3$

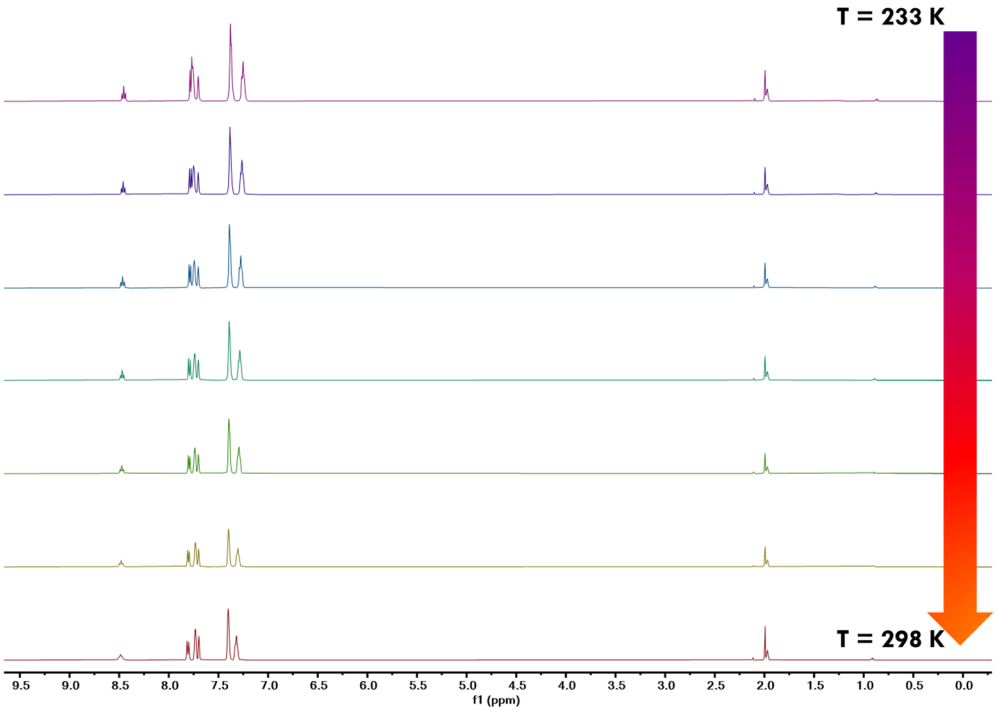

Figure S29. Variable-temperature ^{1}H NMR using 1-BAr$^{F}_{4}$ and 2f in CD_3CN

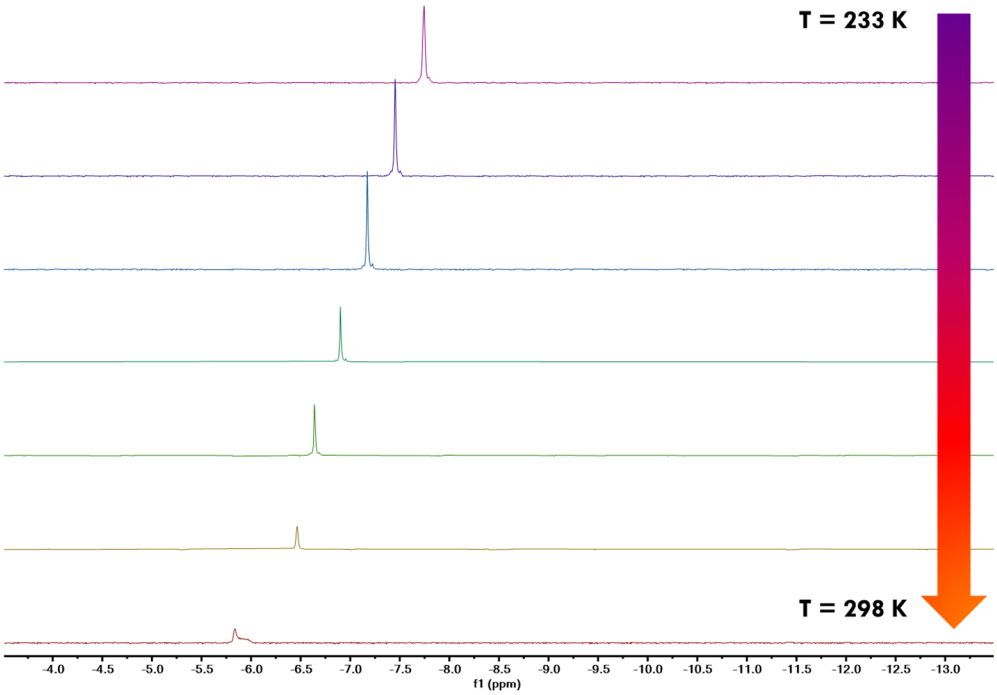

Figure S30. Variable-temperature ^{31}P NMR using 1-BAr$^{F}_{4}$ and 2f in CD_3CN

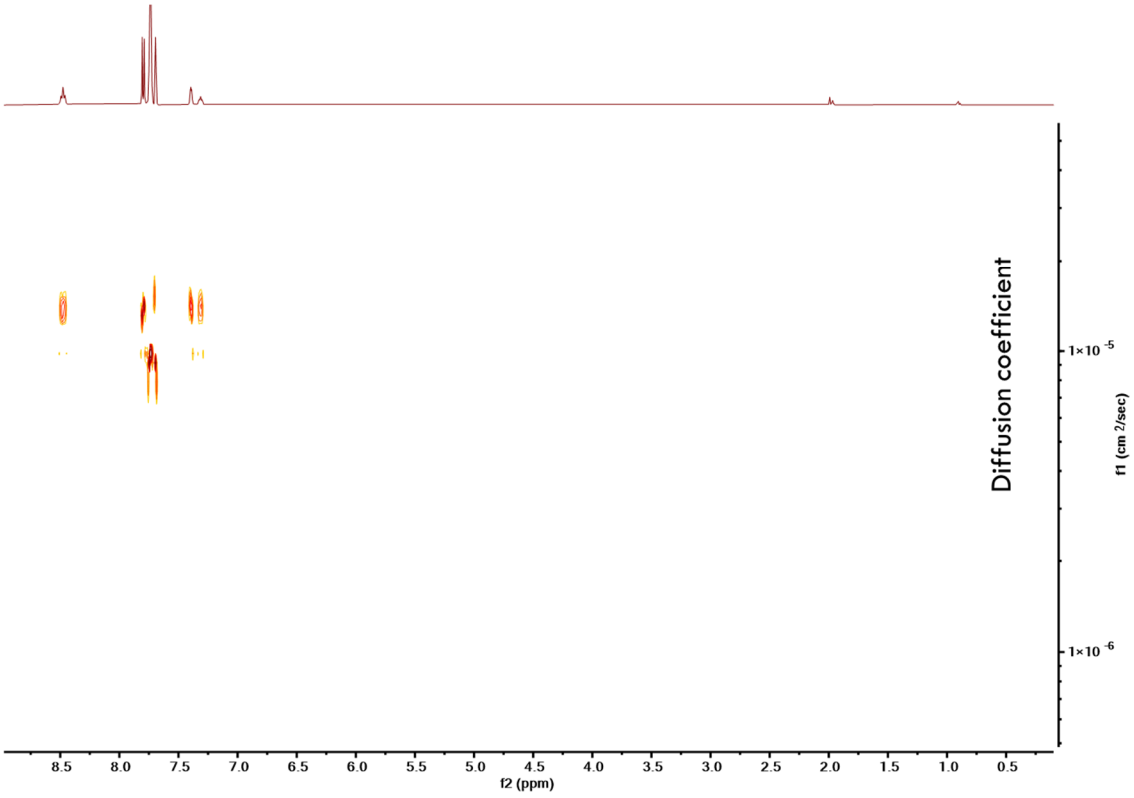

Figure S31. ^{1}H-DOSY experiment using 1-BAr$^{F}_{4}$ and 2f (5:1) in CD_3CN

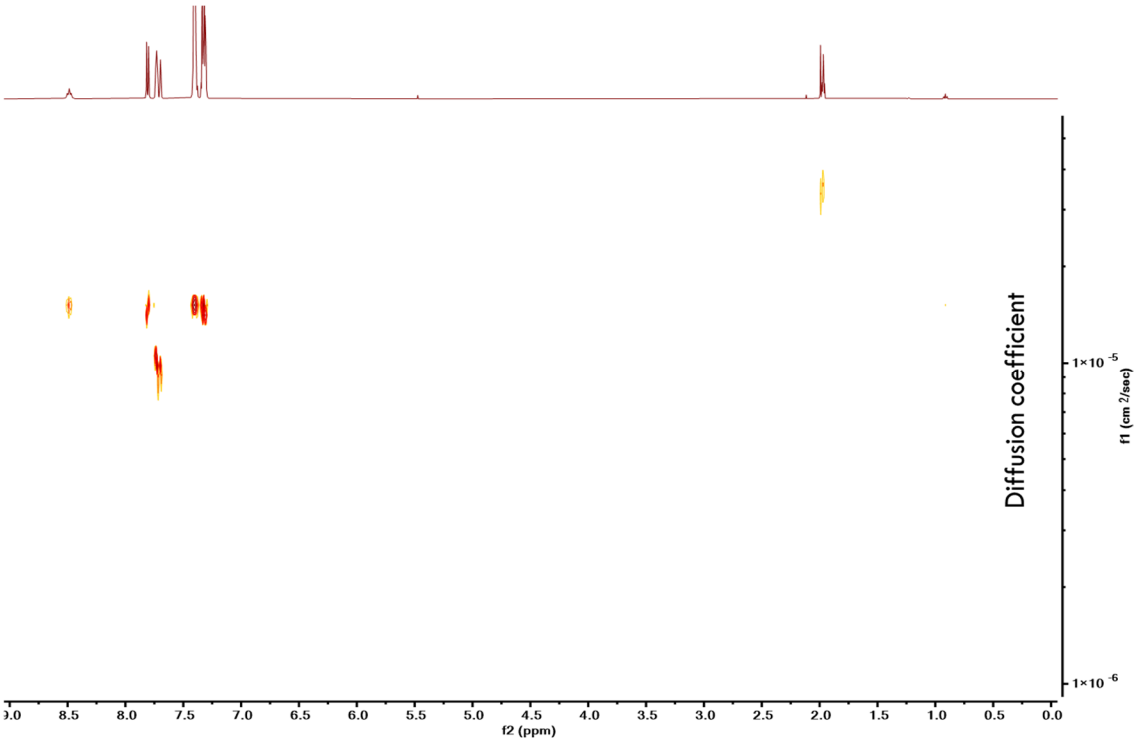

Figure S32. ^{1}H-DOSY experiment using 1-BAr$^{F}_{4}$ and 2f (1:5) in CD$_3$CN

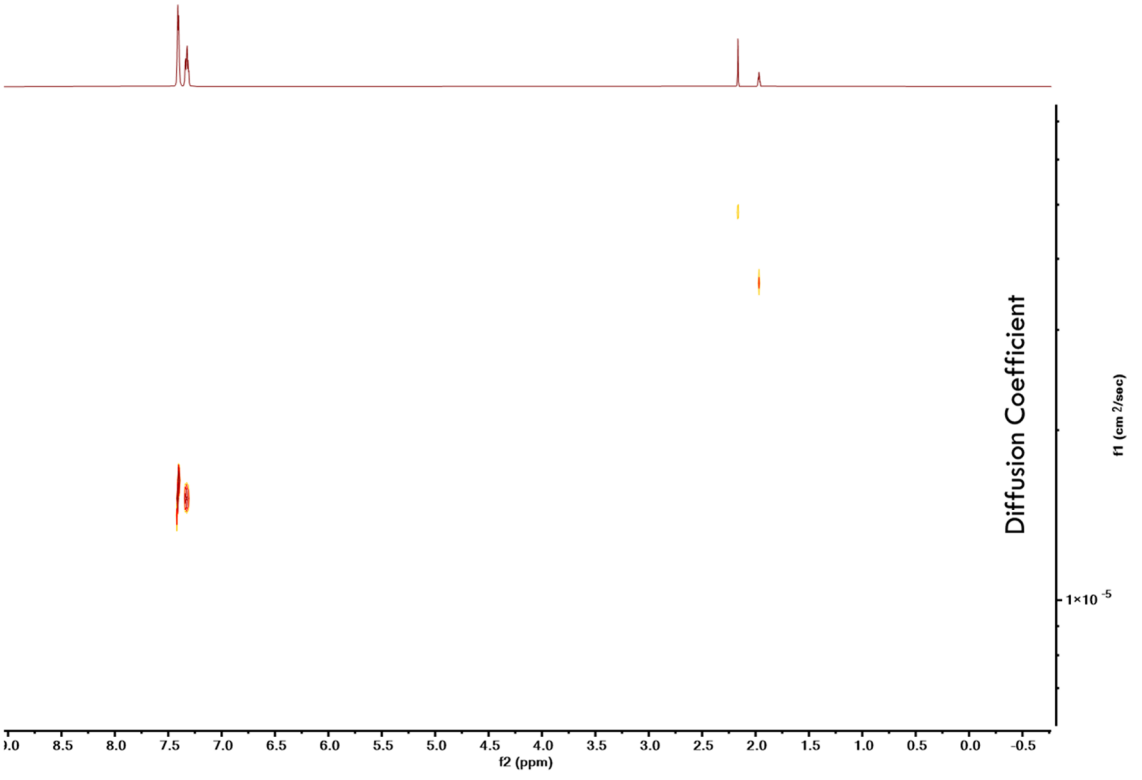

Figure S33. ^{1}H-DOSY experiment using PPh$_3$ (2f) in CD$_3$CN

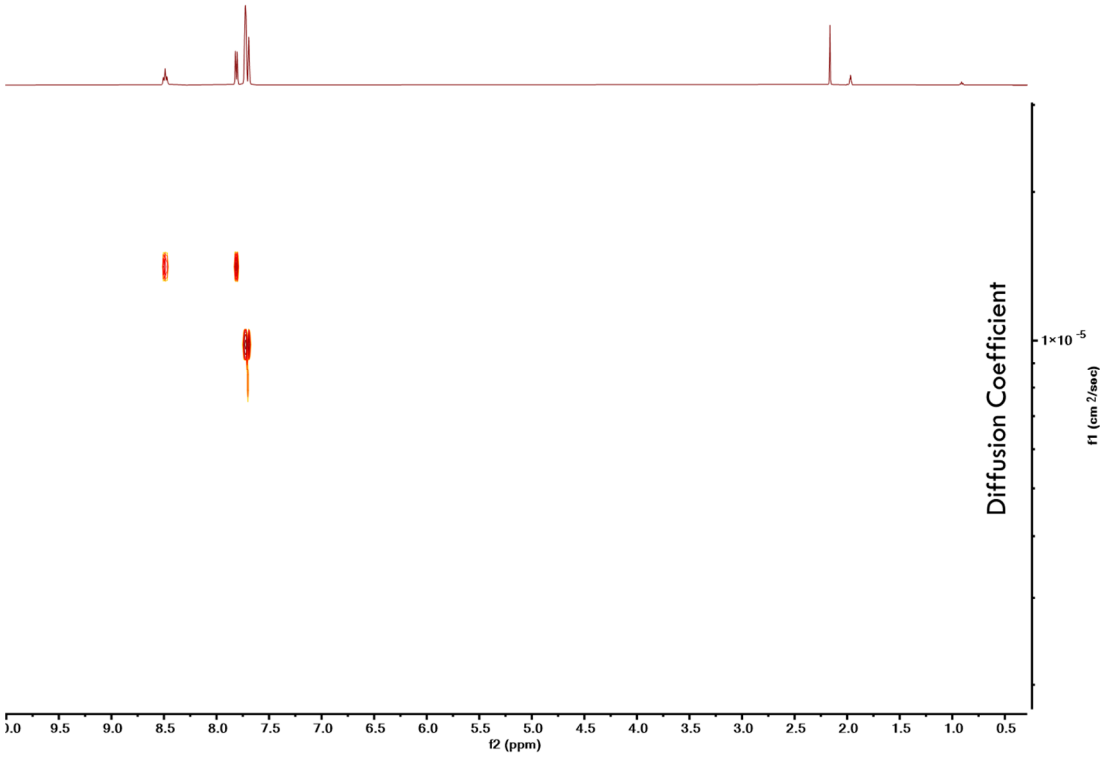

Figure S34. ^{1}H-DOSY experiment using 1-BAr$^{F}_{4}$ in CD$_3$CN

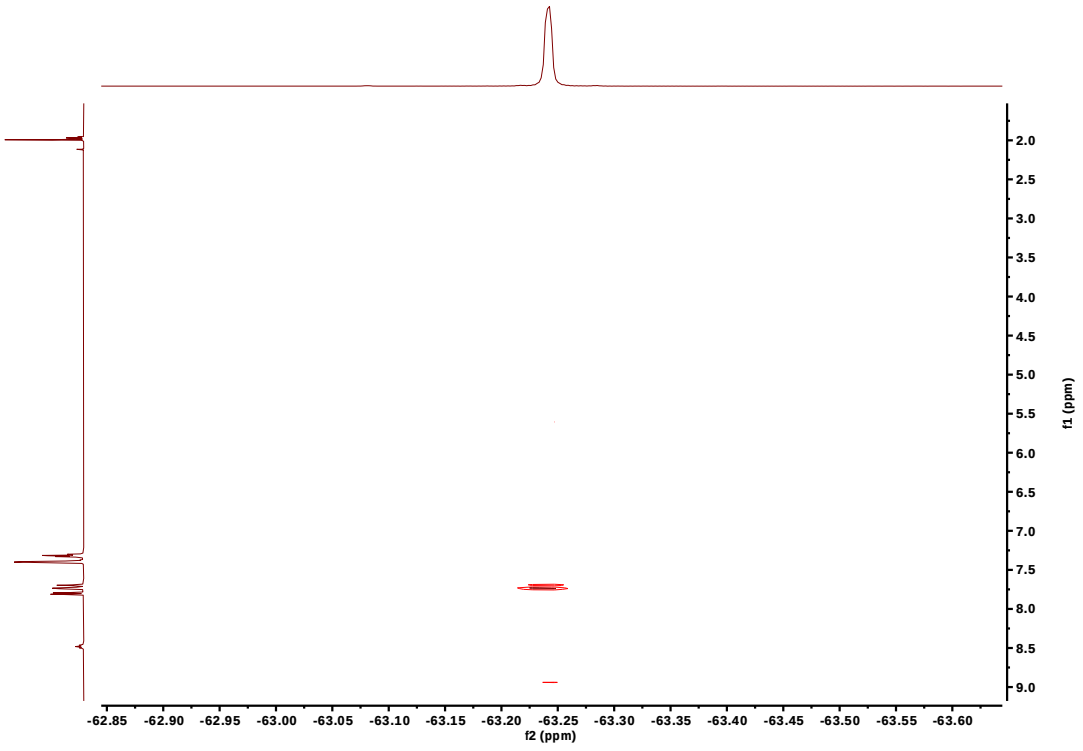

Figure S35. ^{1}H-^{19}F 2-D HOESY NMR spectrum of 1-BAr$^{F}_{4}$ and 2f in CD$_3$CN

II.2g Reaction between 1-BAr$^{F}_{4}$ and ^{t}Bu$_3$P:

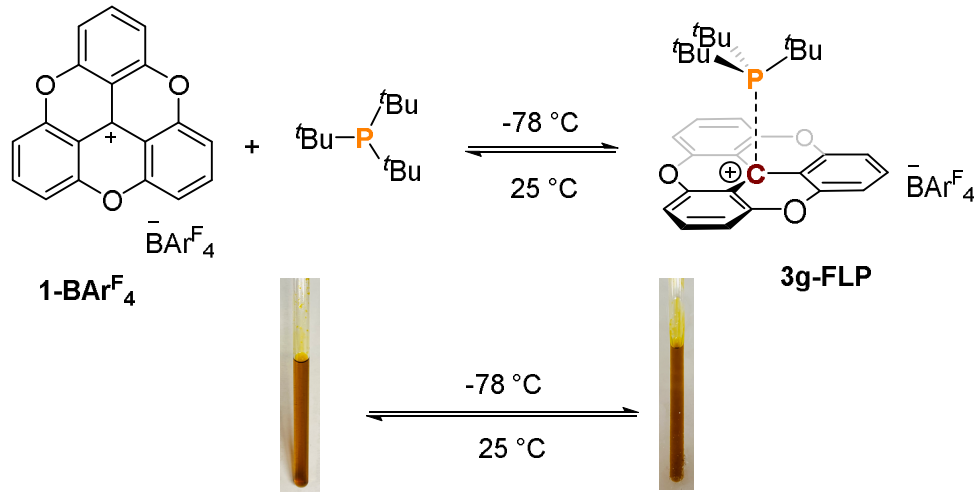

Procedure: In the glove box, a J. Young NMR tube was charged with **1-BAr$^{F}_{4}$** (12 mg, 0.010 mmol), P(^{t}Bu$_3$) (4.0 mg, 0.020 mmol), and CD_2Cl_2 (0.5 mL) or CD_3CN (0.5 mL). Then, ^{1}H, ^{19}F, and ^{31}P NMR were recorded at 25˚C followed by lowering the temperature to -80˚C. NMR spectra were recorded every 10 ˚C. After that, the reaction mixture was warmed to 30 ˚C, and NMR measurements were conducted again. These results are shown in Figure S34. Similarly, VT-experiment for 3g-FLP was performed in CD_3CN.

No additional signals were observed in ^{1}H, ^{13}C, or ^{31}P NMR spectroscopy, even at –80°C, showing that no covalent Lewis adduct was formed. The broadening and coalescence of the TOTA^{+} aromatic peaks and ^{t}butyl group of phosphine indicated that only a weak van der Waals adduct is formed, as observed in the case of Frustrated Lewis pairs derived from B(C_6F_5)$_3$ and P(*o*-tolyl)$_3$, PMes$_3$, or P(^{t}Bu$_3$).[5] At low temperature, the spectrum shows a sharp resonance at (d = 56.0 ppm, -60˚C) as compared to room temperature. Also, it should be noted that the ^{31}P NMR resonance for P(^{t}Bu$_3$) also moves by c.a. Dd = 1 ppm over the same temperature range and the behaviour is likely due to a temperature-induced shift for both species.

A mixture of **1-BAr$^{F}_{4}$** and P(^{t}Bu)$_3$ in CD_3CN was subjected to 1H-Diffusion Ordered Spectroscopy (DOSY). The data revealed that both **1-BAr$^{F}_{4}$** and P(^{t}Bu)$_3$ have almost identical diffusion constants, supporting the inter-molecular interaction between these two species in solution (See Figure S41). Semiquantitative spectra were recorded using a 1 s relaxation delay and 800 ms mixing time.

The values of Diffusion Coefficient (***D***) for the separate components are

1-BAr$^{F}_{4}$ = ~1.42 x 10^{-9} m^2 Sec^{-1}

P(^{t}Bu)$_3$ = ~1.88 x 10^{-9} m^2 Sec^{-1}

The values of Diffusion Coefficient (***D***) for upon combination of two species are

1-BAr$^{F}_{4}$ = ~1.80 x 10^{-9} m^2 Sec^{-1}

P(^{t}Bu)$_3$ = ~1.75 x 10^{-9} m^2 Sec^{-1}

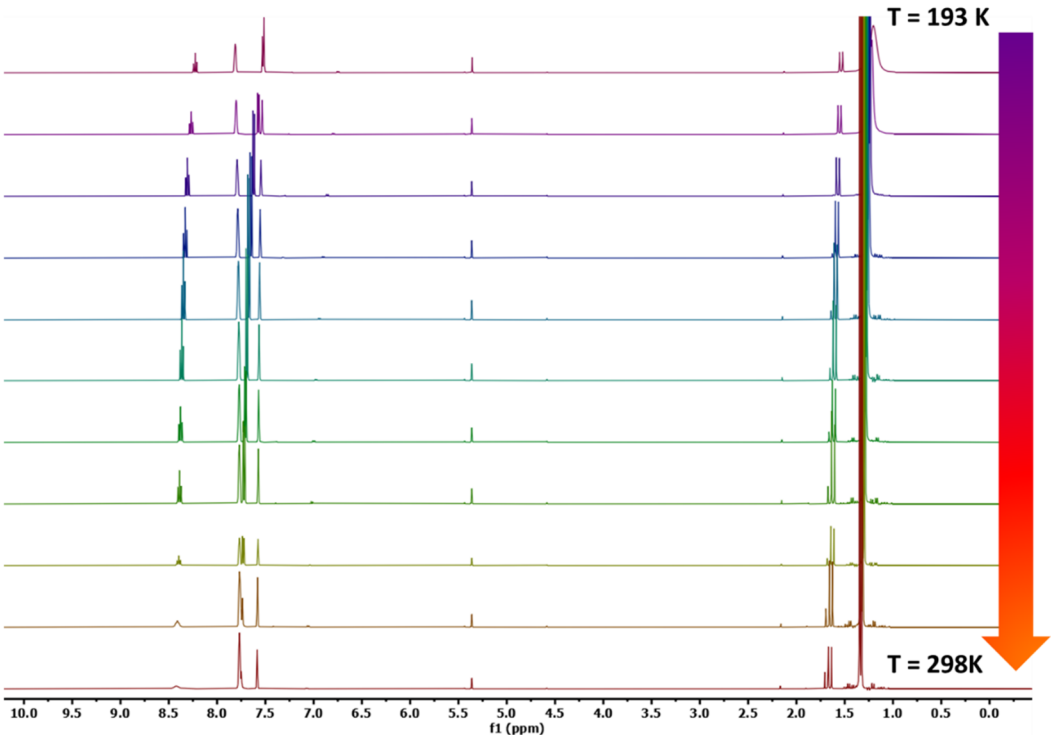

Figure S36. Variable-temperature ^{1}H NMR using 1-BAr$^{F}_{4}$ and 2g in CD_2Cl_2

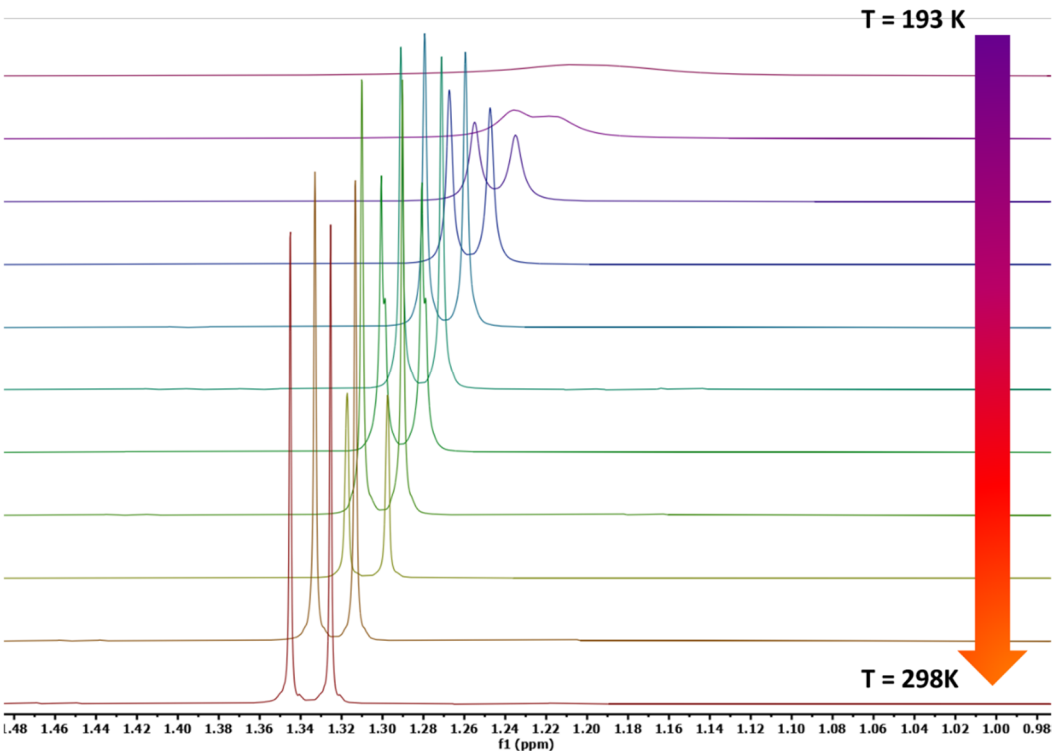

Figure S37. Variable-temperature ^{1}H NMR (zoom section for ^{t}butyl group)

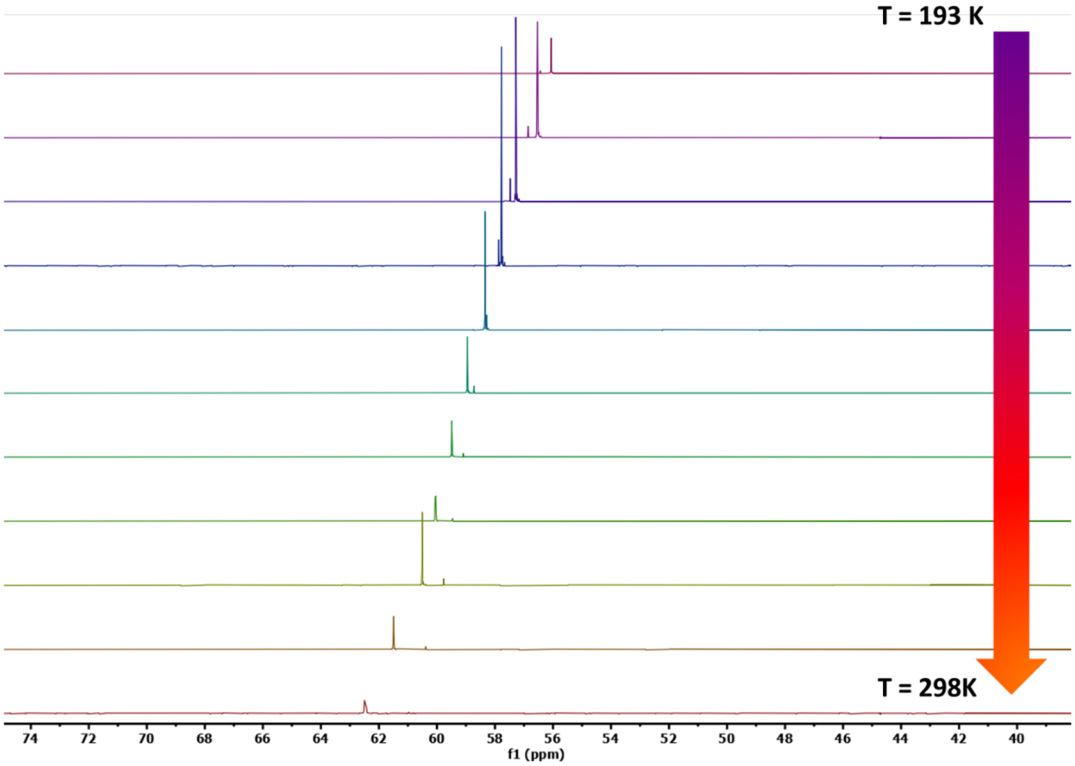

Figure S38. Variable-temperature ^{31}P NMR using 1-BAr$^{F}_{4}$ and 2g in CD_2Cl_2

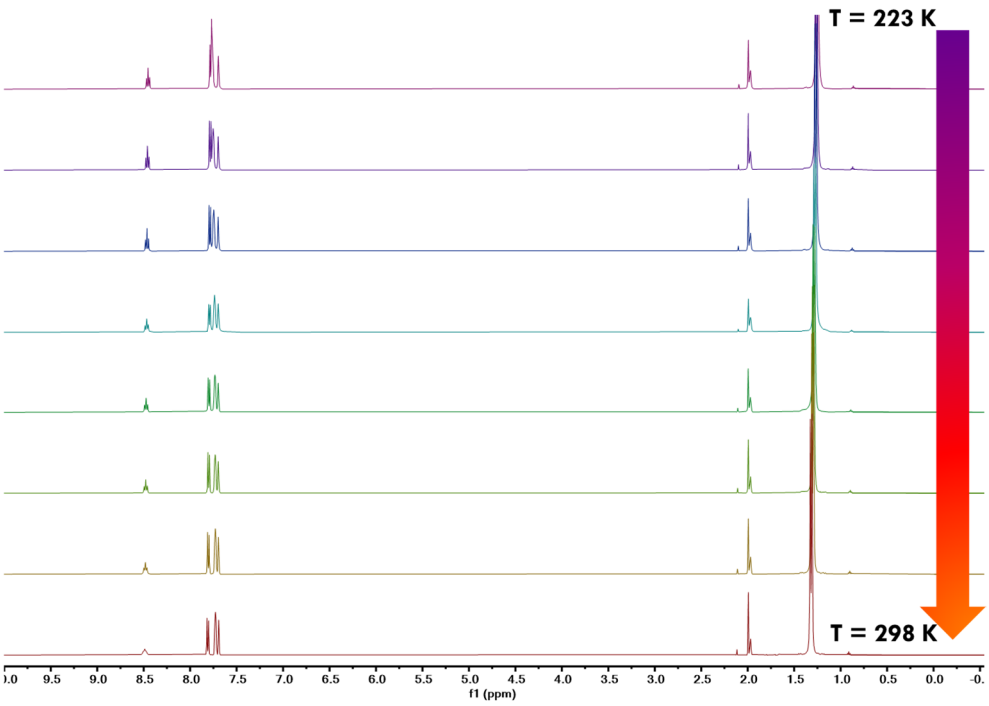

Figure S39. Variable-temperature ^{1}H NMR using 1-BAr$^{F}_{4}$ and 2g in CD_3CN

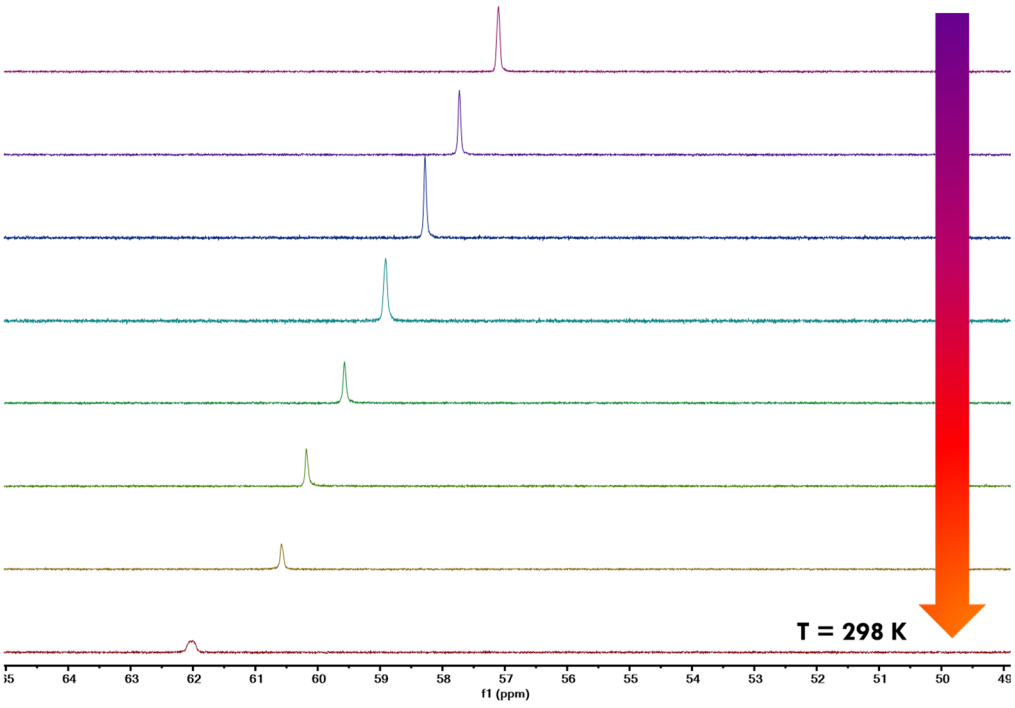

Figure S40. Variable-temperature ^{31}P NMR using 1-BAr$^{F}_{4}$ and 2g in CD_3CN

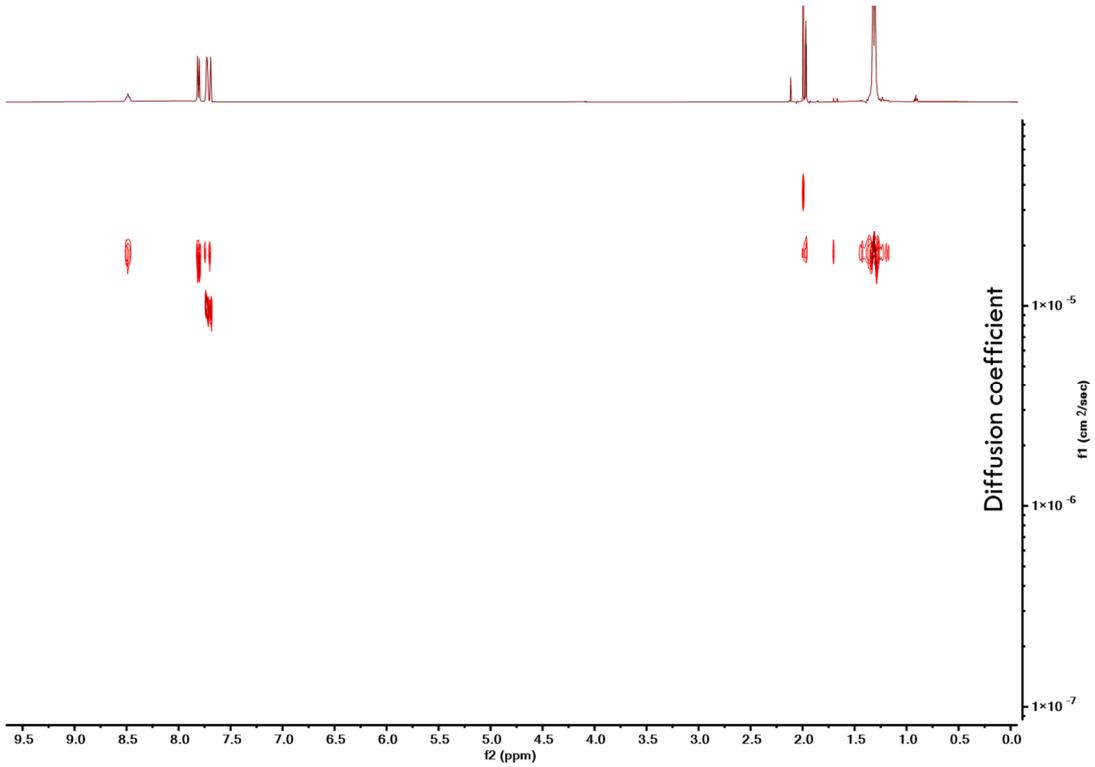

Figure S41. ^{1}H-DOSY experiment using 1-BAr$^{F}_{4}$ and 2g in CD_3CN (Bayesian method)

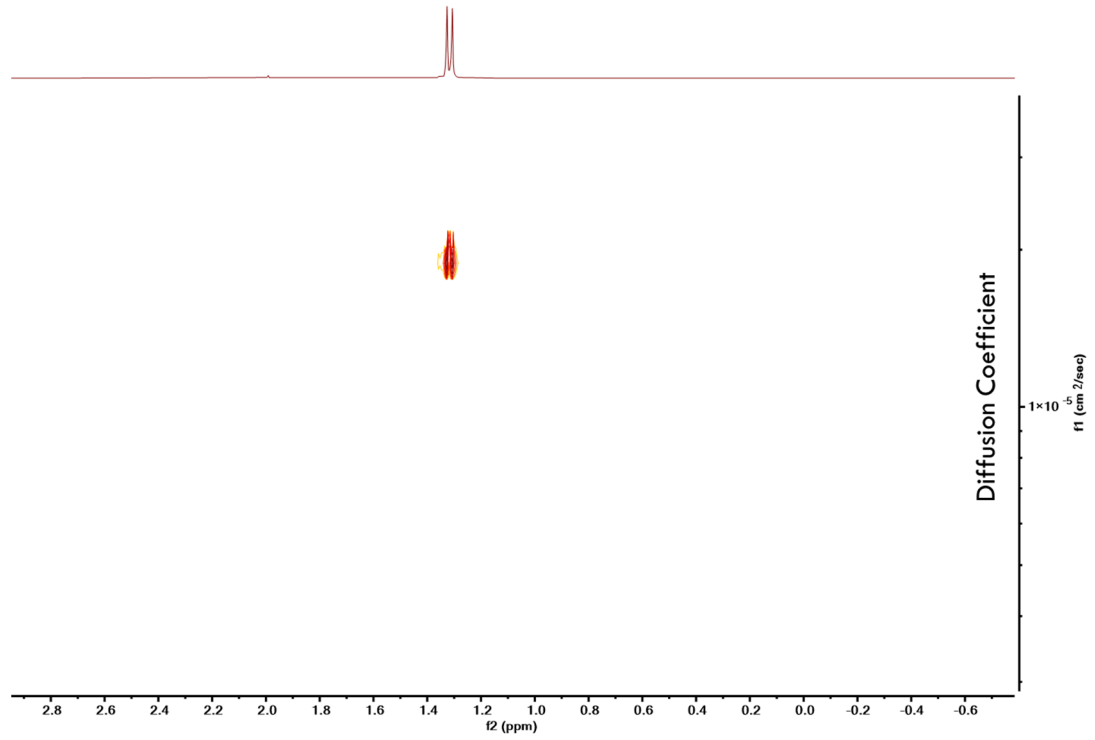

Figure S42. ^{1}H-DOSY experiment using P(^{t}Bu)$_3$ (2g) in CD_3CN

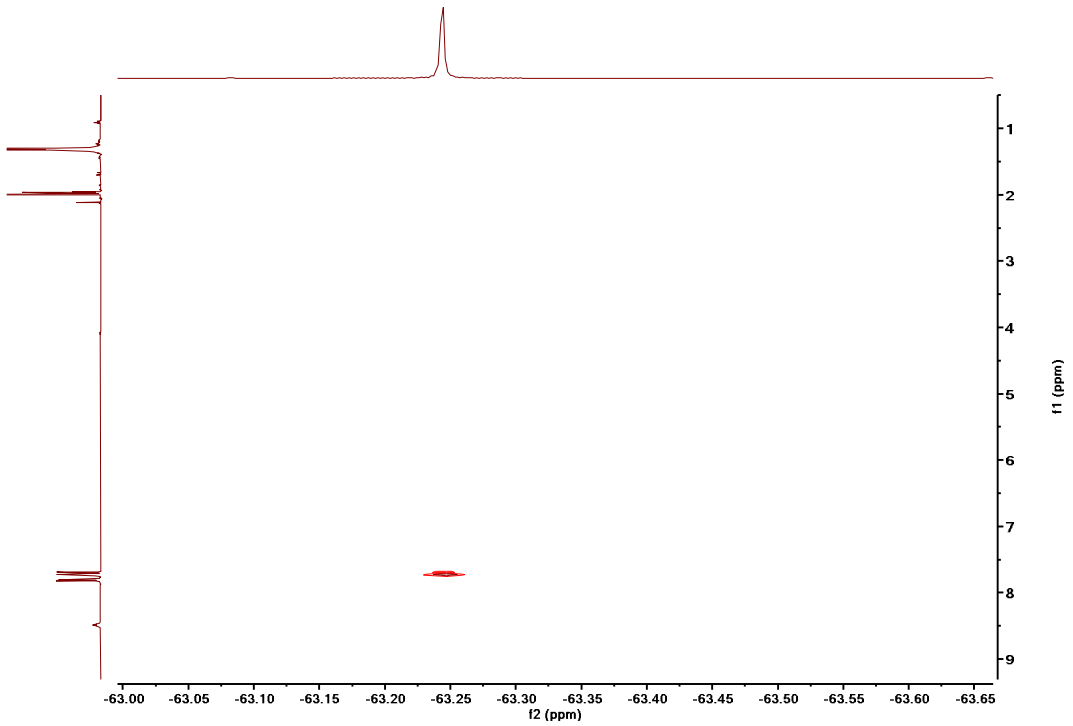

Figure S43. ^{1}H-^{19}F 2-D HOESY NMR spectrum of 1-BAr$^{F}_{4}$ and 2g in CD_3CN

II.3 Frustrated Lewis pair mediated disulfide bond cleavage

II.3a Reaction between 1-BF_4/$^{t}Bu_3P$ and diphenyl disulfide:

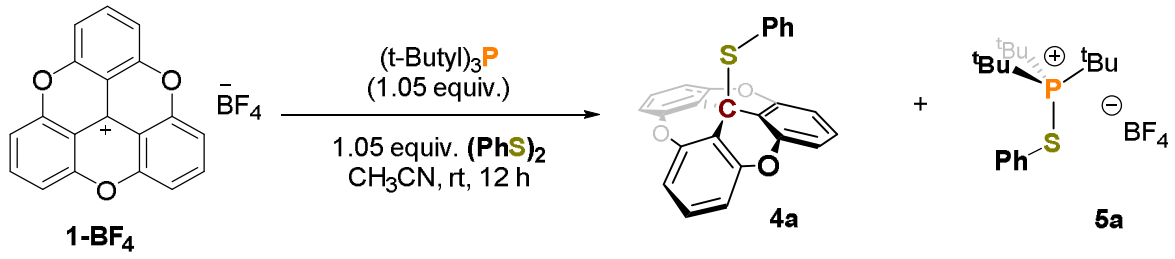

Representative Procedure: A acetonitrile solution (1 mL) of diphenyl disulfide (27 mg, 0.01 mmol) was added to an acetonitrile solution (2 mL) of **1-BF_4** (37.2 mg, 0.01 mmol) and P(^{t}Bu)$_3$ (21 mg, 0.01 mmol), and the solution stood at room temperature for overnight. The solution was concentrated by half under vacuum, and 4 mL of *n*-pentane was added with vigorous stirring which induced precipitation of a solid. After decanting the supernatant, the precipitate was washed with *n*-pentane (3 x 4 mL) and dried under vacuum to give tri-*tert*-butyl(phenylthio)phosphonium tetrafluoroborate (**5a**) as a pale yellow solid (33 mg, 89%

yield). The *n*-pentane washings were combined and evaporated under vacuum to give a white solid. The solid was recrystallized in *n*-pentane solution at -20 °C to give off white crystals, and the crystals were dried under vacuum to give Trioxo-triangulium phenyl sulfide as an off white solid (**4a**, 31 mg, 79% yield). Single crystals of **5a** were obtained by slow diffusion of *n*-pentane into a dichloromethane solution at -20°C.

Note: We attempted the disulfide cleavage in wet acetonitrile using **1-BF$_4$**/P(^{t}Bu)$_3$ (0.01mmol) and it works excellent, giving TOTA-SPh adduct (92% yield) and thio-phosphonium salt in 94% yield. (See crude NMR figure S48, NMR yield are given with internal standard 2,4,6 trimethoxy benzene).

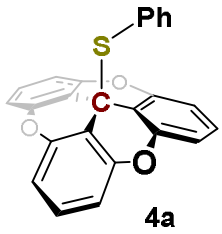

4a

3a^2-(phenylthio)-3a^2*H*-4,8,12-trioxadibenzo[*cd,mn*]pyrene (5a):

Off white solid; **MP** = 160-162 ºC (decomposed; colour change noted)

^{1}H NMR (400 MHz, CDCl$_3$) δ = 7.42 – 7.33 (m, 1H), 7.31 – 7.21 (m, 3H), 7.15 – 7.04 (m, 2H), 6.86 (d, *J* = 8.3 Hz, 6H), 6.83 – 6.76 (m, 2H).

^{13}C NMR (100 MHz, CDCl$_3$) δ = 152.42, 137.77, 131.04, 129.96, 129.12, 128.42, 111.28, 109.82, 40.95. **HRMS (ESI) m/z**: $[M+H]^+$ Calcd. for $C_{25}H_{15}O_3S$ 395.0736; Found: 395.0750. Major fragmentation for TOTA$^+$ $[M^+-C_6H_5S]$ 285.0545 is noted.

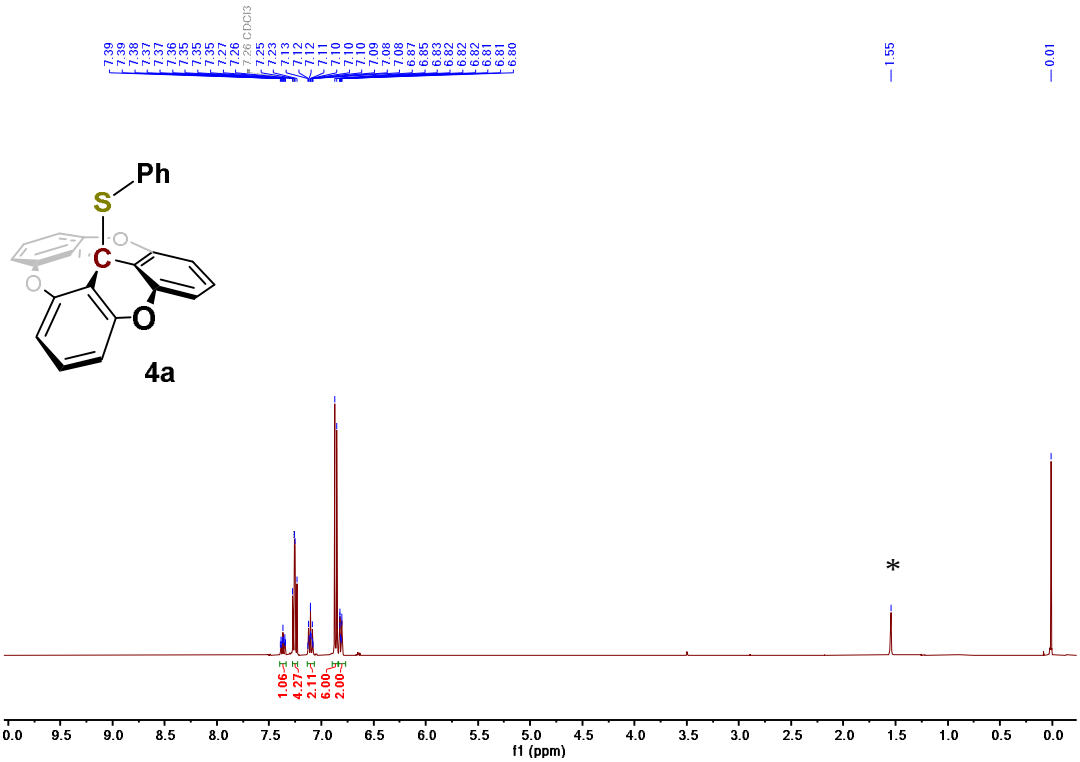

Figure S44: ^{1}H NMR spectrum of 4a in $CDCl_3$ (* indicates residual water)

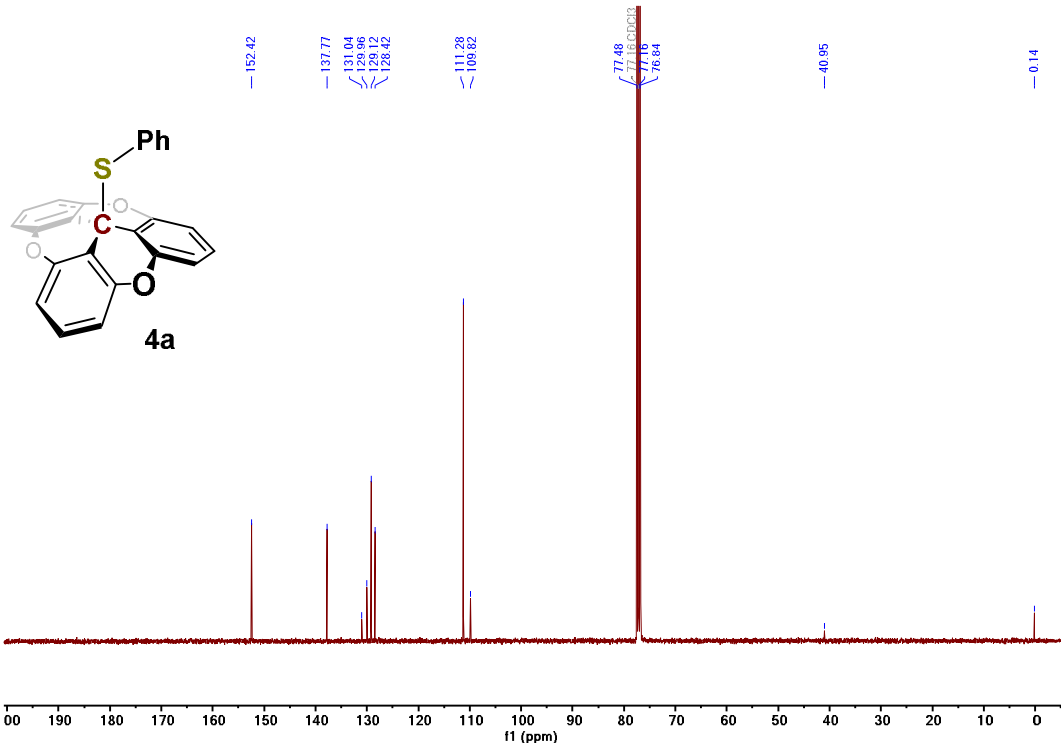

Figure S45: ^{13}C NMR spectrum of 4a in $CDCl_3$

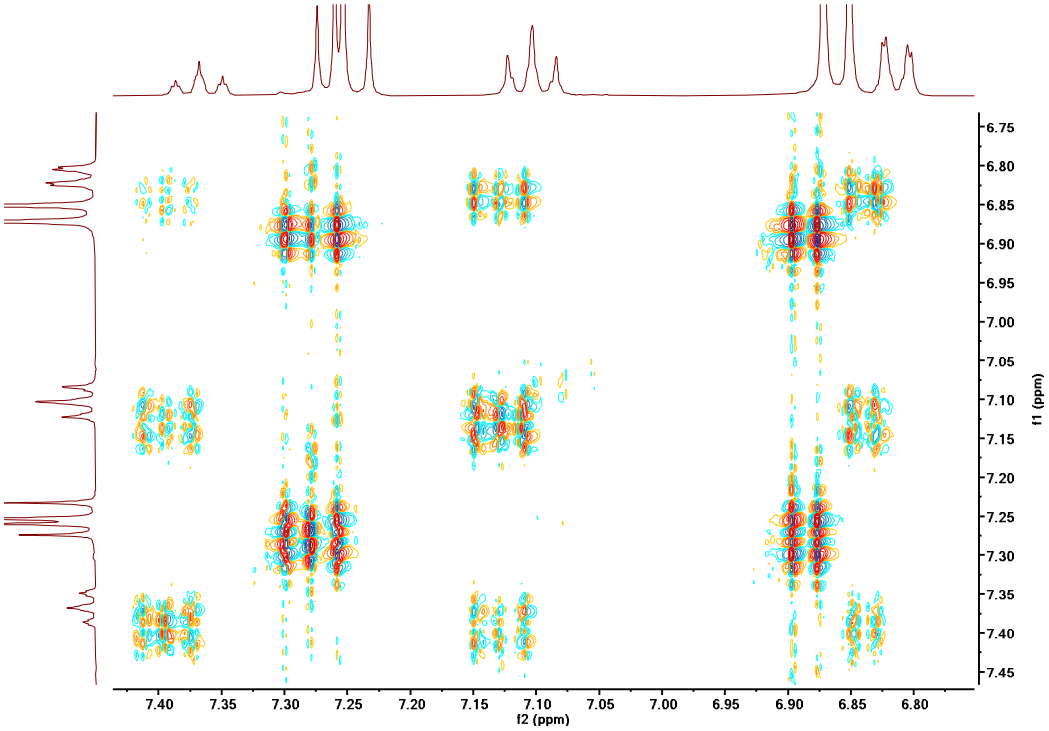

Figure S46: ^{1}H-^{1}H COSY spectrum of 4a in $CDCl_3$ (zoomed aromatic section)

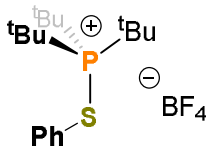

5a

tri-*tert*-butyl(phenylthio)phosphonium tetrafluoroborate (5a):[6]

^{1}H NMR (400 MHz, CD_2Cl_2) δ = 7.88 (dt, *J* = 8.5, 1.4 Hz, 2H), 7.67 – 7.54 (m, 1H), 7.52 (ddd, *J* = 8.4, 7.3, 1.2 Hz, 2H), 1.70 (d, *J* = 15.9 Hz, 27H).

^{13}C NMR (101 MHz, CD_2Cl_2) δ = 138.31 (d, *J* = 3.0 Hz), 132.84 (d, *J* = 2.6 Hz), 131.11 (d, *J* = 2.2 Hz), 121.88 (d, *J* = 9.9 Hz), 46.31 (d, *J* = 15.1 Hz), 30.83.

^{31}P NMR (162 MHz, CD_2Cl_2) δ = 85.23, (ddq, *J* = 47.8, 31.4, 16.0, 15.6 Hz).

^{19}F NMR (376 MHz, CD_2Cl_2) δ = -152.93 (d, *J* = 19.6 Hz).

^{11}B NMR (160 MHz, CD_2Cl_2) δ = -0.96 (d, *J* = 1.0 Hz).

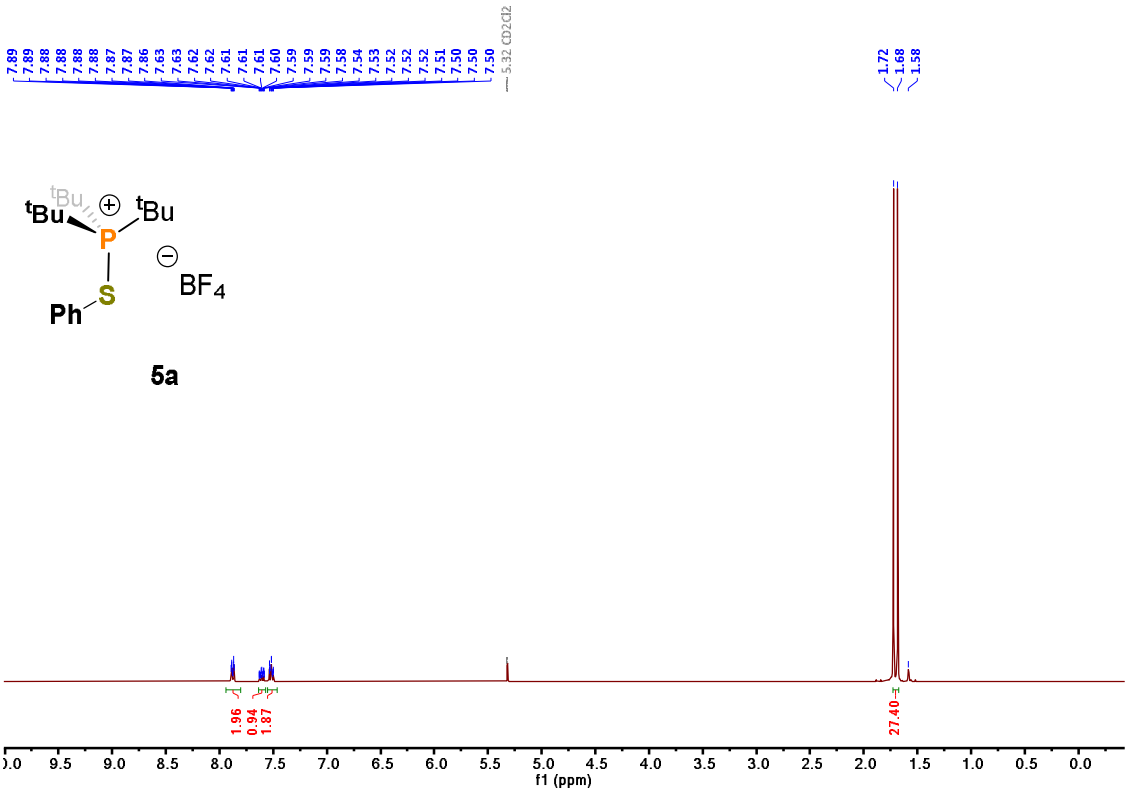

Figure S47: ^{1}H NMR spectrum of 5a in CD_2Cl_2

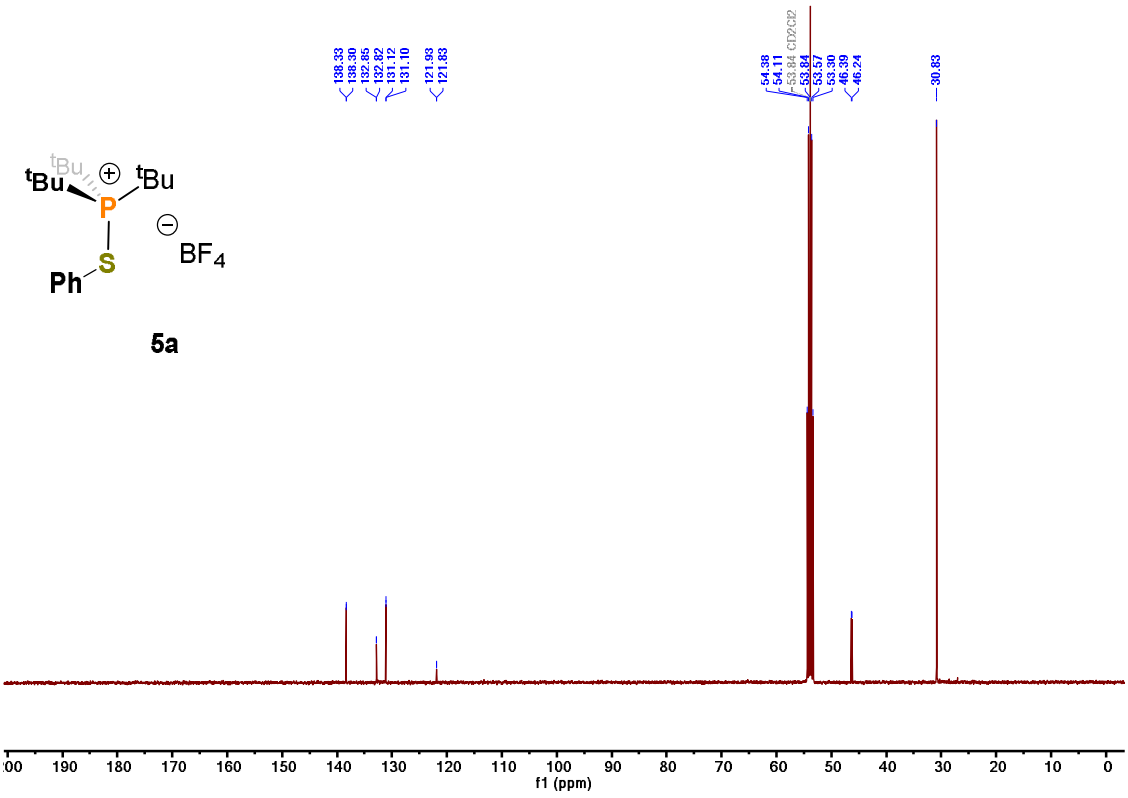

Figure S48: ^{13}C NMR spectrum of 5a in CD_2Cl_2

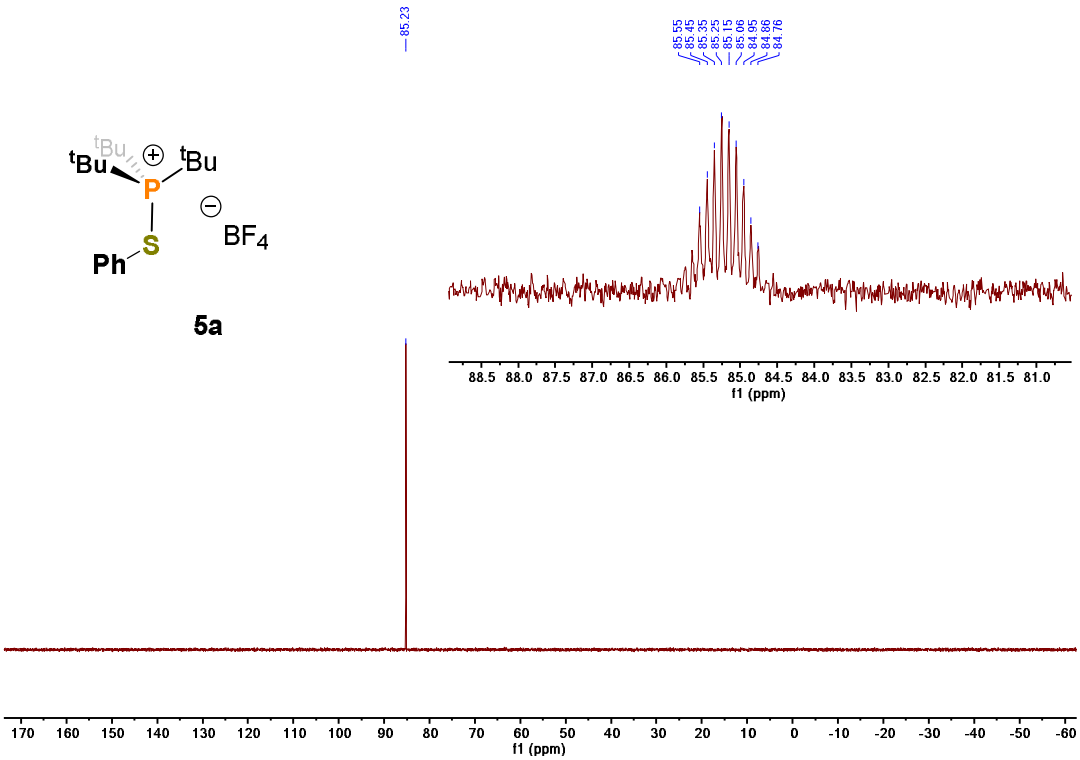

Figure S49: ^{31}P NMR spectrum of 5a in CD_2Cl_2

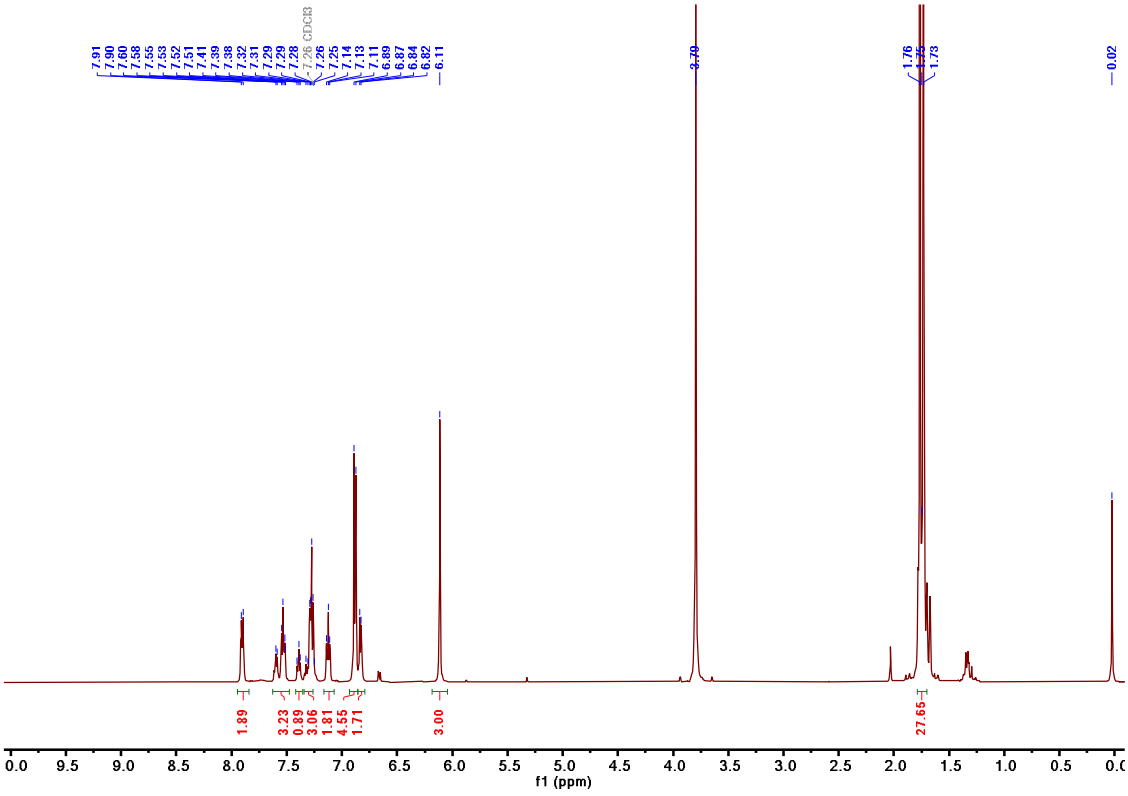

Figure S50: ^{1}H NMR spectrum of crude reaction for S-S cleavage in wet CH_3CN

II.3b. Reaction between 1-BF_4/^{t}Bu$_3$P and di-*p*-tolyl disulfide:

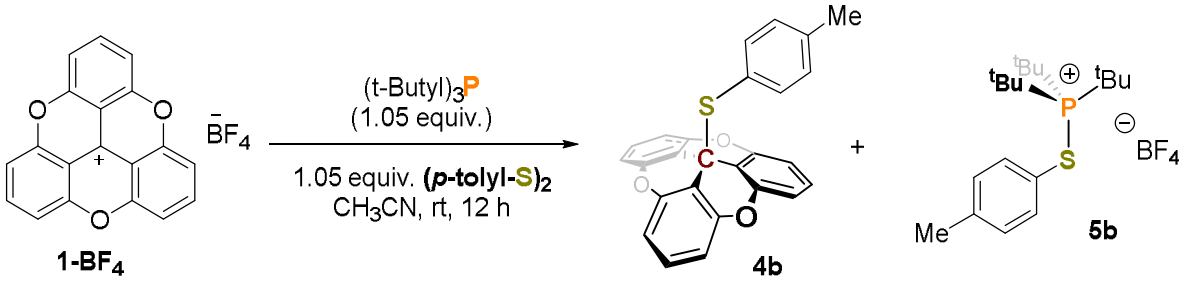

Following the representative procedure by using **1-BF_4** (37.2 mg, 0.1 mmol), tri-*ter*-butylphosphine (20.2 mg, 0.1 mmol) and *p*-tolyl disulphide (24.6 mg, 0.1 mmol) as starting materials.

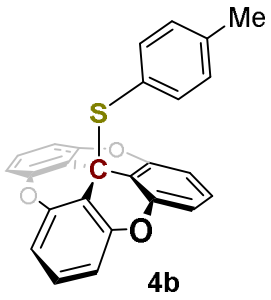

3a^2-(*p*-tolylthio)-*3a^{2}H*-4,8,12-trioxadibenzo[*cd,mn*]pyrene (6b):

Colourless solid, 32 mg, 80% yield; **MP =** 172-174 ºC;

^{1}H NMR (400 MHz, $CDCl_3$) δ = 7.25 (t, *J* = 8.2 Hz, 3H), 6.96 – 6.88 (m, 2H), 6.86 (d, *J* = 8.3 Hz, 6H), 6.69 (d, *J* = 8.0 Hz, 1H), 2.35 (s, 3H).

^{13}C NMR (101 MHz, $CDCl_3$) δ = 152.41, 140.21, 137.55, 129.25, 129.03, 127.57, 111.25, 109.92, 40.66, 21.60.

HRMS (ESI) m/z: $[M+H]^+$ Calcd. for $C_{26}H_{17}O_3S$ 409.0892; Found: 409.0899. Major fragmentation for TOTA$^+$ $[M^+-C_7H_7S]$ 285.0545 is noted.

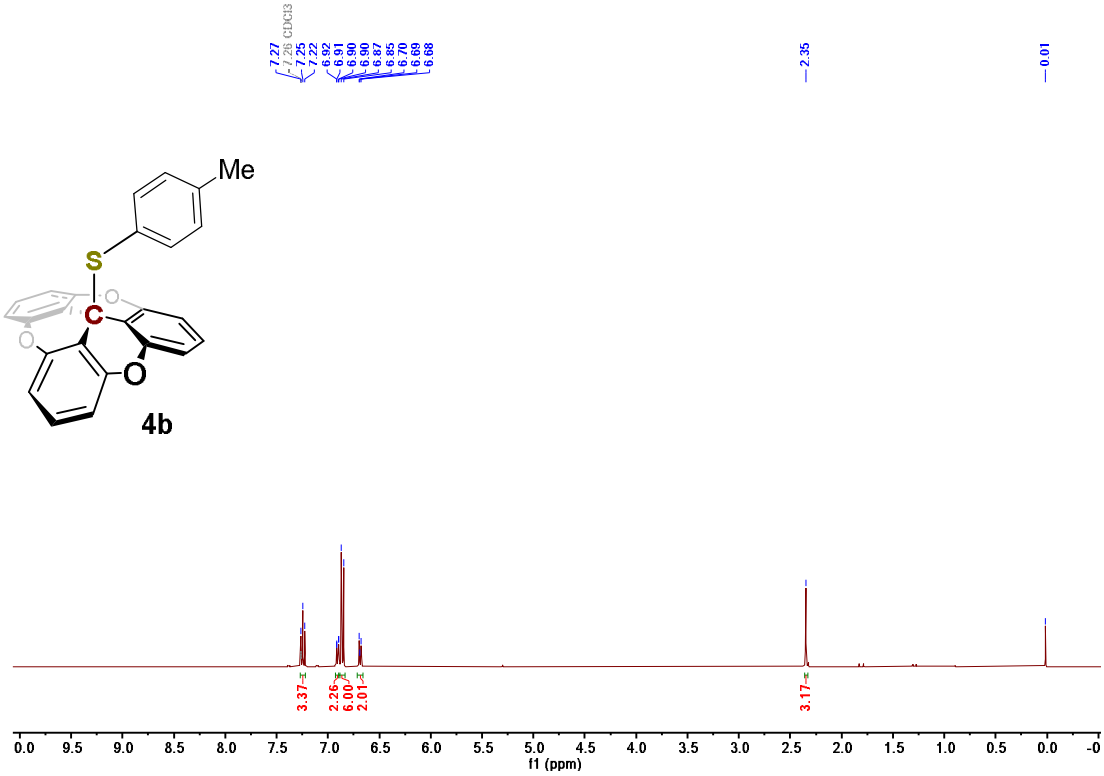

Figure S51: ^{1}H NMR spectrum of 4b in $CDCl_3$

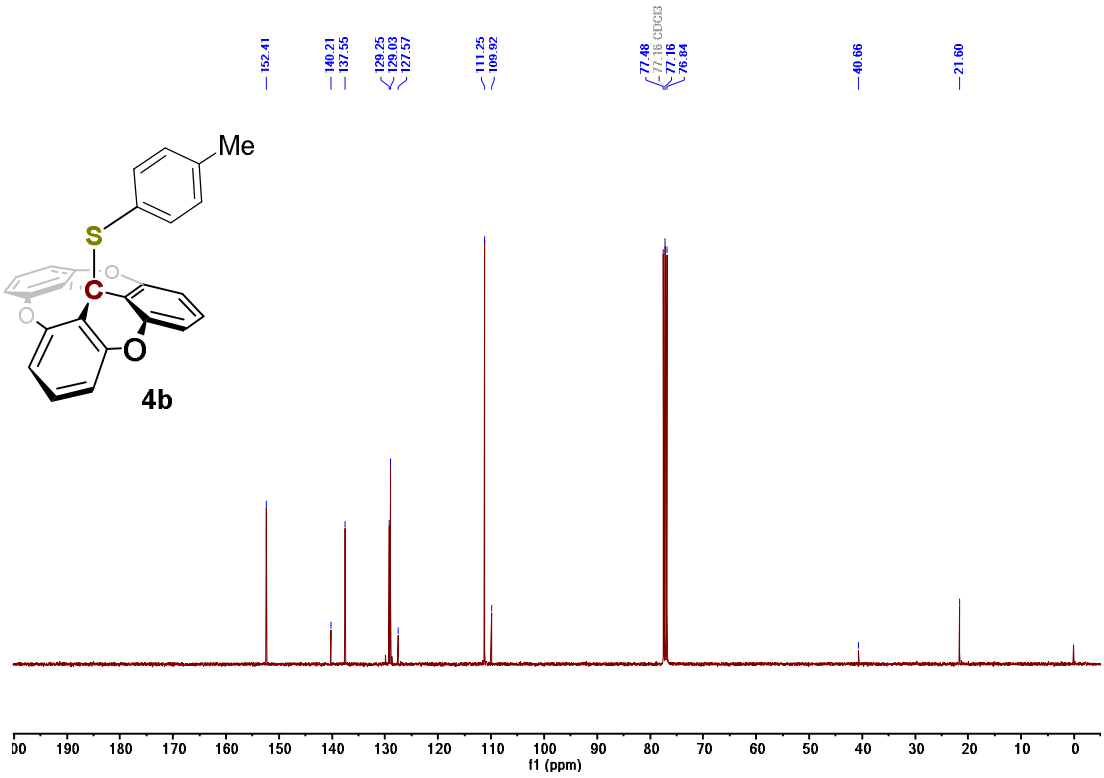

Figure S52: ^{13}C NMR spectrum of 4b in $CDCl_3$

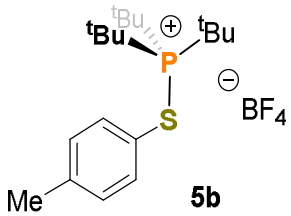

tri-tert-butyl(p-tolylthio)phosphonium tetrafluoroborate (5b)[6]:

Pale yellow solid, 36 mg, 87% yield:

^{1}H NMR (400 MHz, CD_2Cl_2) δ 7.74 (dd, *J* = 8.3, 1.7 Hz, 2H), 7.31 (d, *J* = 8.1 Hz, 2H), 2.41 (d, *J* = 2.1 Hz, 3H), 1.70 (d, *J* = 15.8 Hz, 27H).

^{13}C NMR (101 MHz, CD_2Cl_2) δ = 144.08 (d, *J* = 2.8 Hz), 138.11 (d, *J* = 2.9 Hz), 131.83 (d, *J* = 2.3 Hz), 117.87 (d, *J* = 9.9 Hz), 46.17 (d, *J* = 15.3 Hz), 30.81, 21.49.

^{31}P NMR (162 MHz, CD_2Cl_2) δ = 84.15.

^{19}F NMR (376 MHz, CD_2Cl_2) δ = -152.94.

^{11}B NMR (160 MHz, CD_2Cl_2) δ = -0.96 (d, *J* = 1.0 Hz).

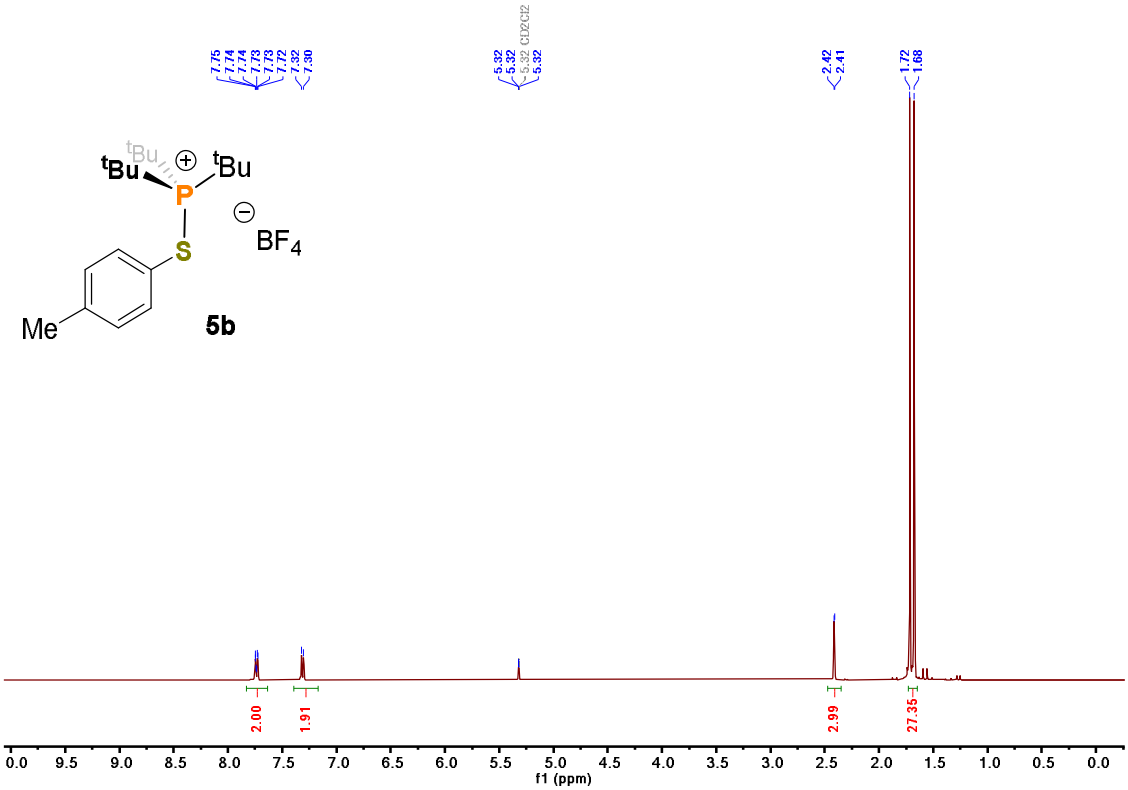

Figure S53: ^{1}H NMR spectrum of 5b in CD_2Cl_2

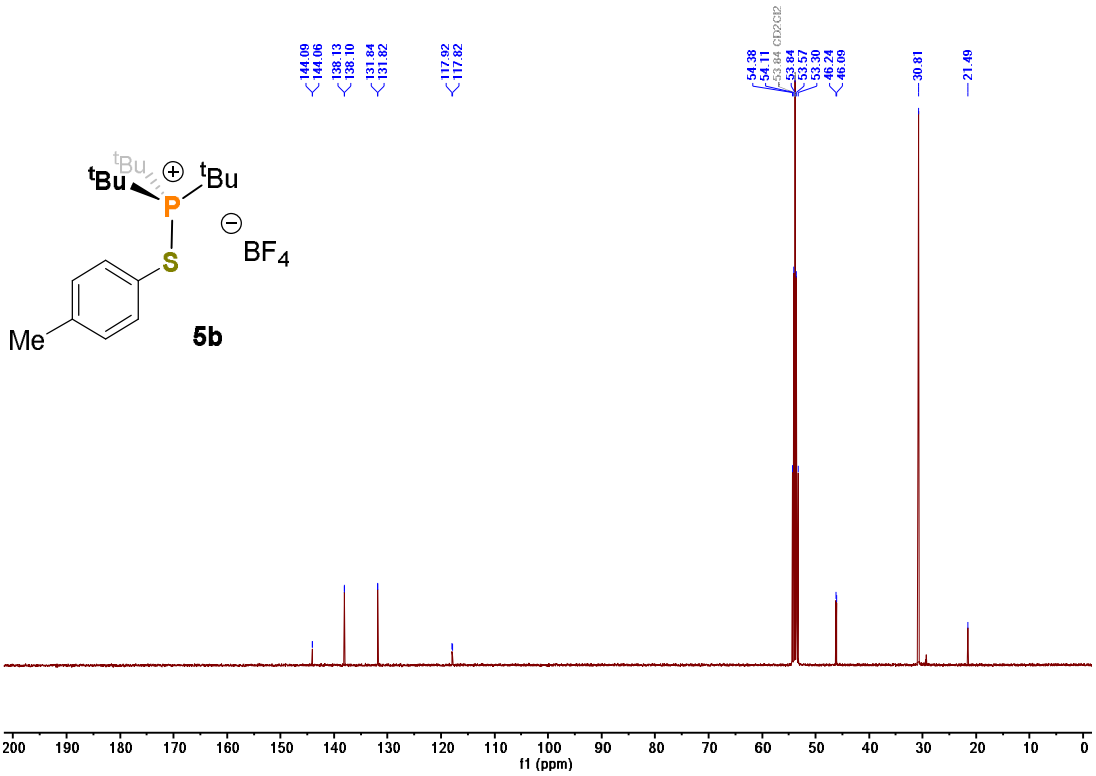

Figure S54: ^{13}C NMR spectrum of 5b in CD_2Cl_2

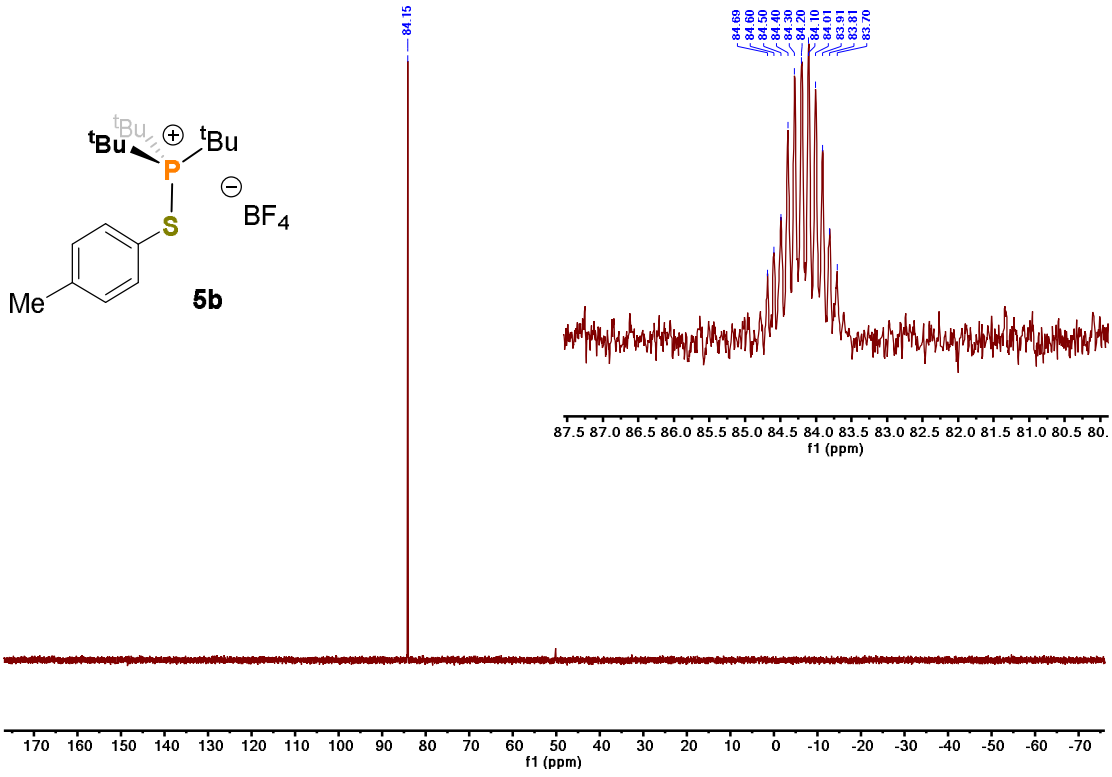

Figure S55: ^{31}P NMR spectrum of 5b in CD_2Cl_2

II.3c Reaction between 1-BF_4/^{t}Bu_3P and bis(4-chlorophenyl) disulfide:

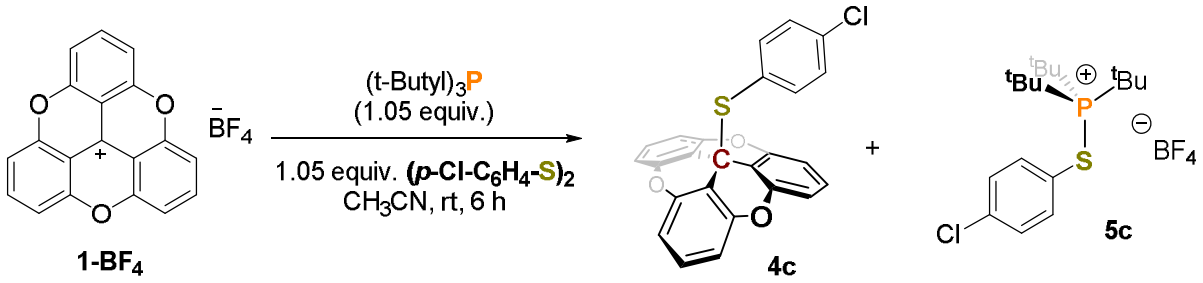

Following the representative procedure by using **1-BF_4** (37.2 mg, 0.1 mmol), tri-*ter*-butylphosphine (20.2 mg, 0.1 mmol) and bis(4-chlorophenyl) disulfide (25.5 mg, 0.1 mmol) as starting materials.

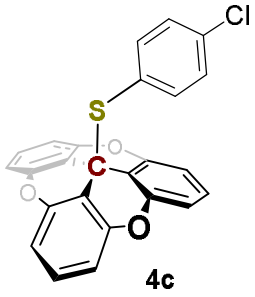

3a^2-((4-chlorophenyl)thio)-3a^2*H*-4,8,12-trioxadibenzo[*cd,mn*]pyrene (4c):

Off white solid, 32 mg, 76% yield; **MP =** 62-64 ºC;

^{1}H NMR (400 MHz, $CDCl_3$) = δ 7.28 (t, *J* = 8.3 Hz, 3H), 7.13 – 6.99 (m, 2H), 6.88 (d, *J* = 8.3 Hz, 6H), 6.77 – 6.64 (m, 2H).

^{13}C NMR (126 MHz, $CDCl_3$) δ = 152.53, 138.97, 136.83, 129.56, 129.39, 128.73, 111.43, 109.65. (Quaternary central carbon not seen in NMR, low abundance)

HRMS (ESI) m/z: $[M+H]^+$ Calcd. for $C_{25}H_{14}ClO_3S$ 429.0346; Found: 429.0352. Major fragmentation for TOTA+ [M+-C_6H_4ClS] 285.0545 is noted.

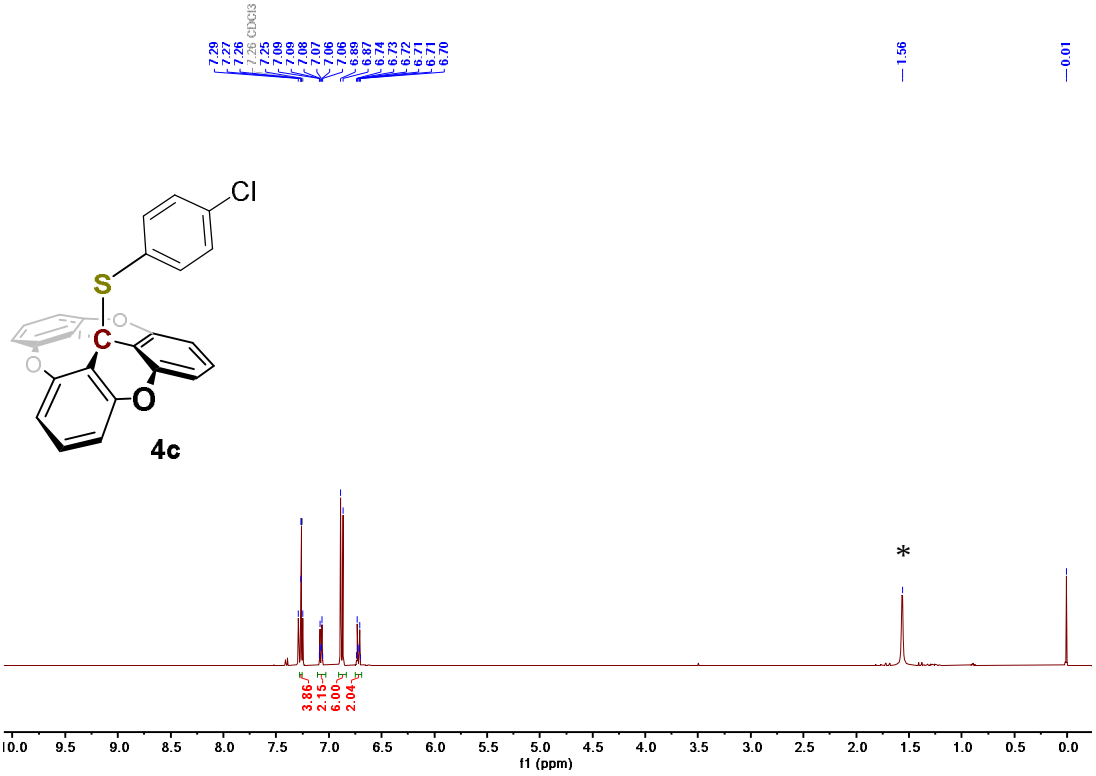

Figure S56: ^{1}H NMR spectrum of 4c in $CDCl_3$ (* indicates residual water)

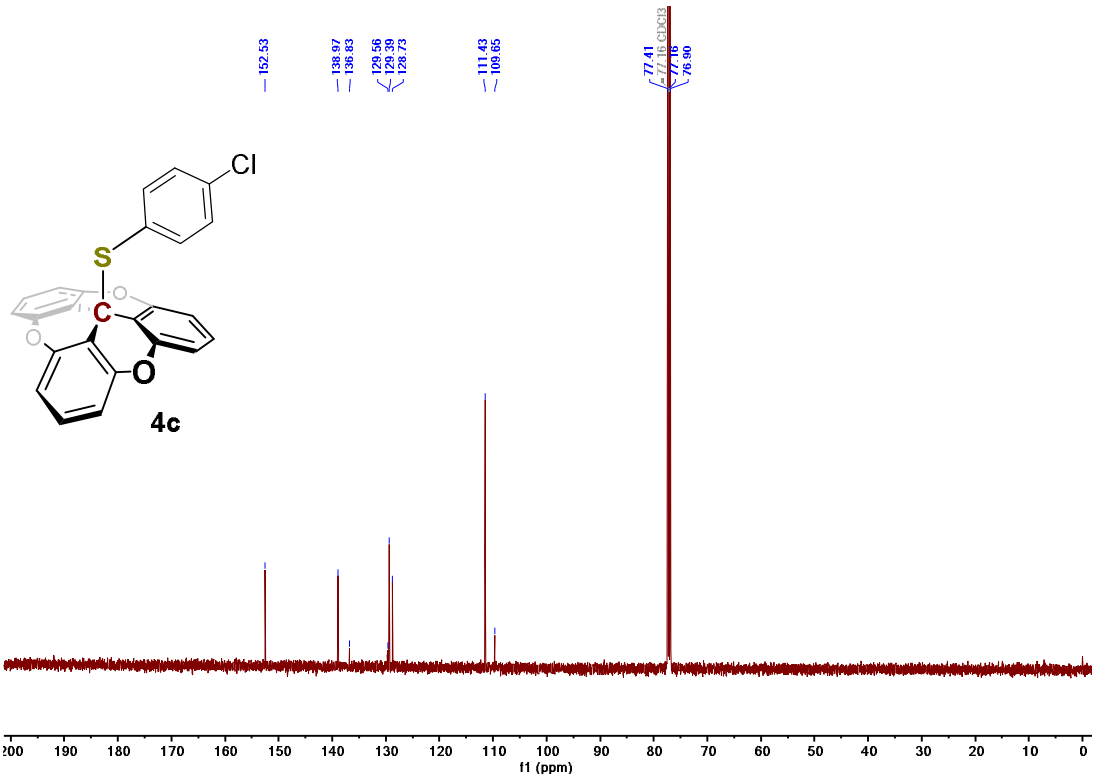

Figure S57: ^{13}C NMR spectrum of 4c in $CDCl_3$

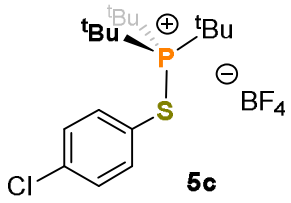

tri-tert-butyl((4-chlorophenyl)thio)phosphonium tetrafluoroborate (5c):

Light pink solid, 36 mg, 83% yield **MP** = 116-118 ºC

^{1}H NMR (400 MHz, CD_2Cl_2) δ = 8.38 – 7.62 (m, 2H), 7.69 – 7.29 (m, 2H), 1.71 (d, *J* = 16.0 Hz, 27H).

^{13}C NMR (100 MHz, CD_2Cl_2) δ = 139.64 (d, *J* = 2.9 Hz), 139.51 (d, *J* = 2.9 Hz), 131.35 (d, *J* = 2.2 Hz), 120.37 (d, *J* = 10.0 Hz), 46.44 (d, *J* = 14.6 Hz), 30.84.

^{31}P NMR (162 MHz, $CDCl_3$) δ = 86.39.

^{19}F NMR (376 MHz, CD_2Cl_2) δ = -152.81.

^{11}B NMR (160 MHz, CD_2Cl_2) δ = -0.96 (d, *J* = 1.0 Hz).

HRMS (ESI) m/z: [M^+] Calcd. for $C_{18}H_{31}ClPS$ 345.1567; found 345.1564.

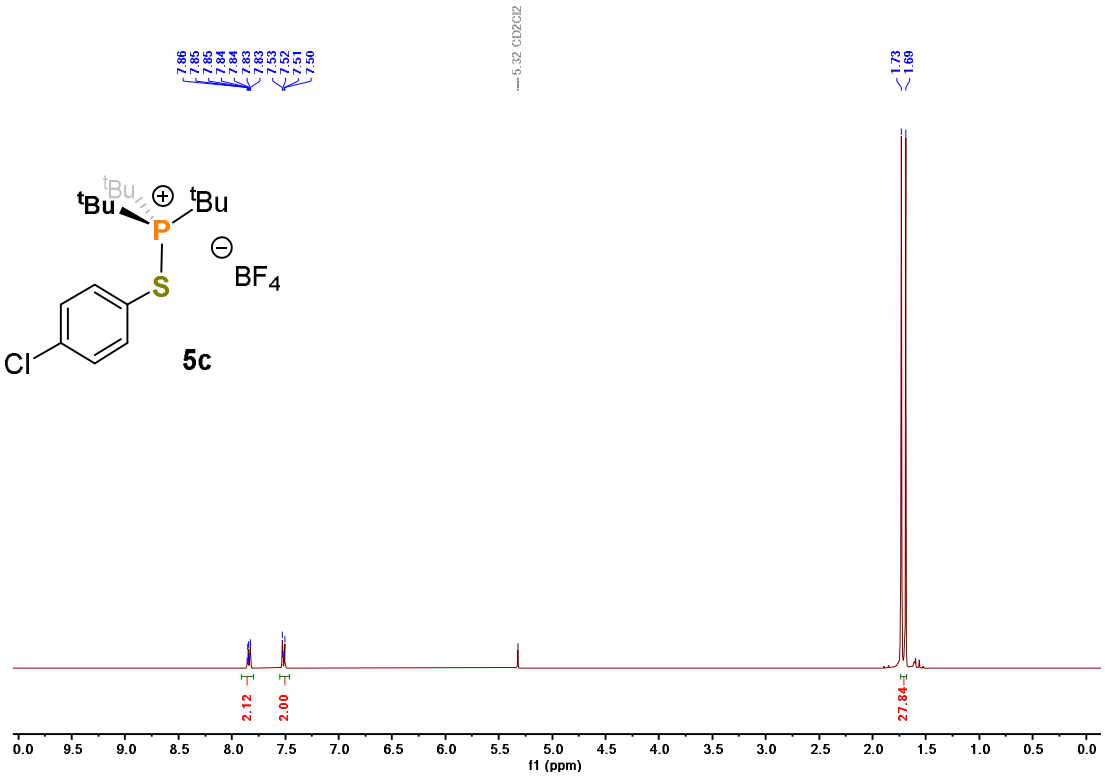

Figure S58: ^{1}H NMR spectrum of 5c in CD_2Cl_2

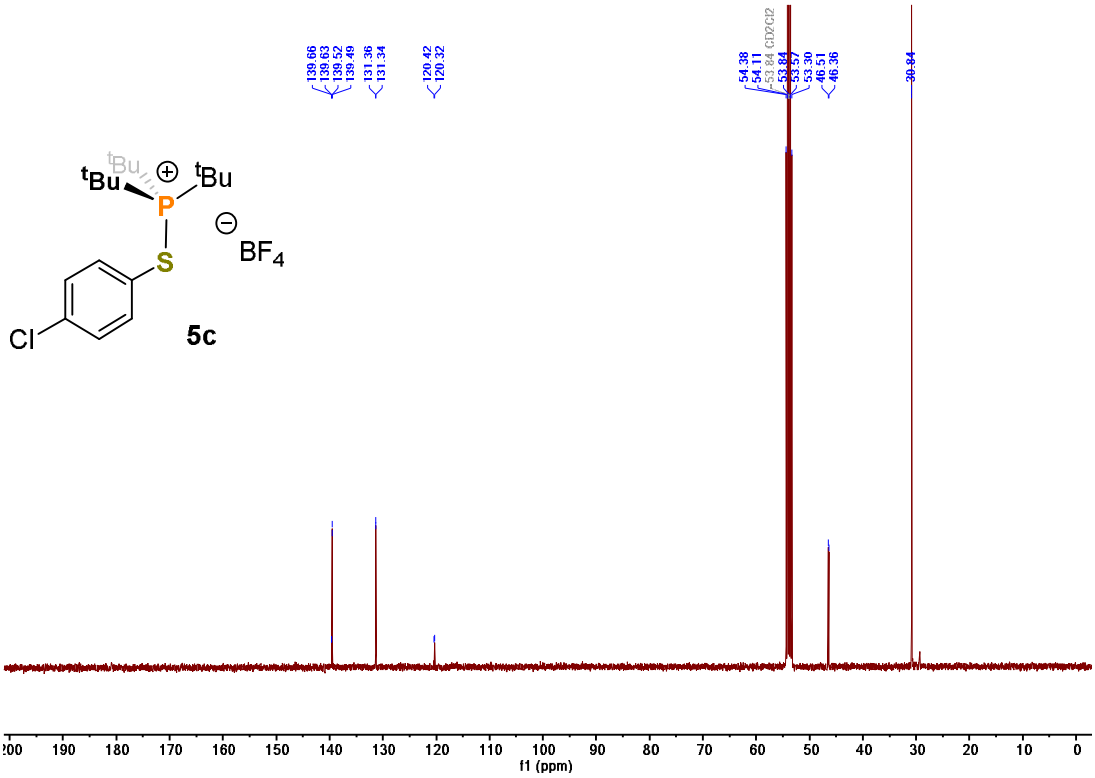

Figure S59: ^{13}C NMR spectrum of 5c in CD_2Cl_2

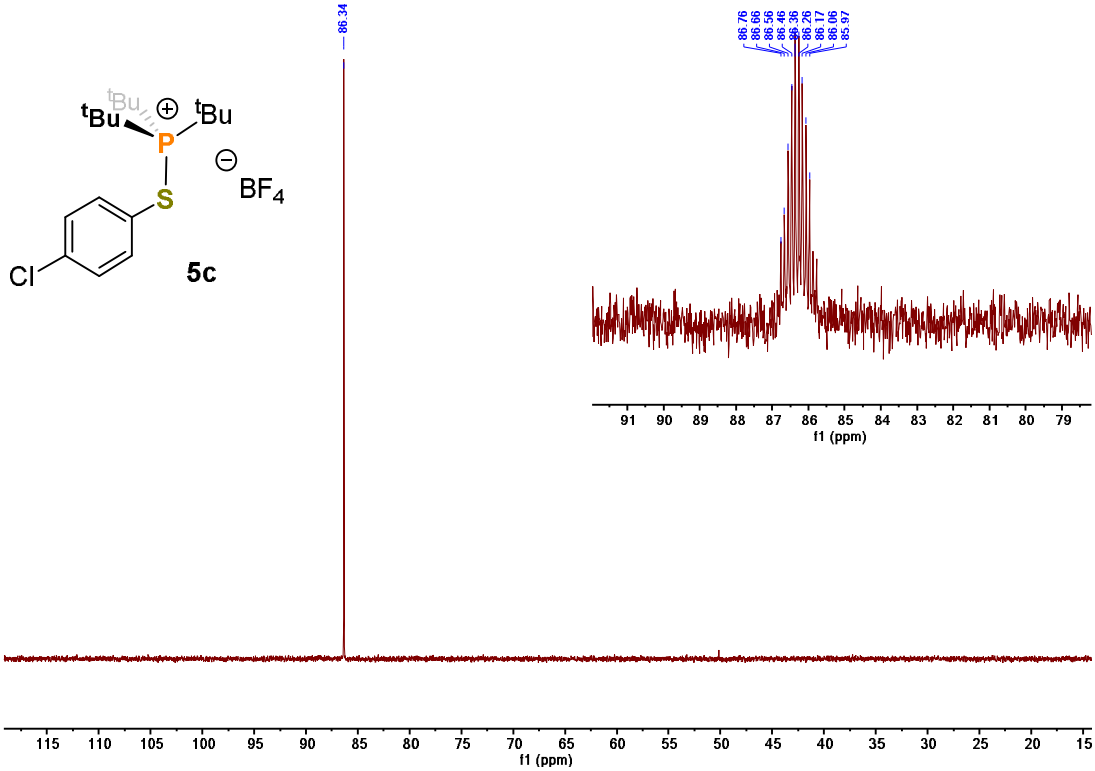

Figure S60: ^{31}P NMR spectrum of 5c in CD_2Cl_2

II.3d Reaction between 1-BF_4/$^tBu_3P$ and bis(4-chlorophenyl) disulfide:

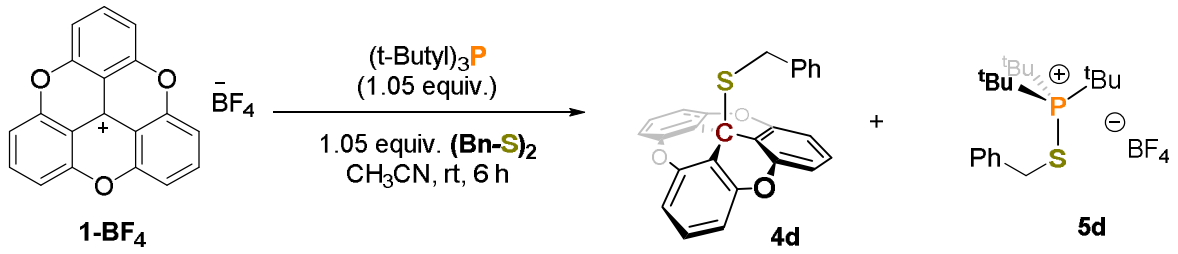

Following the representative procedure by using **1-BF_4** (37.2 mg, 0.1 mmol), tri-*ter*-butylphosphine (20.2 mg, 0.1 mmol) and dibenzyl disulfide (25.5 mg, 0.1 mmol) as starting materials.

NOTE- After overnight stand, the crystal of **4d** were observed in the reaction mixture

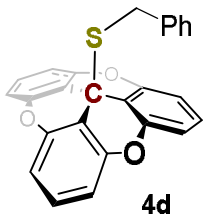

3a^2-(benzylthio)-*3a^{2}H*-4,8,12-trioxadibenzo[*cd,mn*]pyrene (4d):[6]

Pale yellow solid, 36 mg, 88% yield; **MP** = 210-212 ºC decomposition

^{1}H NMR (500 MHz, $CDCl_3$) δ = 7.30 – 7.26 (m, 3H), 7.15 – 7.06 (m, 3H), 7.05 – 7.00 (m, 2H), 6.96 (d, *J* = 8.3 Hz, 6H), 3.64 (s, 2H).

^{13}C NMR (126 MHz, $CDCl_3$) δ = 152.58, 136.32, 129.28, 129.07, 128.42, 127.00, 111.75, 110.35, 35.73, 34.94.

MALDI (TOF) m/z: $[M+H]^+$ Calcd. for $C_{26}H_{17}O_3S$ 409.0892; Found: 409.0898. In **HRMS (ESI)** m/z: major fragmentation for $TOTA^+$ $[M+-C_7H_7S]$ 285.0545 is noted.

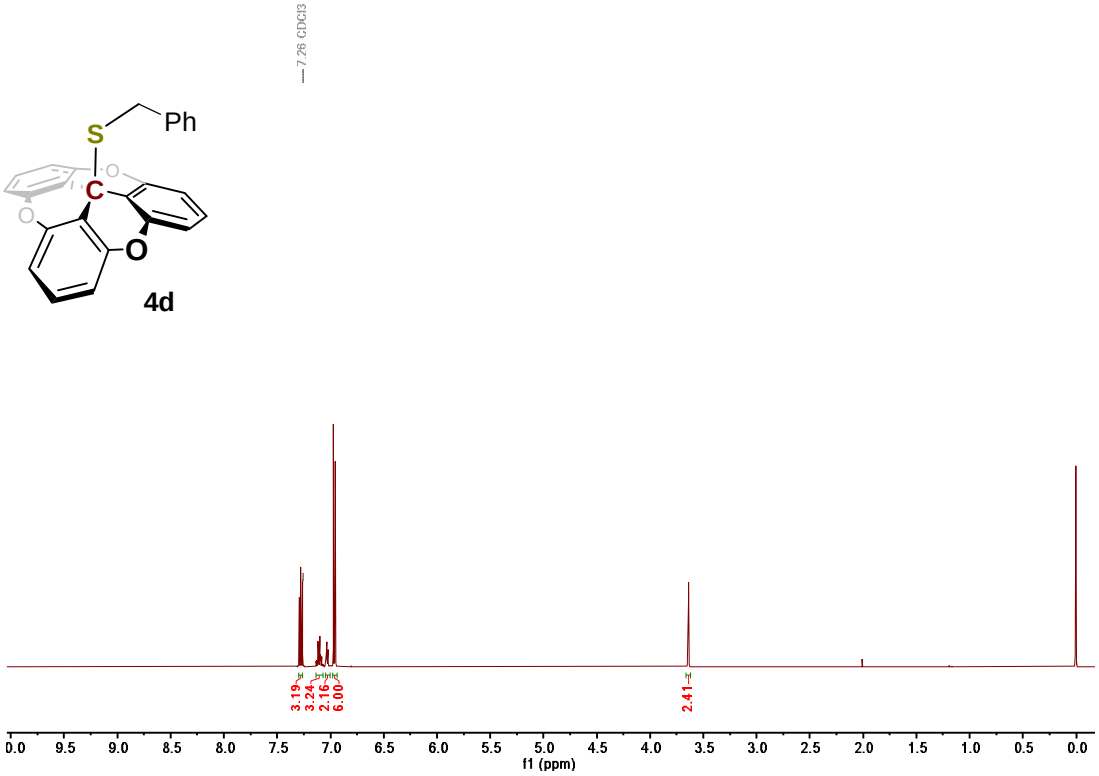

Figure S61: ^{1}H NMR spectrum of 4d in $CDCl_3$

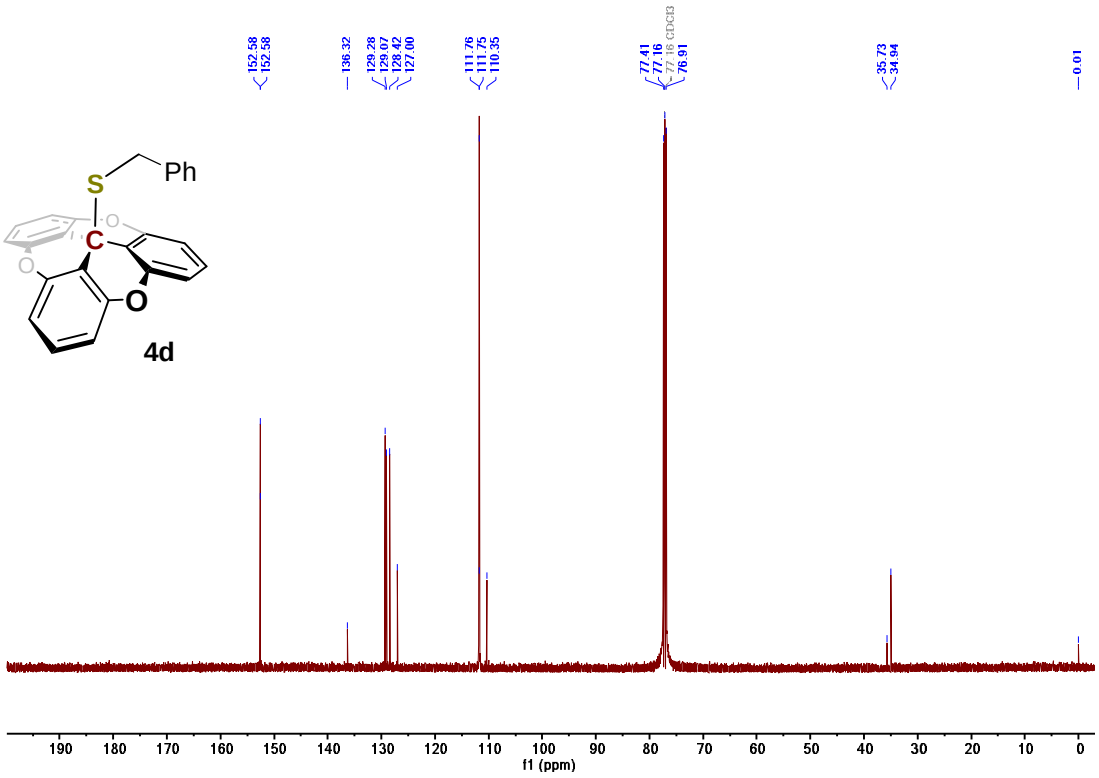

Figure S62: ^{13}C NMR spectrum of 4d in $CDCl_3$

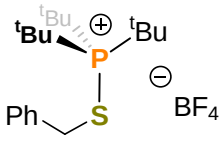

5d

Off white solid, 31 mg, 75% yield; **MP** = 150-152 ºC

^{1}H NMR (500 MHz, $CDCl_3$) δ = 7.45 – 7.32 (m, 5H), 4.51 (d, *J* = 2.7 Hz, 2H), 1.74 (d, *J* = 15.9 Hz, 27H).

^{13}C NMR (126 MHz, $CDCl_3$) δ = 134.08 (d, *J* = 6.4 Hz), 129.96, 129.91, 111.99, 45.50 (d, *J* = 17.7 Hz), 38.11 (d, *J* = 6.2 Hz), 30.37.

^{31}P NMR (202 MHz, $CDCl_3$) δ = 83.20 (t, *J* = 2.0 Hz).

^{11}B NMR (160 MHz, $CDCl_3$) δ = -0.94 (q, *J* = 1.0 Hz).

^{19}F NMR (376 MHz, $CDCl_3$) δ = -152.75 (d, *J* = 20.3 Hz).

HRMS (ESI) m/z: [M^+] Calcd. for $C_{19}H_{34}PS$ 325.2113; found 325.2111.

NOTE- The compound **5d** is undergoing debenzylation according to a previous report by Stephen and co-workers.[6] The side of the product $S{=}P^tBu_3$ is indicated in NMR spectra.

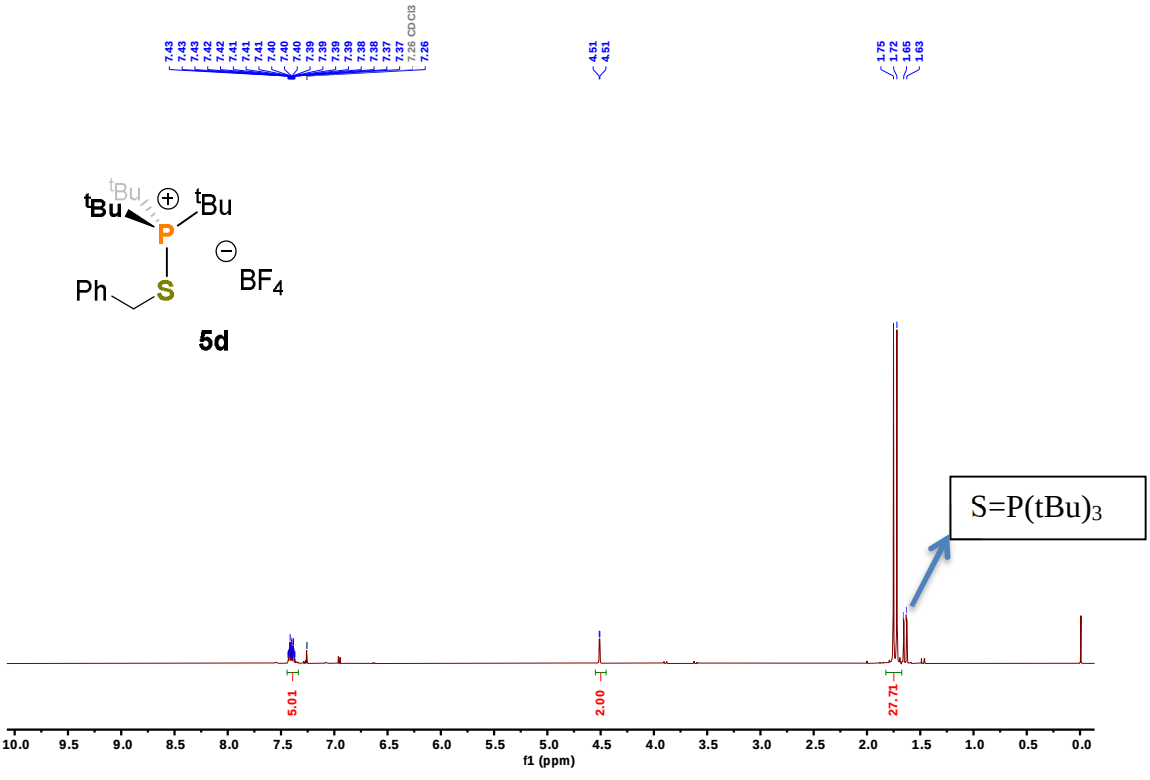

Figure S63: ^{1}H NMR spectrum of 5d in $CDCl_3$

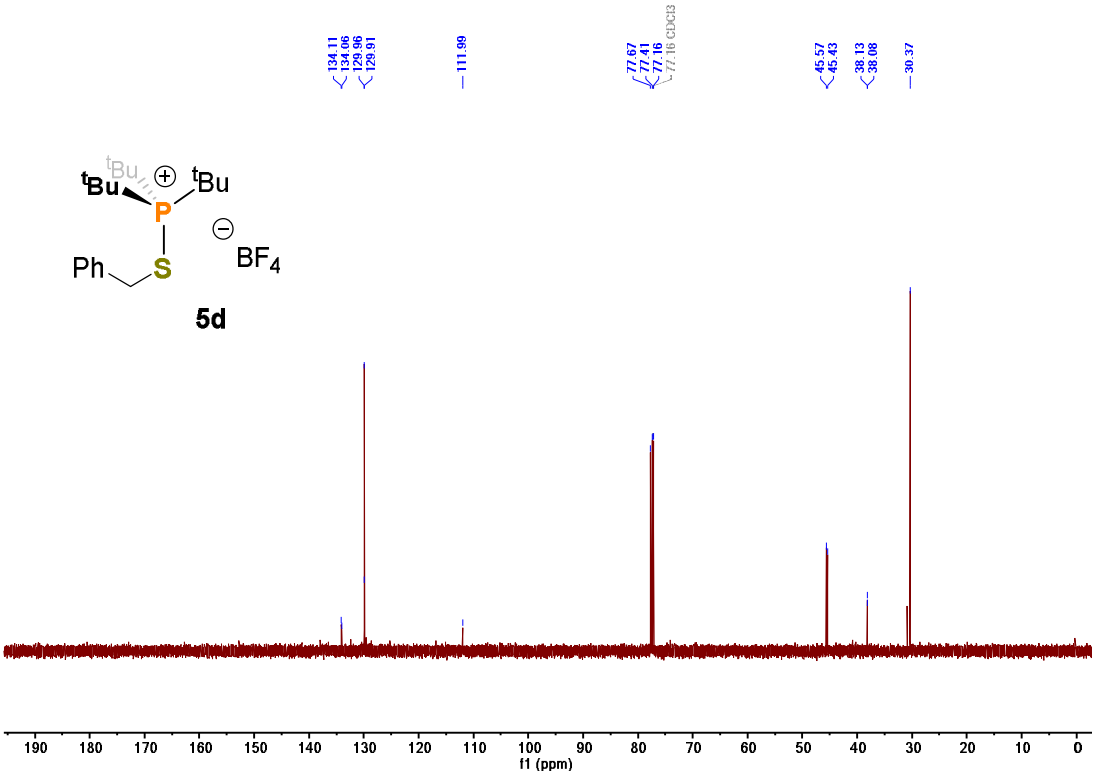

Figure S64: ^{13}C NMR spectrum of 5d in $CDCl_3$

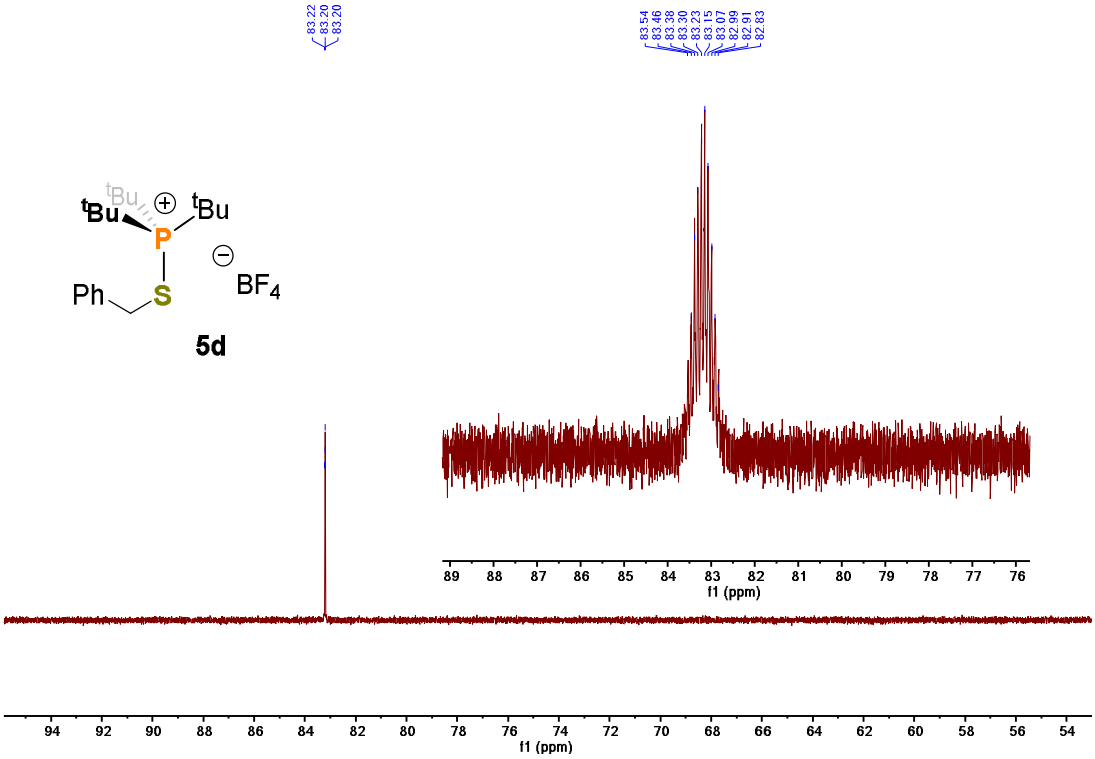

Figure S65: ^{31}P NMR spectrum of 5d in $CDCl_3$

II.3e Reaction between 1-BAr$^{F}_{4}$/^{t}PPh$_3$ and diphenyl disulfide:

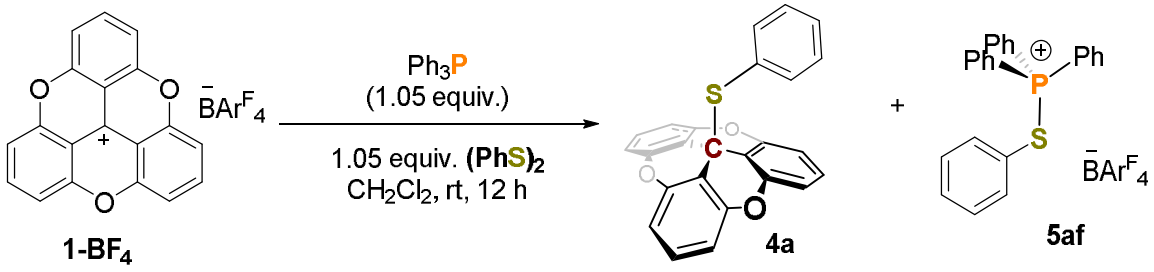

Following the representative procedure by using **1-BAr$^{F}_{4}$** (57.0 mg, 0.05 mmol), triphenylphosphine (14 mg, 0.055 mmol) and diphenyl disulfide (10.5 mg, 0.055 mmol). **NOTE**- Reaction of **[1]$^{+}$BF$_4$** in CH_3CN formed the desired cleavage products but solubility issues resulted in lower yields. The compound **4a** was isolated in 89% yield after recrystallization from pentane.

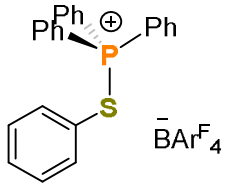

5af

triphenyl(phenylthio)phosphonium tetrakis(3,5-bis(trifluoromethyl)phenyl)borate(5af):[7]
Light yellow solid, 51 mg, 85% yield;

^{1}H NMR (500 MHz, CDCl3) δ = 7.78 (td, *J* = 7.5, 1.9 Hz, 3H), 7.70 (dt, *J* = 4.9, 2.3 Hz, 8H), 7.58 (td, *J* = 7.8, 4.1 Hz, 6H), 7.49 (d, *J* = 1.8 Hz, 4H), 7.47 – 7.38 (m, 7H), 7.23 (t, *J* = 7.7 Hz, 3H), 7.11 (dt, *J* = 8.3, 1.8 Hz, 2H).

^{13}C NMR (126 MHz, CDCl3) δ = 161.83 (dd, J = 99.7, 49.7 Hz), 148.60 (d, J = 1202.0 Hz), 137.09 (d, J = 3.9 Hz), 136.53 (d, J = 3.2 Hz), 134.92, 133.84 (d, J = 10.8 Hz), 132.97 – 131.28 (m), 131.03 (d, J = 3.1 Hz), 130.76 (d, J = 13.4 Hz), 129.79 – 126.77 (m), 124.64 (d, J = 272.5 Hz), 121.39, 118.23, 117.82 – 116.74 (m), 113.14.

^{31}P NMR (202 MHz, CDCl$_3$) δ = 45.80 (s).

^{11}B NMR (160 MHz, CDCl3) δ = -6.60 (dt, J = 5.6, 2.8 Hz).

^{19}F NMR (376 MHz, CDCl$_3$) δ = -62.43.

HRMS (ESI) m/z: [M+] Calcd. for $C_{24}H_{20}PS^{+}$ 371.1017; found 371.1013.

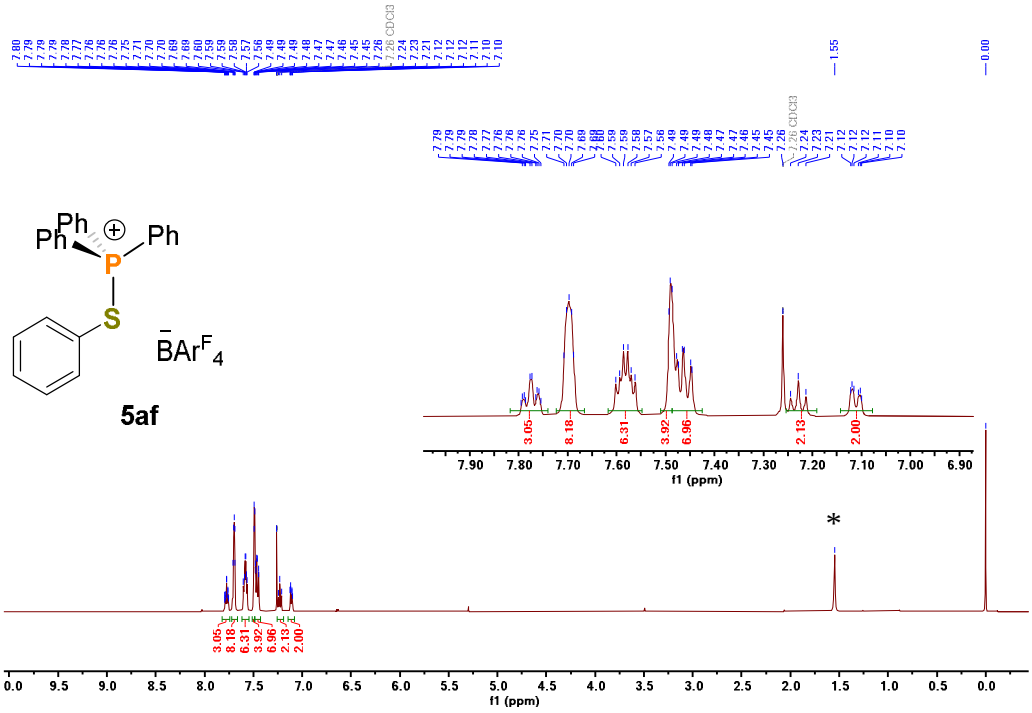

Figure S66: ^{1}H NMR spectrum of 5af in $CDCl_3$ (* indicates residual water)

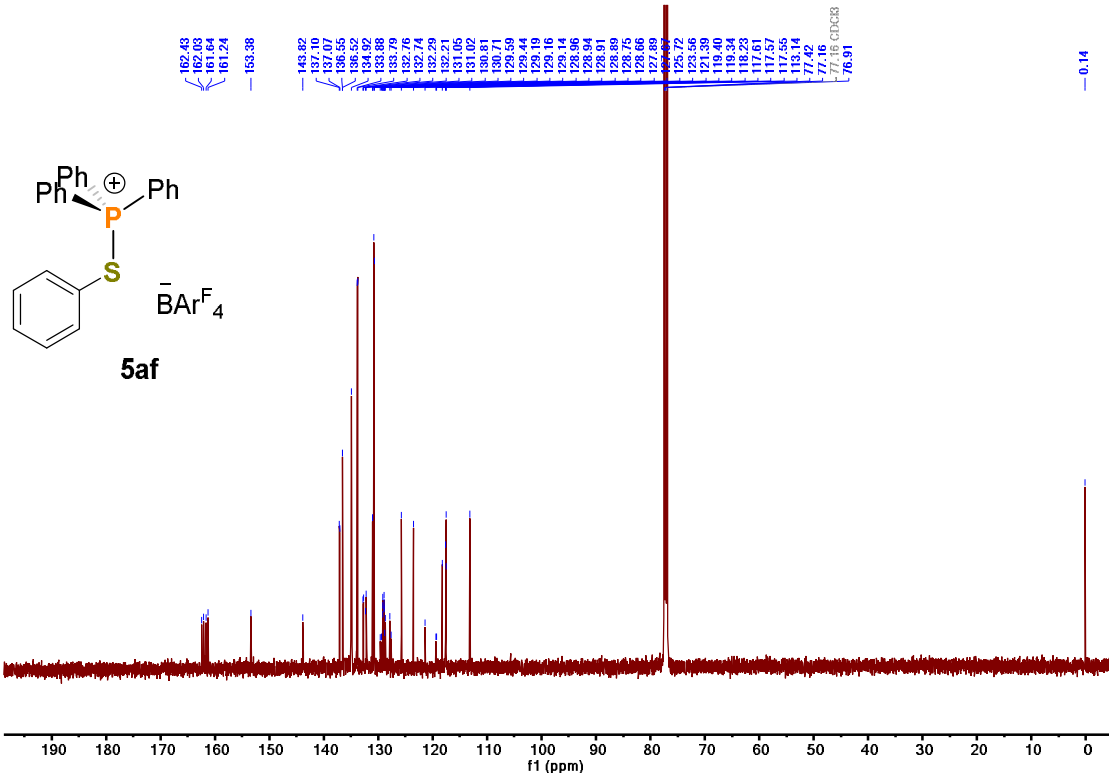

Figure S67: ^{13}C NMR spectrum of 5af in $CDCl_3$

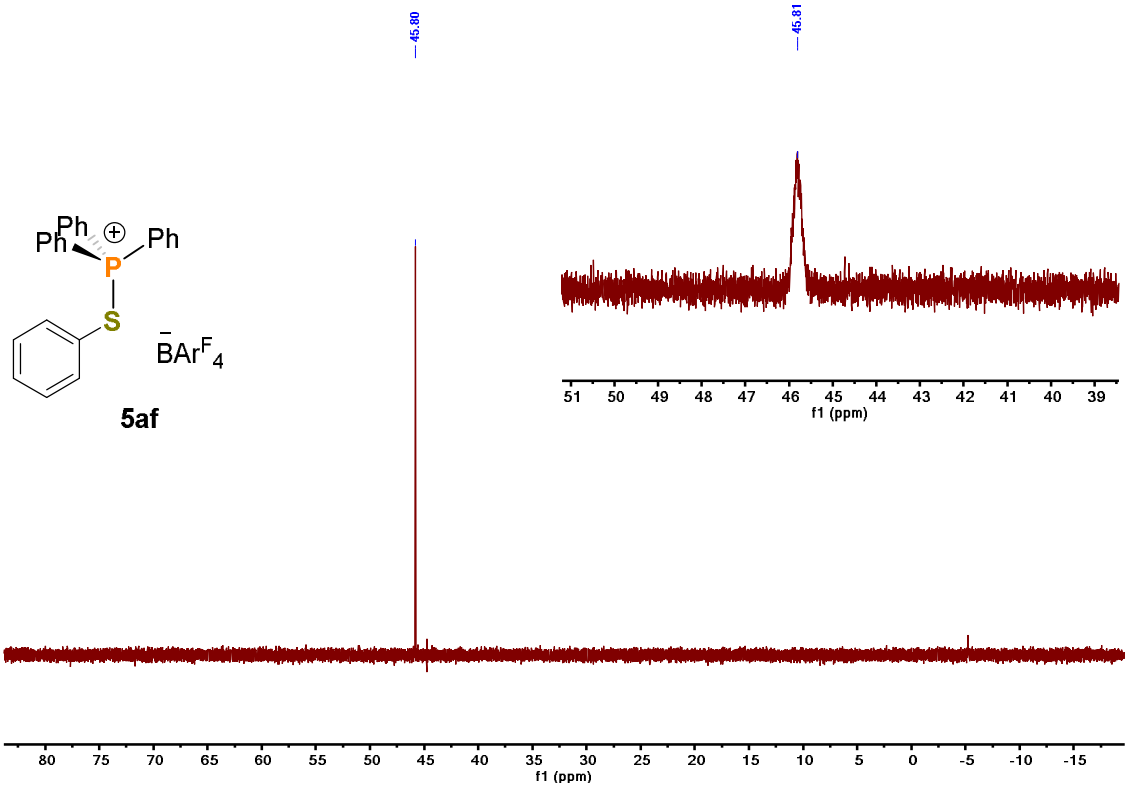

Figure S68: ^{31}P NMR spectrum of 5af in $CDCl_3$

II.3f Reaction between TOTA-PR$_3$ adduct (3a and 3d) and diphenyl disulfide:

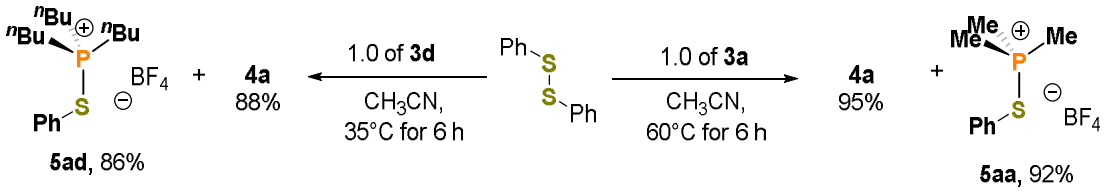

Procedure: An acetonitrile solution (1 mL) of diphenyl disulfide (4.2 mg, 0.02 mmol) was added to a solution of **3a** (9.0 mg, 0.02 mmol) in acetonitrile (1 mL), then heated for 6 h at 60°C. The same procedure and amounts were used for **3d** (9.0 mg, 0.02 mmol), but this was heated at 35°C for 6h. The solution was concentrated by half under vacuum, and 2 mL of *n*-pentane was added with vigorous stirring which induced precipitation of a solid. After decanting the supernatant, the precipitate was washed with *n*-pentane (3 x 2 mL) and dried under vacuum to give **5aa** or **5ad** as a pale-yellow solid. The washing solution was combined and evaporated under vacuum to give **4a** as a white solid.

Note: In case of PMe_3/P^nBu_3, premixig the PMe_3/P^nBu_3 with disulfide at rt, followed by addition of $TOTA^+$, results the formation of desired S–S bond cleavage products with TOTA-PR_3 adducts.

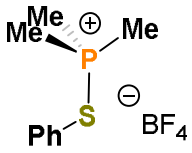

5aa

trimethyl(phenylthio)-λ^4-phosphane tetrafluoroborate (5aa):

Light yellow solid, 5.0 mg, 92% yield;

^{1}H NMR (500 MHz, CD_2Cl_2) δ = 7.89 – 7.26 (m, 5H), 2.13 (d, *J* = 13.7 Hz, 9H).

^{13}C NMR (126 MHz, CD_2Cl_2) δ = 137.12 (d, *J* = 3.8 Hz), 132.79 (d, *J* = 3.3 Hz), 131.54 (d, *J* = 3.1 Hz), 12.60 (d, *J* = 50.7 Hz).

^{31}P NMR (202 MHz, CD_2Cl_2) δ = 52.72 (tt, *J* = 27.5, 14.0 Hz).

^{11}B NMR (160 MHz, CD_2Cl_2) δ = -1.15.

^{19}F NMR (470 MHz, CD_2Cl_2) δ -150.47 (d, *J* = 25.9 Hz).

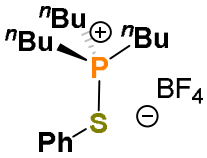

5ad

tributyl(phenylthio)-λ^4-phosphane tetrafluoroborate (5ad) [8]**:**

Light yellow solid, 5.8 mg, 88% yield;

^{1}H NMR (500 MHz, $CDCl_3$) δ = 7.68 – 7.58 (m, 1H), 7.58 – 7.47 (m, 4H), 2.52 – 2.17 (m, 6H), 1.71 – 1.55 (m, 6H), 1.49 (h, *J* = 7.3 Hz, 6H), 0.96 (t, *J* = 7.3 Hz, 9H).

^{13}C NMR (126 MHz, CD_2Cl_2) δ = 136.57 (d, *J* = 3.4 Hz), 132.40, 131.19 (d, *J* = 2.6 Hz), 23.92 (d, *J* = 5.6 Hz), 23.78 (d, *J* = 17.0 Hz), 22.67 (d, *J* = 40.0 Hz), 13.53 (d, *J* = 4.4 Hz).

^{31}P NMR (202 MHz, $CDCl_3$) δ = 65.16

^{11}B NMR (160 MHz, $CDCl_3$) δ = -1.06.

^{19}F NMR (470 MHz, $CDCl_3$) δ = -151.76 (d, *J* = 5.9 Hz).

NOTE- The ^{13}C-NMR shows some unreacted TOTA-P^{n}Bu$_3$ adduct (**3d**) peaks.

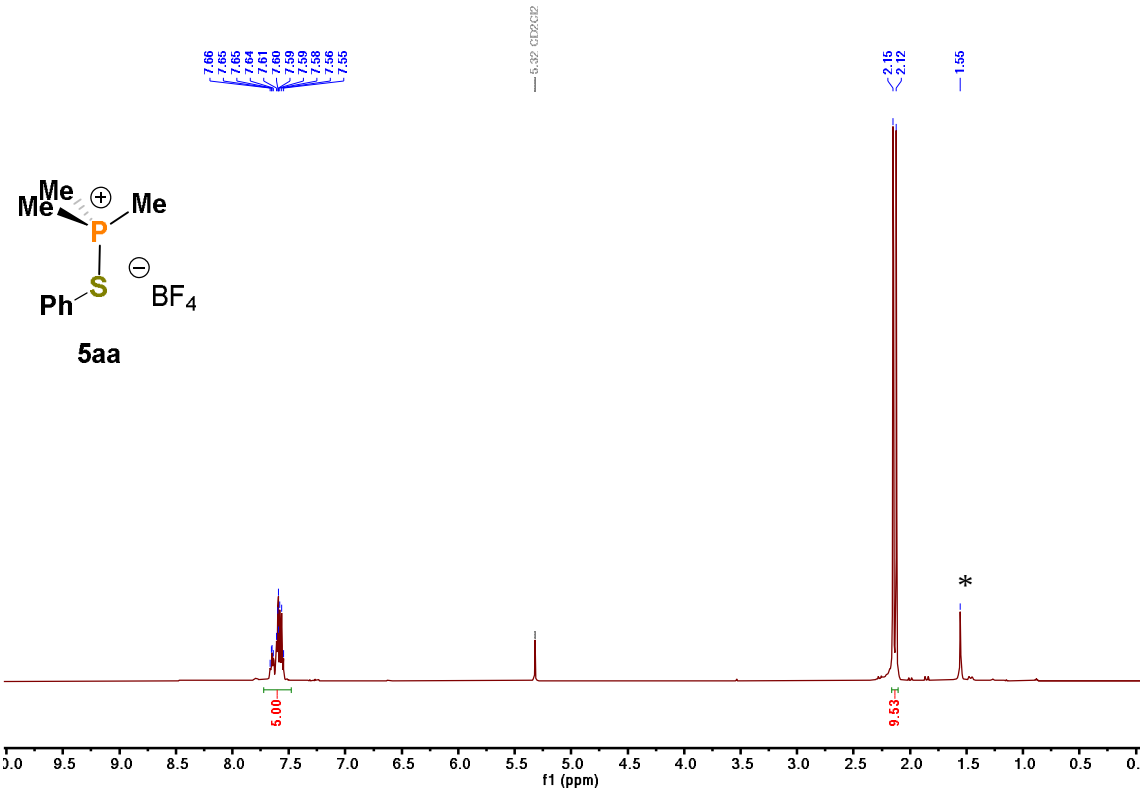

Figure S69: ^{1}H NMR spectrum of 5aa in CD_2Cl_2 (* indicates residual water)

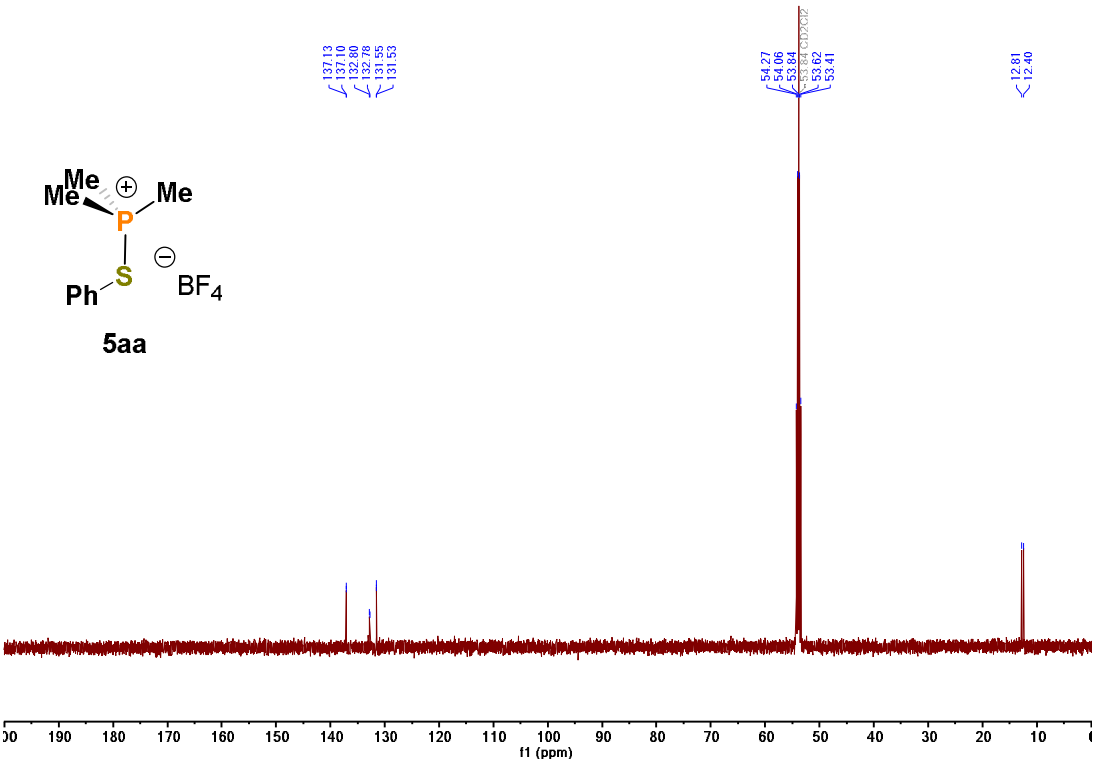

Figure S70: ^{13}C NMR spectrum of 5aa in CD_2Cl_2

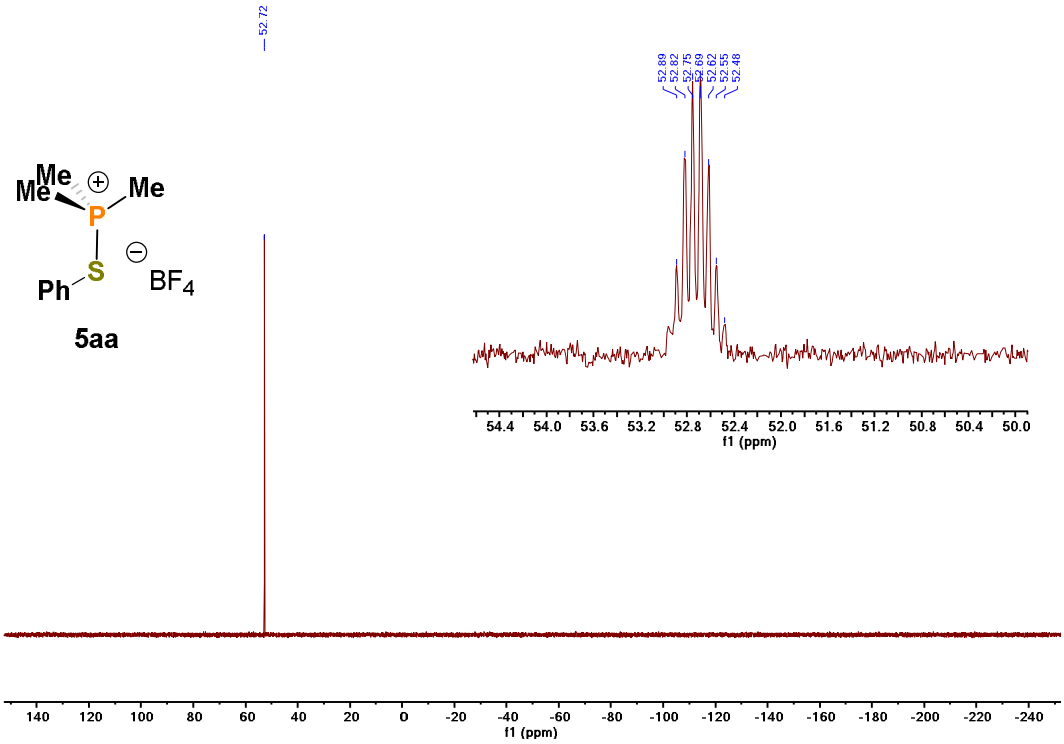

Figure S71: ^{31}P NMR spectrum of 5aa in CD_2Cl_2

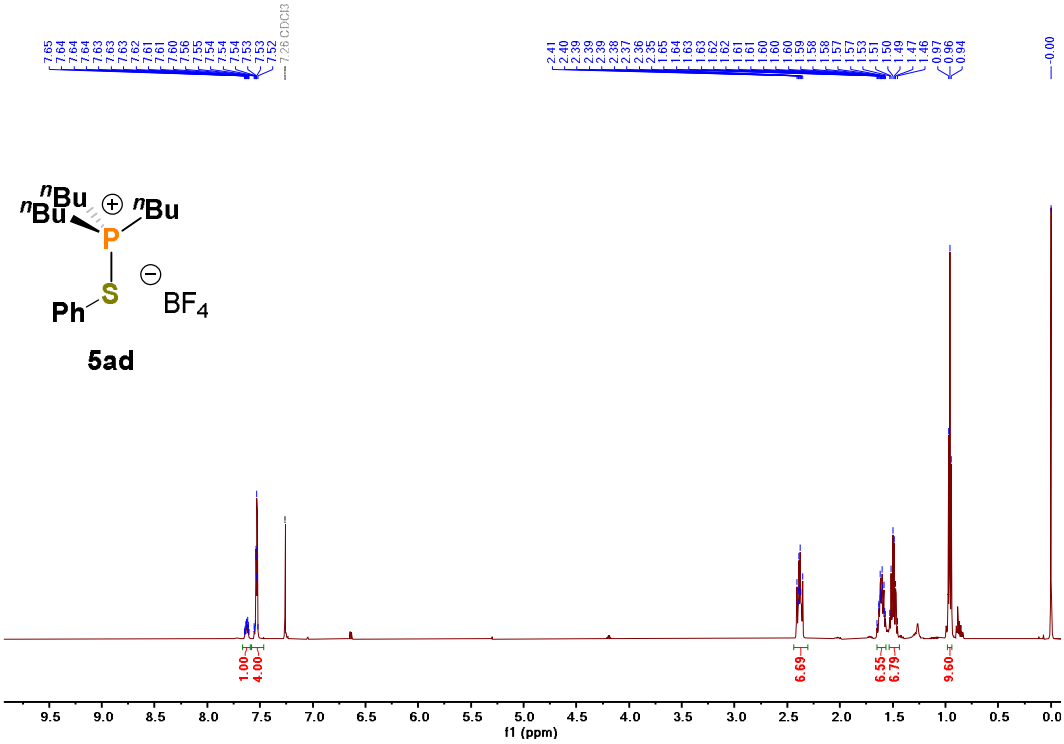

Figure S72: ^{1}H NMR spectrum of 5ad in $CDCl_3$

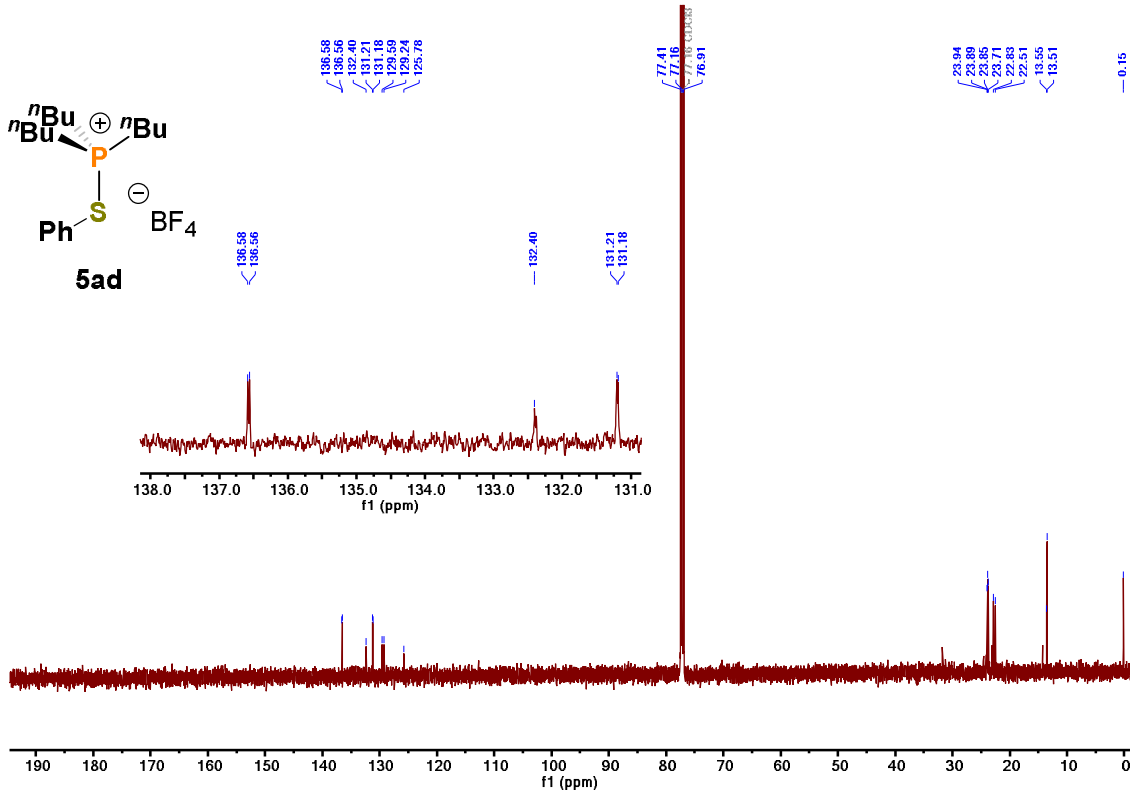

Figure S73: ^{13}C NMR spectrum of 5ad in CD2Cl$_2$

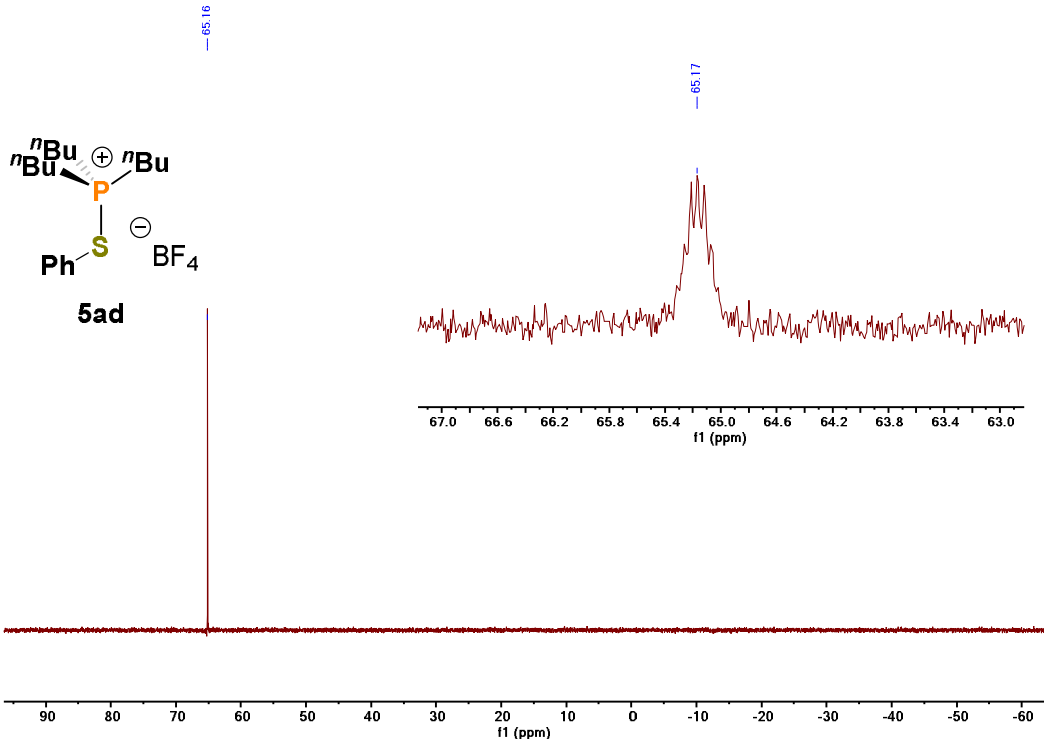

Figure S74: ^{31}P NMR spectrum of 5ad in CD$_2$Cl$_2$

II.4 Frustrated Lewis pair mediated dehydrogenation of cyclohexadiene

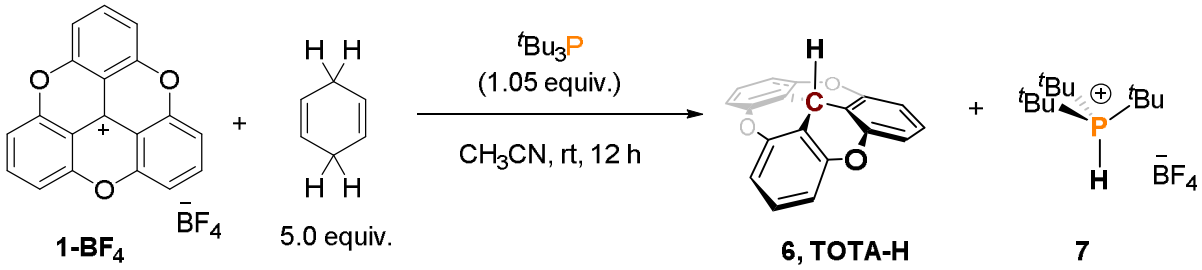

Procedure: An acetonitrile solution (2 mL) of 1,4-cyclohexadiene (40 mg, 0.5 mmol) was added to acetonitrile solution (2 mL) of **1-BF$_4$** (37.2 mg, 0.1 mmol) and ^{t}Bu$_3$P (20.1 mg, 0.1 mmol), and the solution stood at room temperature overnight. The volatiles of the solution were removed under vacuum to give a pale-yellow solid. The solid was washed with n-pentane (3 x 2mL) and ether (3 x 2mL) and dried under vacuum to give **7** as a pale-yellow solid (26 mg, 86% yield). The washing solution was combined and evaporated under vacuum to give TOTA-H (**6**) as an off-white solid after column chromatography (18 mg, 64% yield).

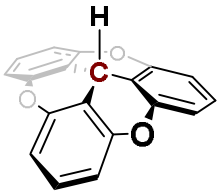

6, TOTA-H

3a^{2}H-4,8,12-trioxadibenzo[*cd,mn*]pyrene (6)[9]:

Off white solid; yield: 64%,

^{1}H NMR (500 MHz, CDCl$_3$) δ = 7.24 (ddd, *J* = 8.0, 0.9 Hz, 3H), 6.91 (d, *J* = 8.1 Hz, 6H), 4.92 (s, 1H).

^{13}C NMR (126 MHz, CDCl$_3$) δ = 153.51, 129.02, 111.76, 109.68, 21.01.

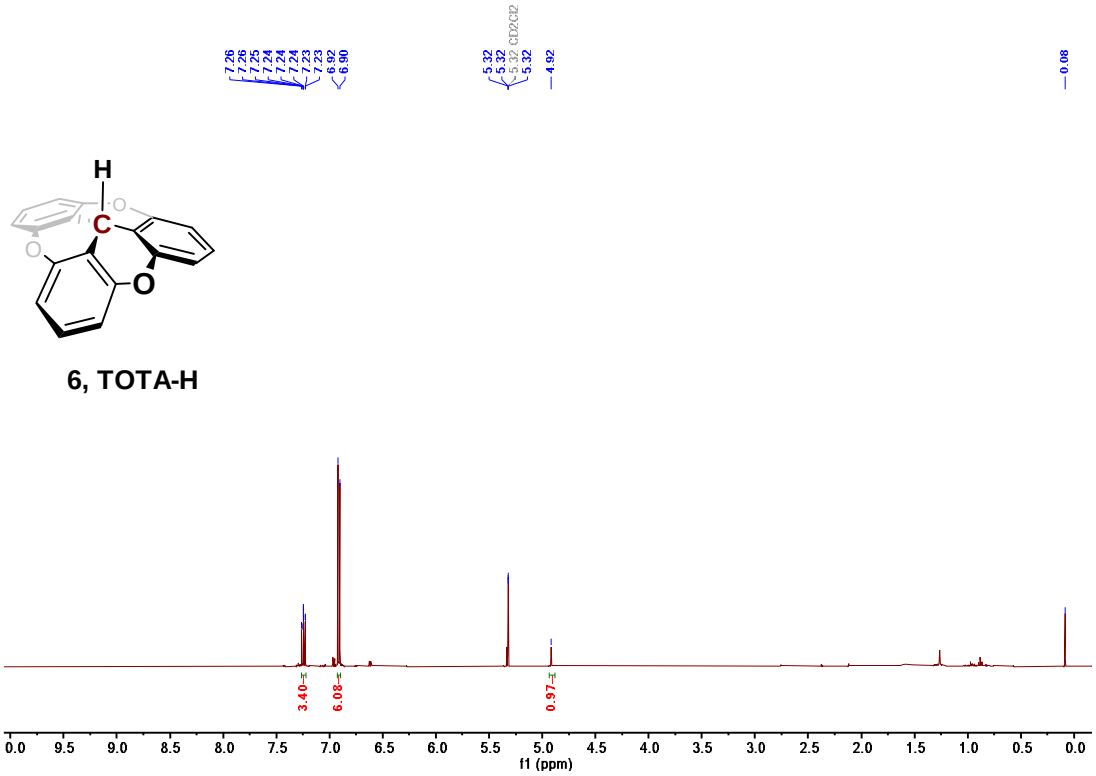

Figure S75: ^{1}H NMR spectrum of 6 in CD_2Cl_2

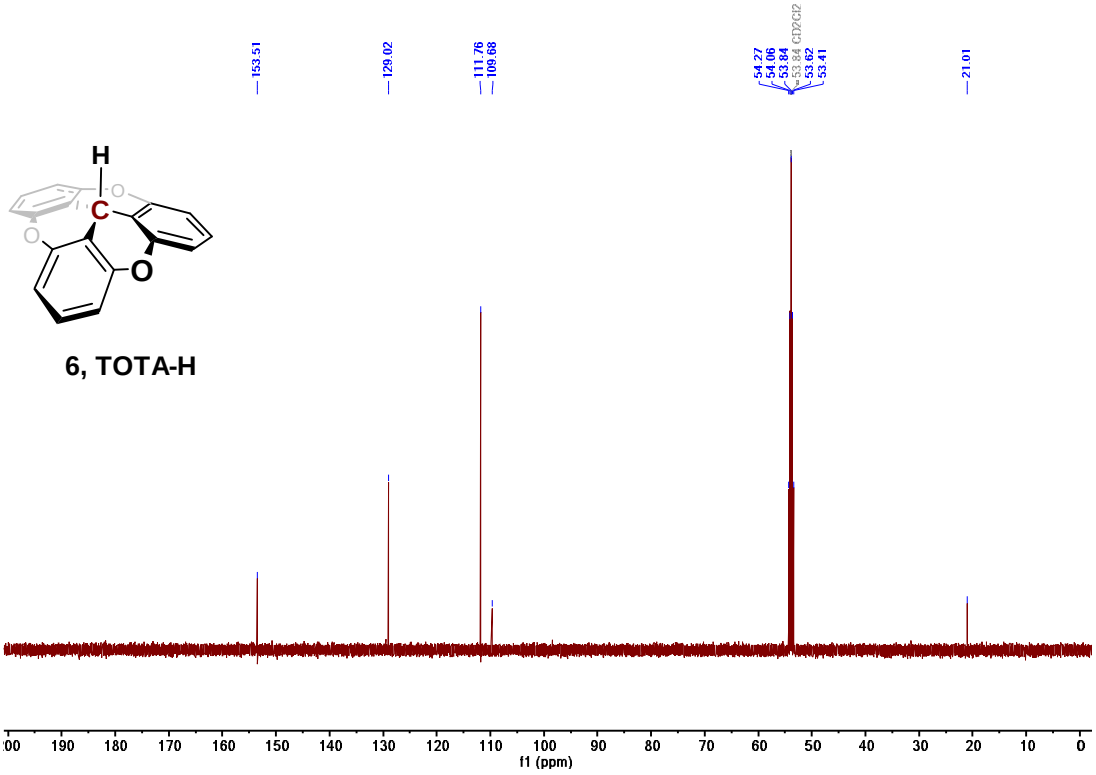

Figure S76: ^{13}C NMR spectrum of 6 in CD_2Cl_2

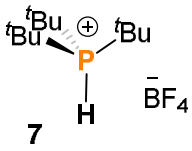

7

tri-*tert*-butylphosphonium tetrafluoroborate (7):

Yield: 86%, Pale yellow solid;

^{1}H NMR (400 MHz, $CDCl_3$) δ = 6.25 (d, *J* = 469.8 Hz, 1H), 1.67 (d, *J* = 15.2 Hz, 27H).

^{13}C NMR (126 MHz, $CDCl_3$) δ = 37.11 (d, *J* = 29.2 Hz), 30.19

^{31}P NMR (202 MHz, $CDCl_3$) δ = 50.52.

^{19}F NMR (376 MHz, $CDCl_3$) δ = -150.14 (d, *J* = 3.7 Hz).

^{11}B NMR (160 MHz, $CDCl_3$) δ = -1.29.

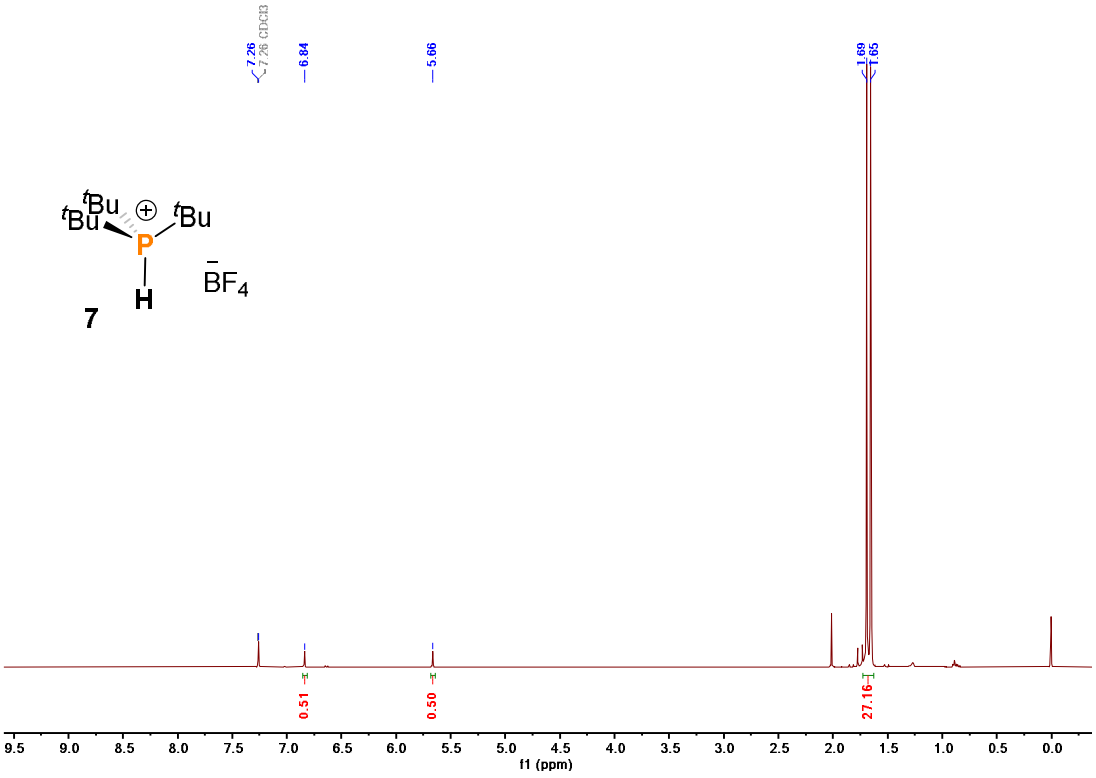

Figure S77: ^{1}H NMR spectrum of 7 in CD_2Cl_2

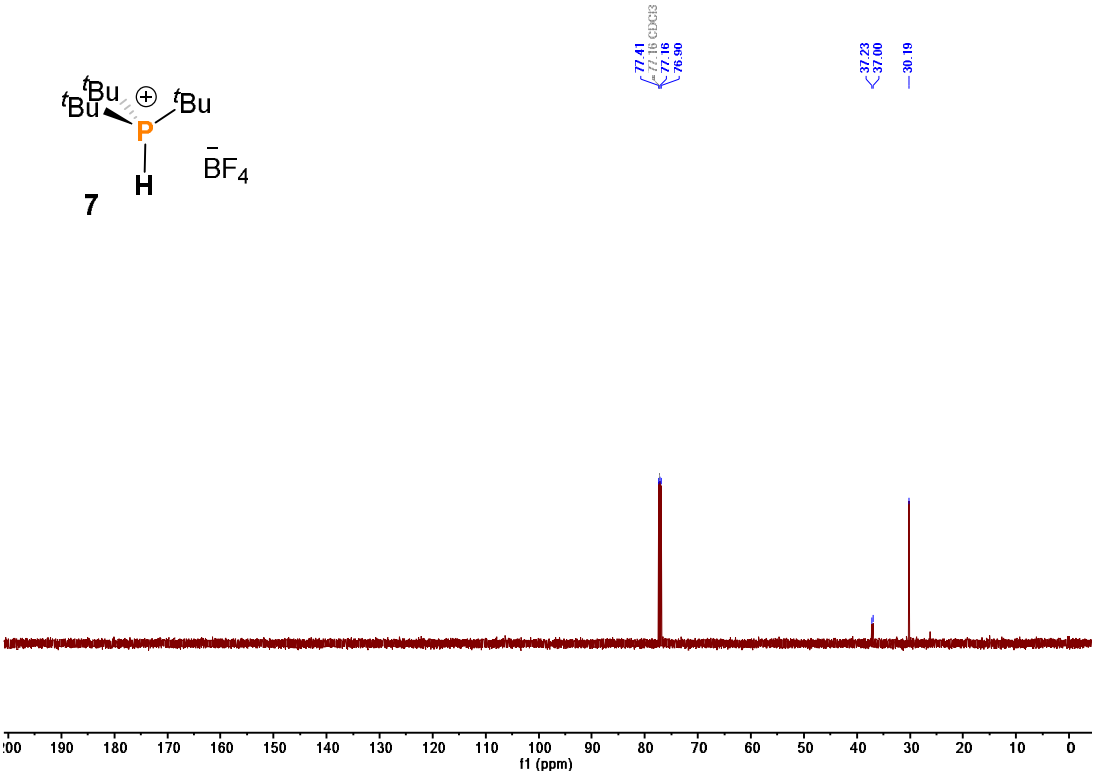

Figure S78: ^{13}C NMR spectrum of 7 in CD_2Cl_2

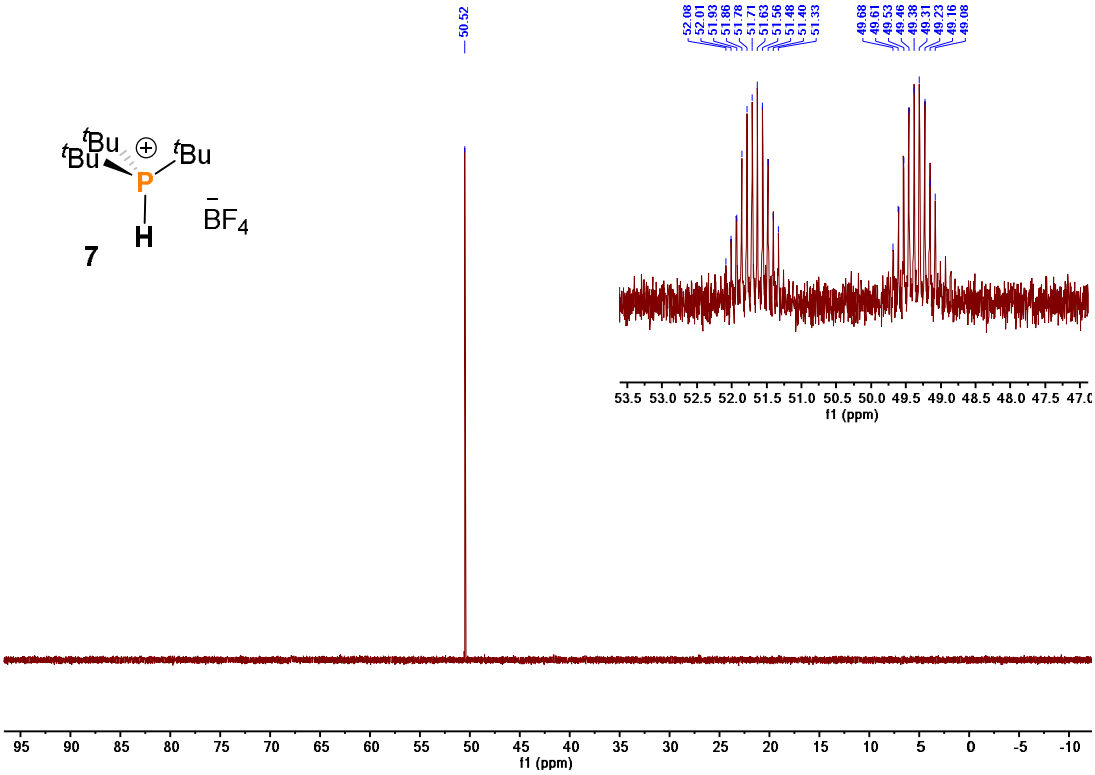

Figure S79: ^{31}P NMR spectrum of 7 in CD_2Cl_2

II.5 Frustrated Lewis pair mediated cleavage of C-Br bond in alkyl halide

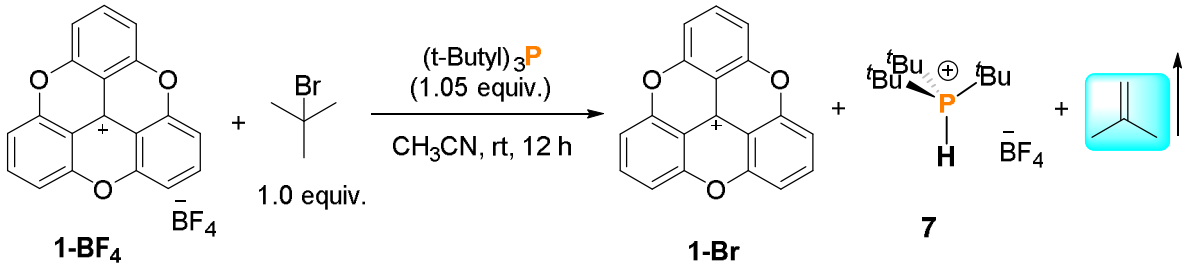

Procedure: An acetonitrile solution (2 mL) of ^{t}butyl bromide (11 µl, 0.1 mmol) was added to acetonitrile solution (2 mL) of **1-BF$_4$** (37.2 mg, 0.1 mmol) and P(^{t}Bu)$_3$ (20.1 mg, 0.1 mmol). After one hour, the reaction mixture turns to yellow to orange was noted, and later orange solid was precipitated from the solution. The solution was stirred overnight at room temperature. The volatiles of the solution were removed under vacuum to give an orange solid. The solid was washed with n-pentane (3 x 3 mL) and ether (2 x 2 mL) and dried under vacuum to give orange solid (62 mg, 96% yield).

The washing solution was combined and evaporated under vacuum did not show any product. ^{1}H NMR indicates both the TOTA signals and the phosphonium signal. Further, the controlled experiment performed where either TOTA^{+} or P(^{t}Bu)$_3$ did not show any phosphonium salt formation.

^{1}H NMR (400 MHz, DMSO) δ = 8.57 (t, *J* = 8.5 Hz, 2H), 7.99 (d, *J* = 8.5 Hz, 4H), 6.18 (d, *J* = 457.5 Hz, 1H).

^{31}P NMR (162 MHz, DMSO) δ = 51.96.

^{19}F NMR (376 MHz, DMSO) δ = -148.27 (d, *J* = 2.2 Hz).

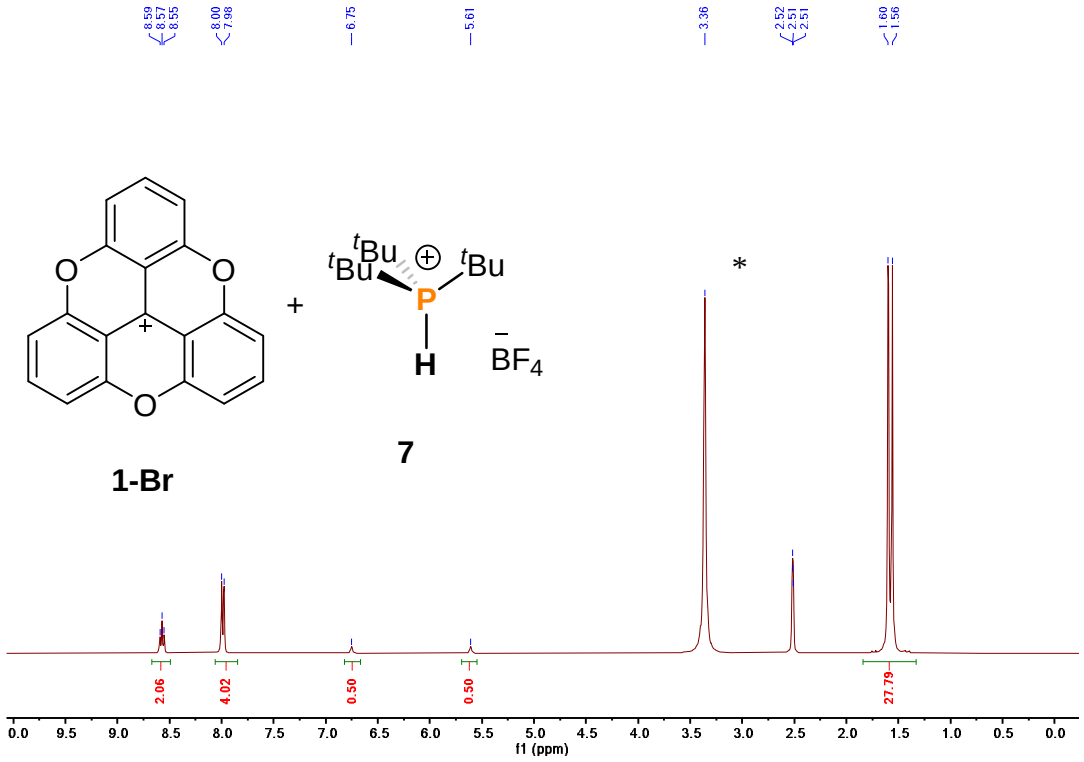

Figure S80: ^{1}H NMR spectrum of reaction crude in DMSO-d^{6} (* indicates residual water)

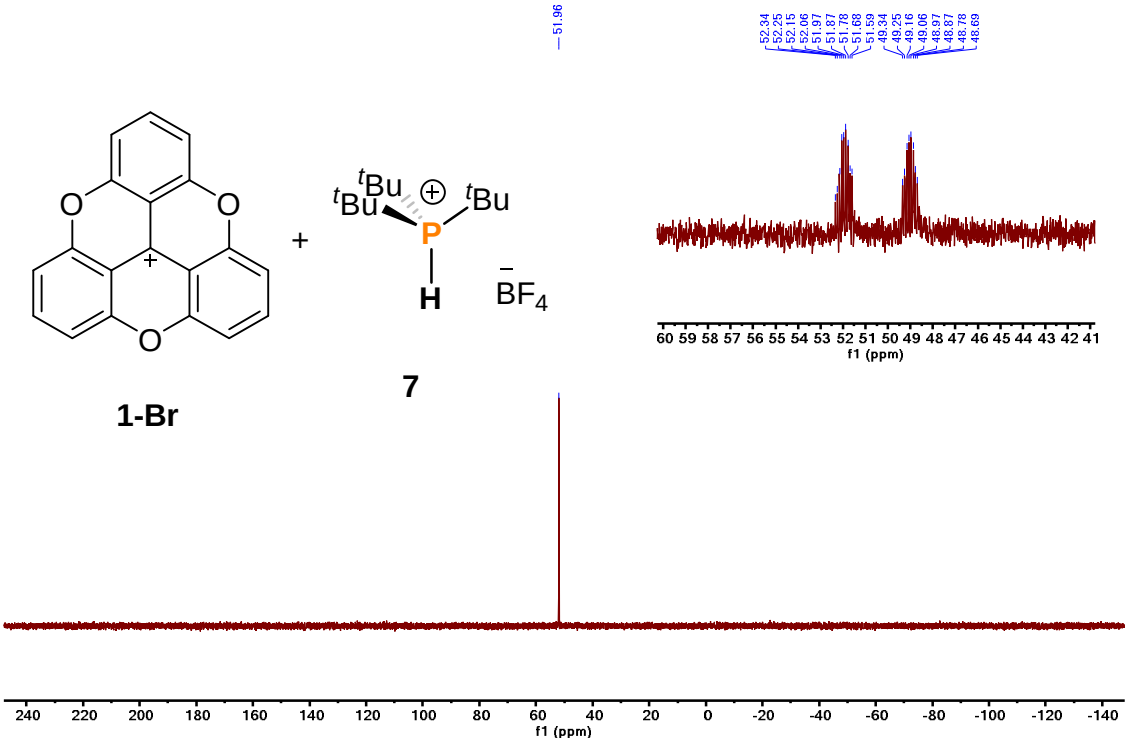

Figure S81: ^{31}P NMR spectrum of reaction crude in DMSO-d^{6}

II.6 Frustrated Lewis pair mediated fixation of formaldehyde

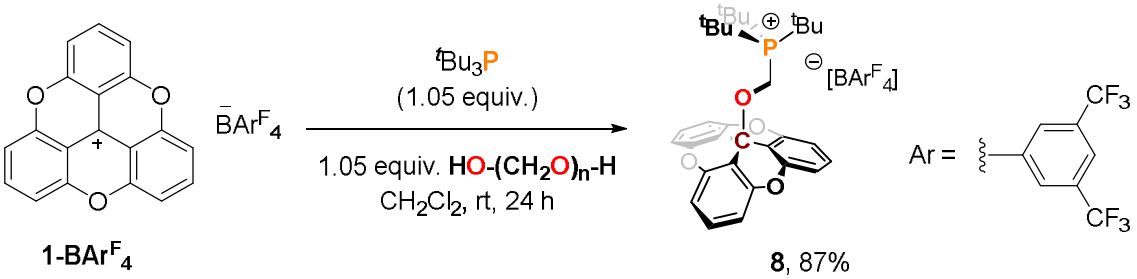

1-BAr$^F_4$ **8**, 87%

Procedure: In a vial (5 mL), **1-BAr$^F_4$** (57.2 mg, 0.05 mmol) and ^{t}Bu$_3$P (10.2 mg, 0.05 mmol) were dissolved in CH_2Cl_2 (2 mL) and stirred for 10 minutes. Then paraformaldehyde (1.5 mg, 0.05 mmol) was added to the reaction mixture. The yellow solution turns colorless after stirring the mixture at room temperature for one hour. The reaction mixture was stirred for an additional 24 hrs at room temperature, whereupon a light precipitate formed which was further diluted with n-pentane. Removing the supernatant by glass pipette and the residue was washed with anhydrous pentane (3 x 3 mL). All volatiles were removed in *vacuo* to yield **6** (58.0 mg, 87 %) as a colorless solid. Crystals suitable for X-ray diffraction analysis were obtained from a mixture of dichloromethane and *n*-pentane at -20 °C.

(((3a^2*H*-4,8,12-trioxadibenzo[*cd,mn*]pyren-3a^2-yl)oxy)methyl)tri-*tert*-butylphosphonium tetrakis(3,5-bis(trifluoromethyl)phenyl)borate (8):

Colourless solid, Yield = 58 mg, 87%; **MP** = 230-232 ºC (decomposition)

1H NMR (500 MHz, CDCl3) δ = 7.81 – 7.61 (m, 8H), 7.52 (d, *J* = 0.7 Hz, 4H), 7.51 – 7.48 (m, 3H), 7.13 (d, *J* = 8.4 Hz, 6H), 3.63 (d, *J* = 5.4 Hz, 2H), 1.24 (d, *J* = 14.3 Hz, 27H).

^{13}C NMR (126 MHz, CDCl$_3$) δ = 164.21 – 158.81 (m), 152.76, 135.01 (dd, *J* = 4.7, 2.6 Hz), 132.00, 130.08 (d, *J* = 6.2 Hz), 129.73 – 128.35 (m), 128.01, 125.84, 123.67, 117.69 (t, *J* = 3.8 Hz), 111.94, 111.60, 111.35, 105.35, 61.01 (d, *J* = 11.0 Hz), 50.27 (d, *J* = 55.5 Hz), 38.95 (d, *J* = 26.4 Hz), 29.11.

^{31}P NMR (202 MHz, CDCl$_3$) δ = 44.17 (td, *J* = 29.1, 28.7, 14.4 Hz).

^{11}B NMR (160 MHz, CDCl$_3$) δ = -6.63 (dt, *J* = 5.6, 2.8 Hz).

^{19}F NMR (376 MHz, CDCl$_3$) = δ -62.85.

MALDI-TOF m/z: [M^+] Calcd. for $C_{32}H_{38}O_4P$ 517.2502; Found: 517.2513. **HRMS (ESI) m/z**; major fragmentation for TOTA$^+$ [M^+-$C_{13}H_{29}OP$]$^+$ at 285.0546 and [$C_{13}H_{29}OP$]$^+$ i.e. [M^+-$C_{19}H_9O_3$]$^+$ at 233.2028 noted.

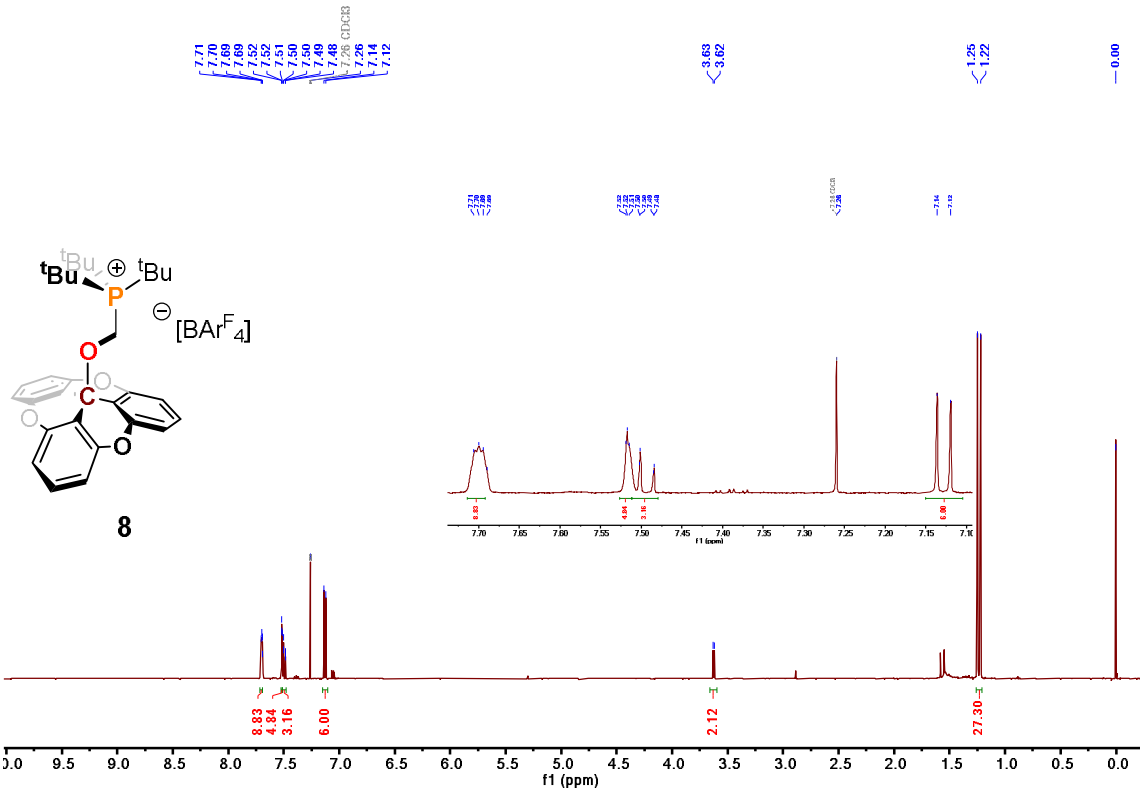

Figure S82: ^{1}H NMR spectrum of 8 in $CDCl_3$

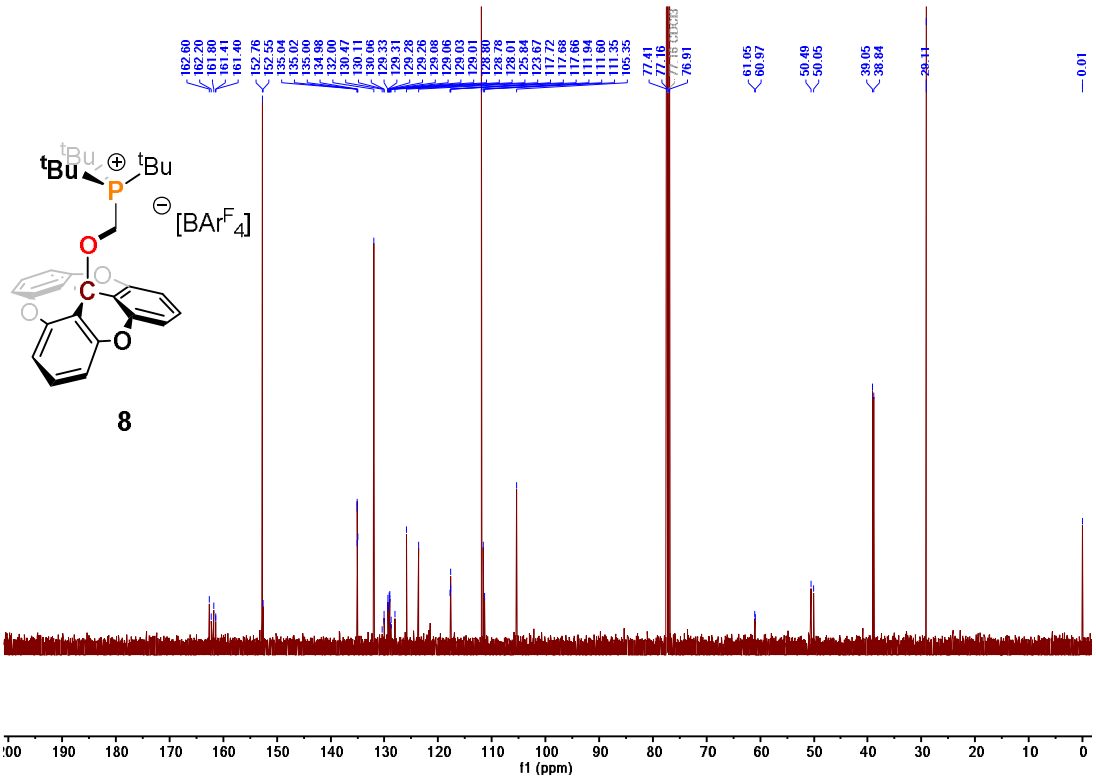

Figure S83: ^{13}C NMR spectrum of 8 in $CDCl_3$

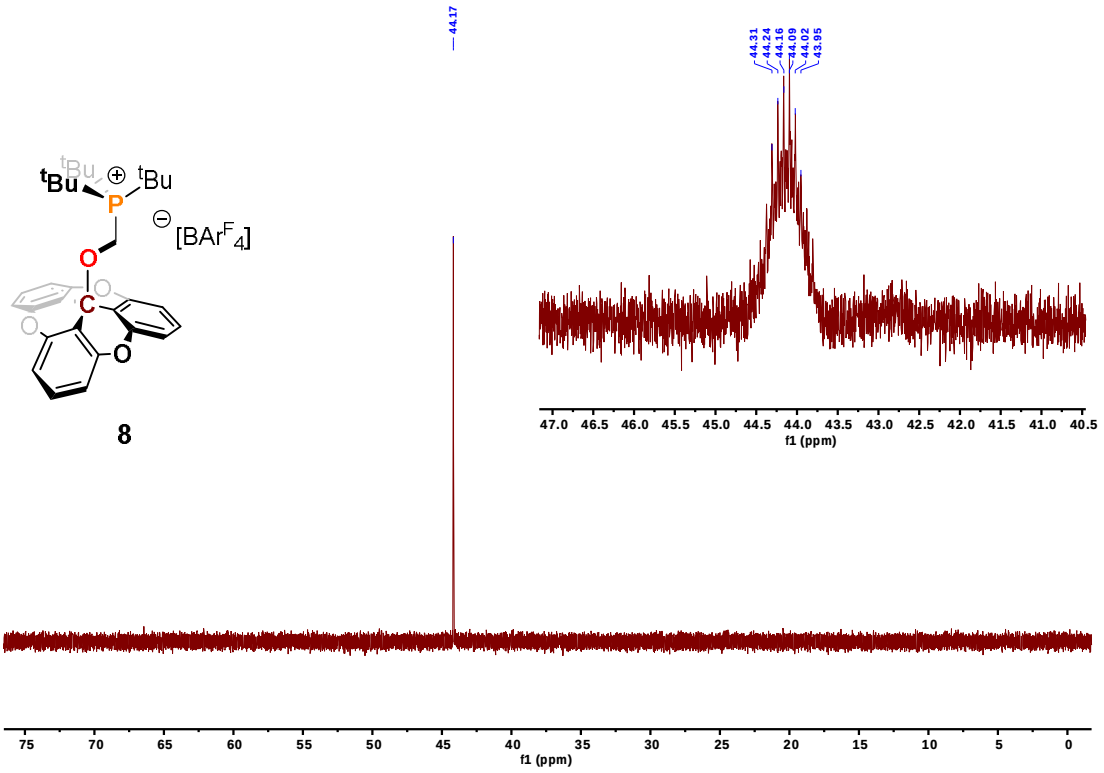

Figure S84: ^{31}P NMR spectrum of 8 in $CDCl_3$

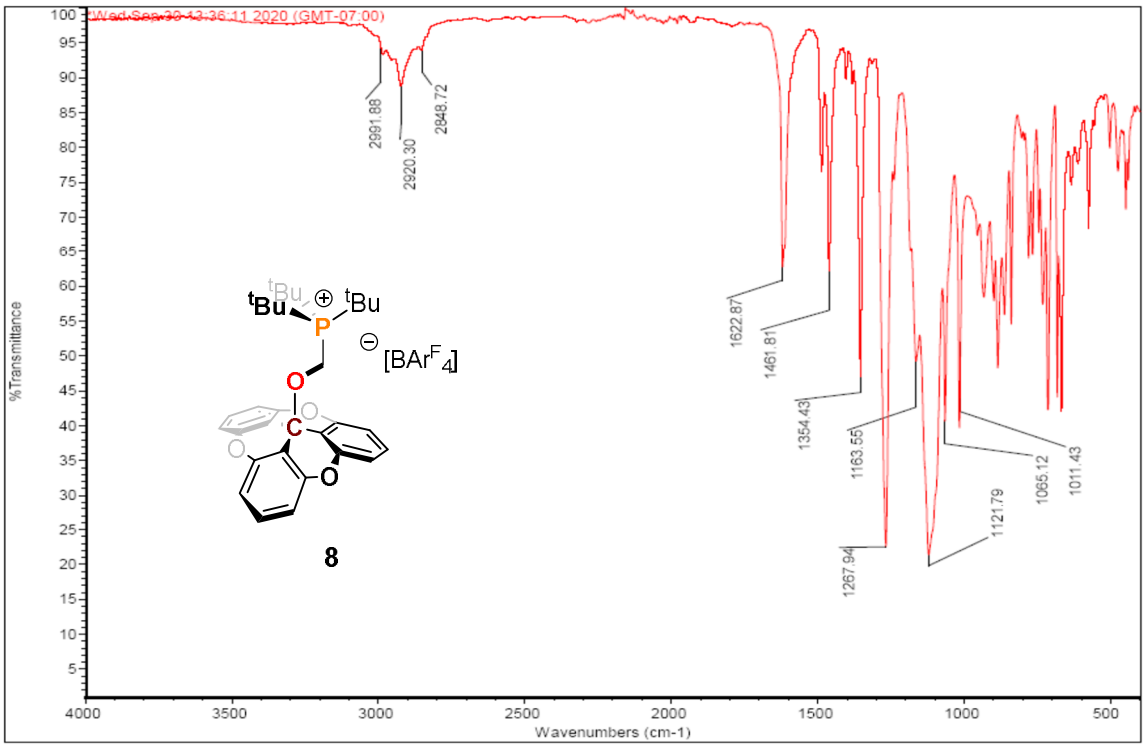

Figure S85: IR spectrum of 8

II.7 Frustrated Lewis pair mediated fixation of Staudinger reaction intermediate

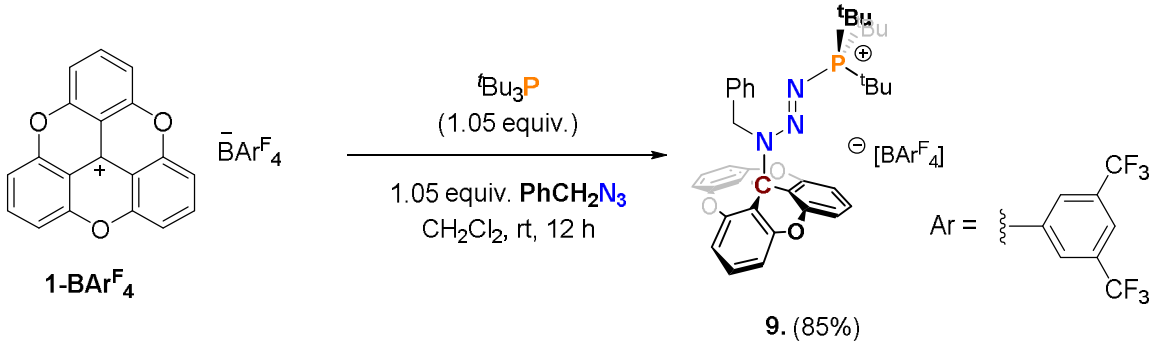

Procedure: A solution of benzyl azide (8.6 mg, 0.065 mmol, 1.3 equiv) in CH_2Cl_2 (2 mL) was added dropwise to a solution of **1-BAr$^F_4$** (57 mg, 0.05 mmol, 1.0 equiv) and P(^{t}Bu)$_3$ (10 mg, 0.05 mmol, 1.0 equiv.) in CH_2Cl_2 (2 mL) at room temperature and let to react for 12 h. The orange to pale yellow color change noted. After subsequent standing overnight at room temperature, half of CH_2Cl_2 were removed under reduced pressure. The addition of pentane (5ml) resulted in the deposition of white crystals which were collected by filtration, washed with pentane (2 x 5 mL) to give **2a** as a pale-yellow solid in 85% yield (68 mg). Crystals suitable for single X-ray diffraction were grown by slow diffusion of pentane into a solution of **9** in CH_2Cl_2.

Note: This compound is slightly air sensitive, undergoes decomposition to the unidentified product.

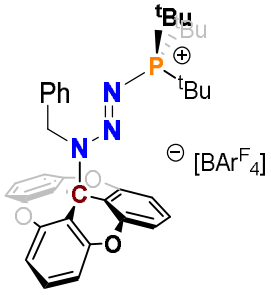

9

(*E*)-(3-(3a^2*H*-4,8,12-trioxadibenzo[*cd,mn*]pyren-3a^2-yl)-3-benzyltriaz-1-en-1-yl)tri-*tert*-butylphosphonium tetrakis(3,5-bis(trifluoromethyl)phenyl)borate (9):

Pale Yellow solid, 85% yield, **MP** = 120-122 ºC;

^{1}H NMR (500 MHz, CD_2Cl_2) δ = 7.73 (m, 8H), 7.56 (dq, *J* = 2.2, 1.2 Hz, 4H), 7.48 (t, *J* = 8.3 Hz, 3H), 7.13 (d, *J* = 8.3 Hz, 6H), 7.11 – 7.04 (m, 3H), 6.51 (ddt, *J* = 5.9, 3.3, 0.9 Hz, 2H), 4.83 (d, *J* = 0.8 Hz, 2H), 1.14 (d, *J* = 14.1 Hz, 27H).

^{13}C NMR (100 MHz, CD_2Cl_2) δ = 162.18 (dd, *J* = 99.7, 49.8 Hz), 153.45, 152.67, 135.22, 132.20, 130.27, 129.92 – 129.05 (m), 129.02, 127.91, 126.37, 125.30, 123.66, 120.95, 119.37 – 115.75 (m), 112.88, 111.72, 107.64, 50.44, 40.97 (d, *J* = 31.8 Hz), 29.74, 29.21.

^{31}P NMR (202 MHz, CD_2Cl_2) δ = 64.65.

^{11}B NMR (160 MHz, CD_2Cl_2) δ = -6.60 (dq, *J* = 5.5, 2.8 Hz).

^{19}F NMR (376 MHz, CD_2Cl_2) δ = -62.83.

HRMS (ESI) m/z: $[M]^+$ Calcd. for $C_{38}H_{43}N_3O_3P$, 620.3036; Found: 620.3039. Major fragmentation TOTA$^+$ $C_{19}H_9O_3^+$ 285.0545.

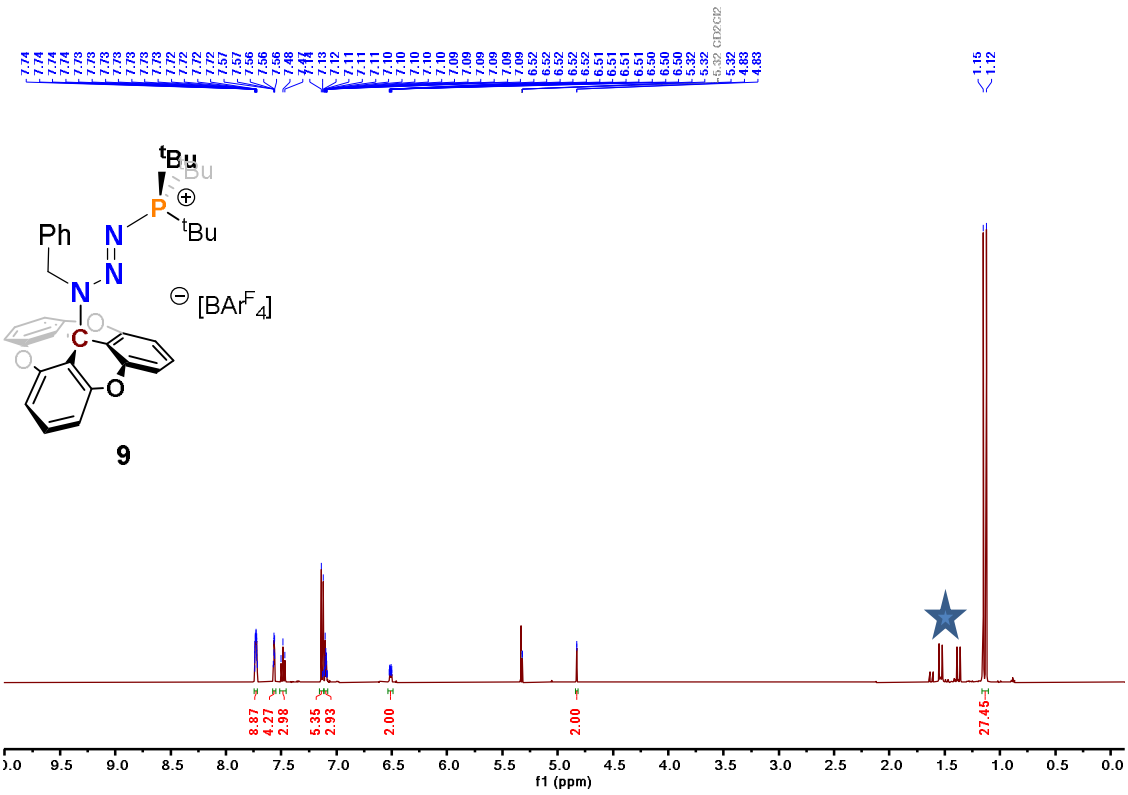

Figure S86: ^{1}H NMR spectrum of 9 in CD_2Cl_2 (*some impurities after degradation of 9)

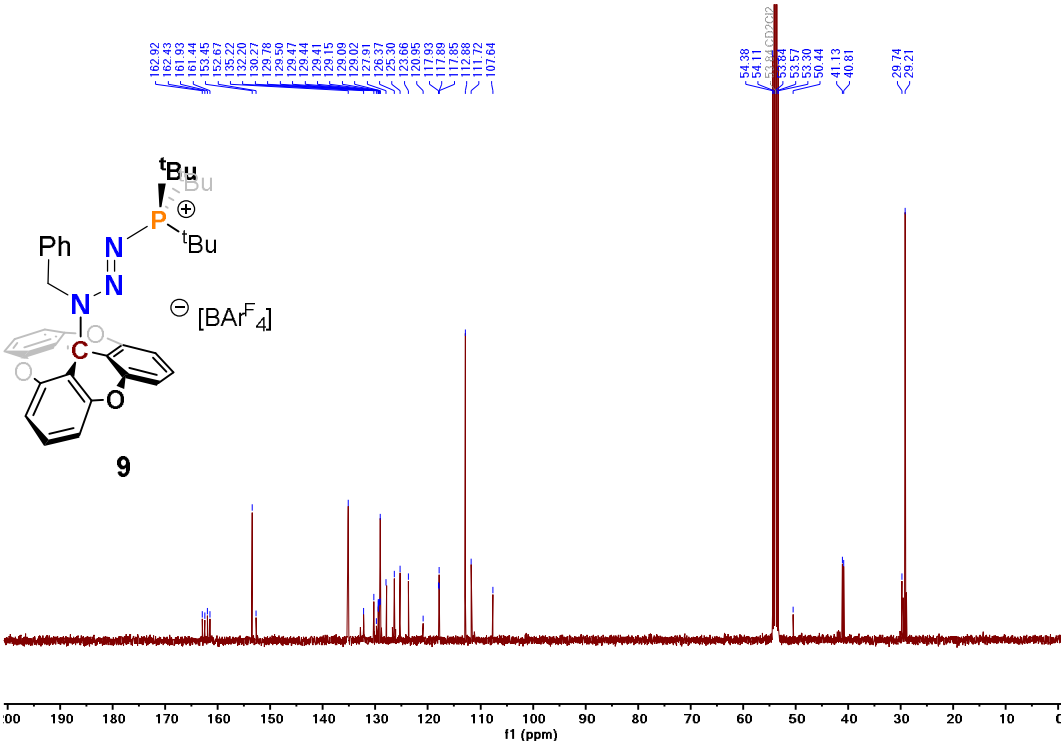

Figure S87: ^{13}C NMR spectrum of 9 in CD_2Cl_2

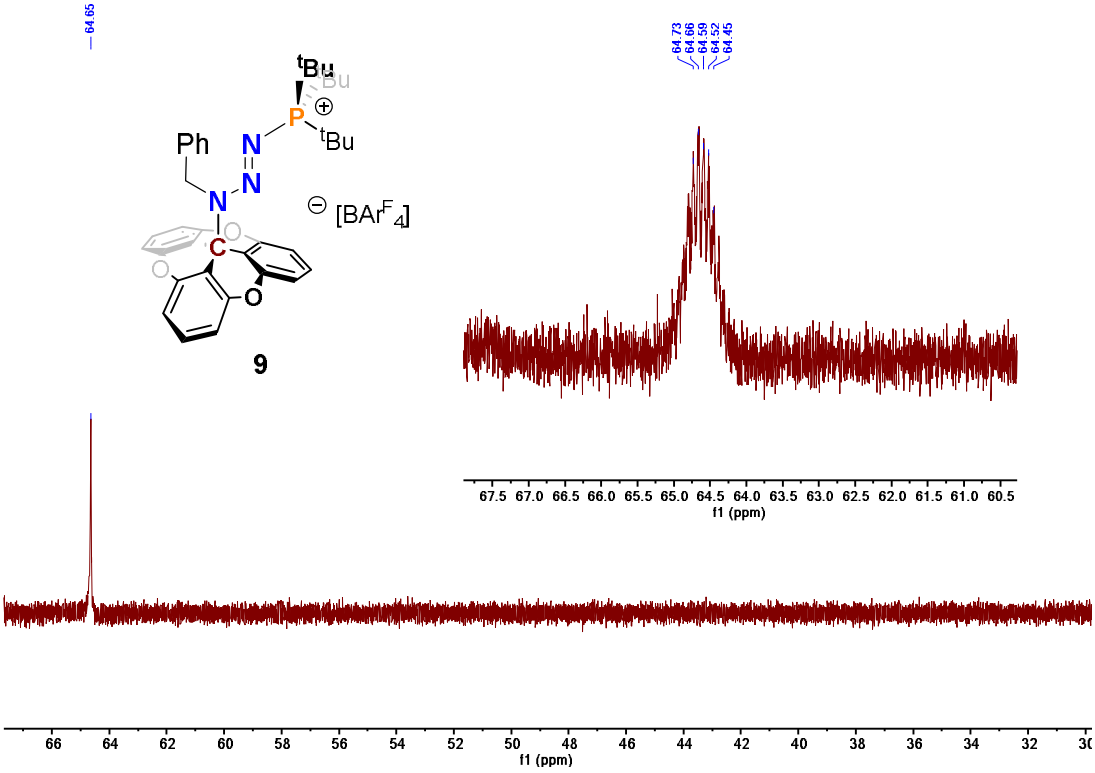

Figure S88: ^{31P} NMR spectrum of 9 in CD_2Cl_2

II.8 The reaction of I*t*Bu with 1-[X]

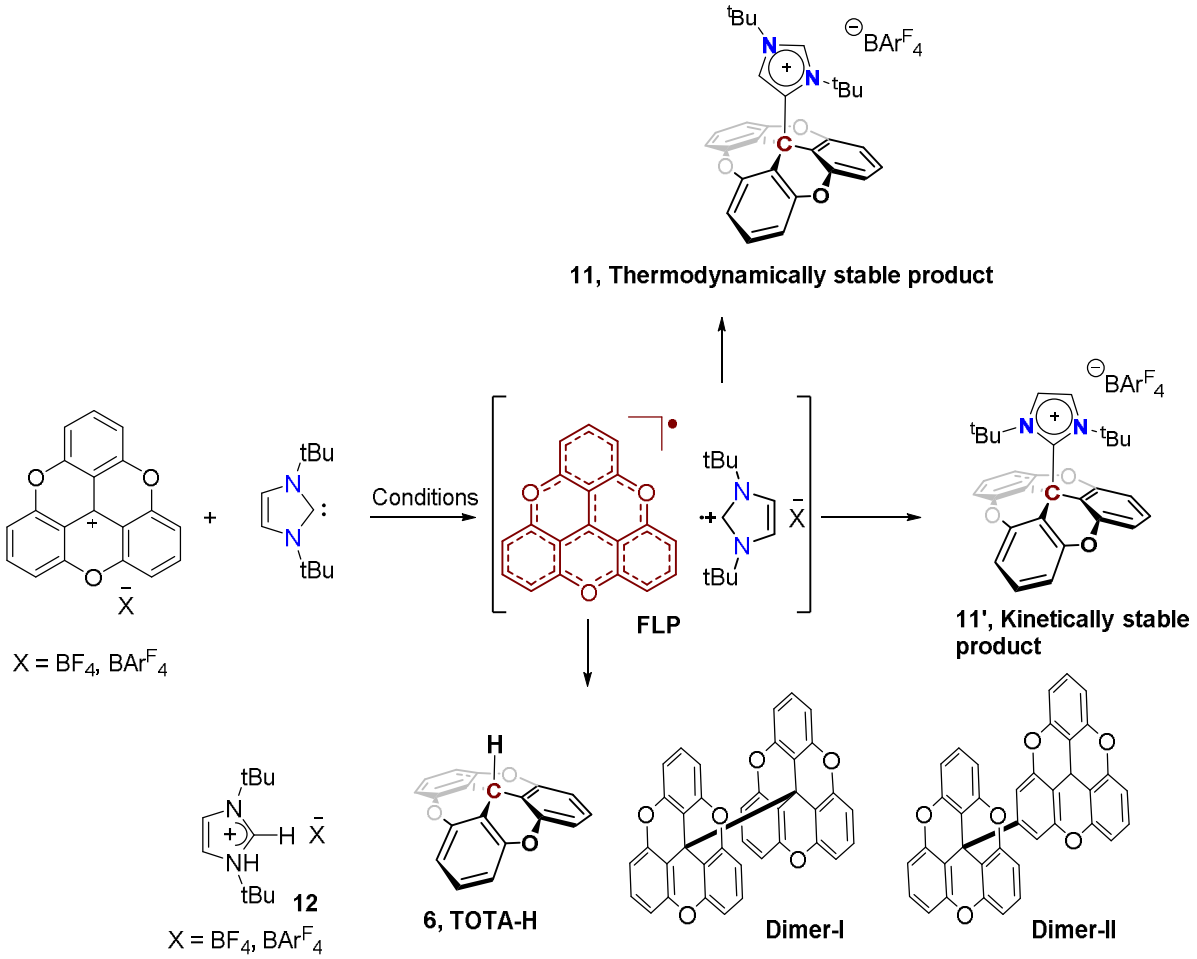

Scheme S1: Possible product formation of reaction between **1**-/NHC.

Table S1: Screening of reaction condition

Sr No	Reaction Conditions	Results
1	Toluene, rt, 1 h	79%(**11**), 10%(**11′**), 10%(**12**),
2	Toluene, -78 °C, 30 min	69%(**11′**), 28%(**12**)
3	CH_3CN, rt, 1 h	<5% (**11** and **11′**), <96% (**12**), 15% (**6**), Dimers
4	Toluene with 25% THF(radical scavenger), rt, 1 h	61%(**11**), 18% (**12**), 14%(**6**),
5	Toluene with 1.0 Equiv. of TEMPO, rt, o/n	58%(**11**), 32%(**12**), no TEMPO adduct formation noted

6	CH_3CN with 1.0 Equiv. of Bz_2O_2, rt, o/n	1-OBz adduct formation not observed
7	CH_3CN, under dark condition, rt, 1 h	18% (**11′**), <74% (**12**), Dimers

Reaction condition: (a) 1-BAr^F_4 (12 mg, 0.01 mmol), I*t*Bu (1.6 mg, 0.01 mmol), 2 ml of solvent, room temperature, 1 h. (b) 2,4,6 tri-methoxy benzene is used as internal standard for NMR yield determination.

II.9a. The reaction of I^{t}Bu with 1-[BAr^F_4] in toluene at room temperature:

A toluene solution (1 mL) of I^{t}Bu (9 mg, 0.05 mmol) was added to a stirred toluene solution (1mL) of **1-BAr^F_4** (57 mg, 0.05 mmol) at room temperature. The color of the solution changed from yellow to light purple, and then to light yellow. The resulting reaction mixture was stirred for another 1 h. After that, the solvent was removed under vacuum, and the light-yellow solid was obtained. Further, the adduct (**11**) was purified by neutral alumina with CH_2Cl_2/Hexane as the mobile phase.

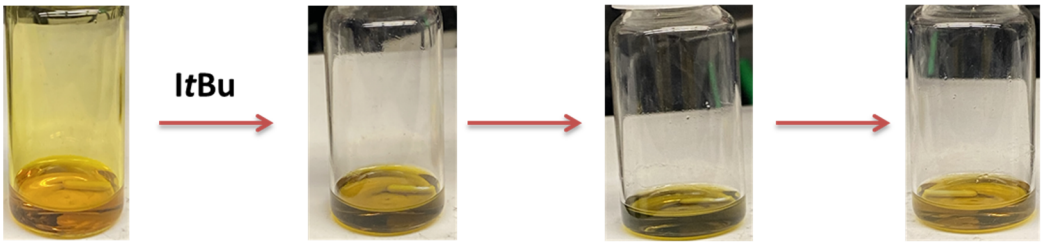

Figure S89: Colour change of reaction of I^{t}Bu with **1-[BAr^F_4]** in Toluene

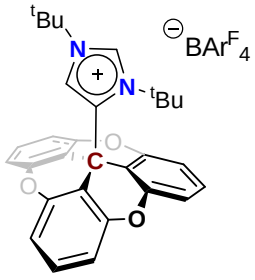

11

Off white solid, 51 mg; 79% yield; **MP** = 136-138 ºC;

^{1}H NMR (500 MHz, $CDCl_3$) δ = 7.90 (d, *J* = 2.2 Hz, 1H), 7.70 (p, *J* = 2.2 Hz, 8H), 7.53 (s, 4H), 7.44 (dd, *J* = 8.1 Hz, 3H), 7.09 (d, *J* = 8.3 Hz, 6H), 6.53 (d, *J* = 2.2 Hz, 1H), 1.36 (s, 9H), 1.34 (s, 9H).

^{13}C NMR (126 MHz, $CDCl_3$) δ = 162.20 (dd, *J* = 99.8, 50.1 Hz), 142.18, 135.27, 131.82, 131.43, 130.08 – 128.29 (m), 128.26, 126.09, 124.59, 123.92, 121.75, 117.96, 113.30, 112.25, 65.22, 61.23, 32.45, 30.37, 29.35.

^{19}F NMR (376 MHz, $CDCl_3$) δ = -62.37.

^{11}B NMR (160 MHz, $CDCl_3$) δ = -6.65 (dt, *J* = 5.7, 2.9 Hz).

HRMS (ESI) m/z: [M^+] Calcd. for $C_{30}H_{29}N_2O_3$ 465.2172; 465.2169.

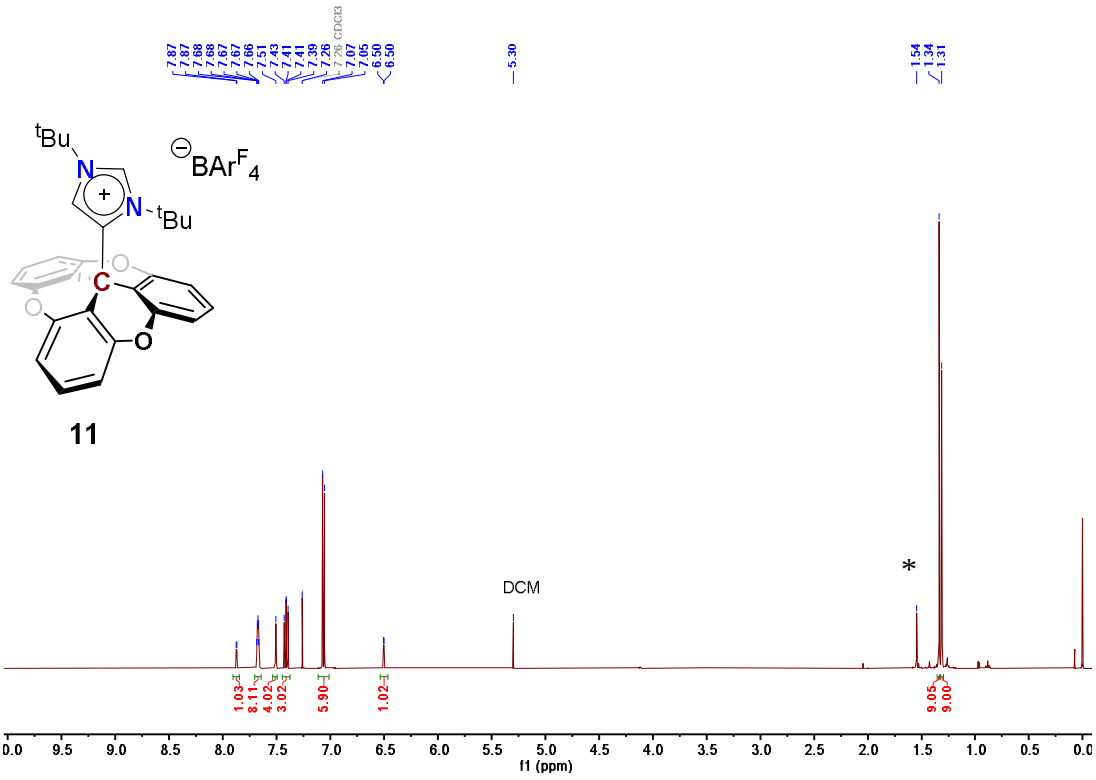

Figure S90: ^{1}H NMR spectrum of 11 in $CDCl_3$ (* indicates residual water)

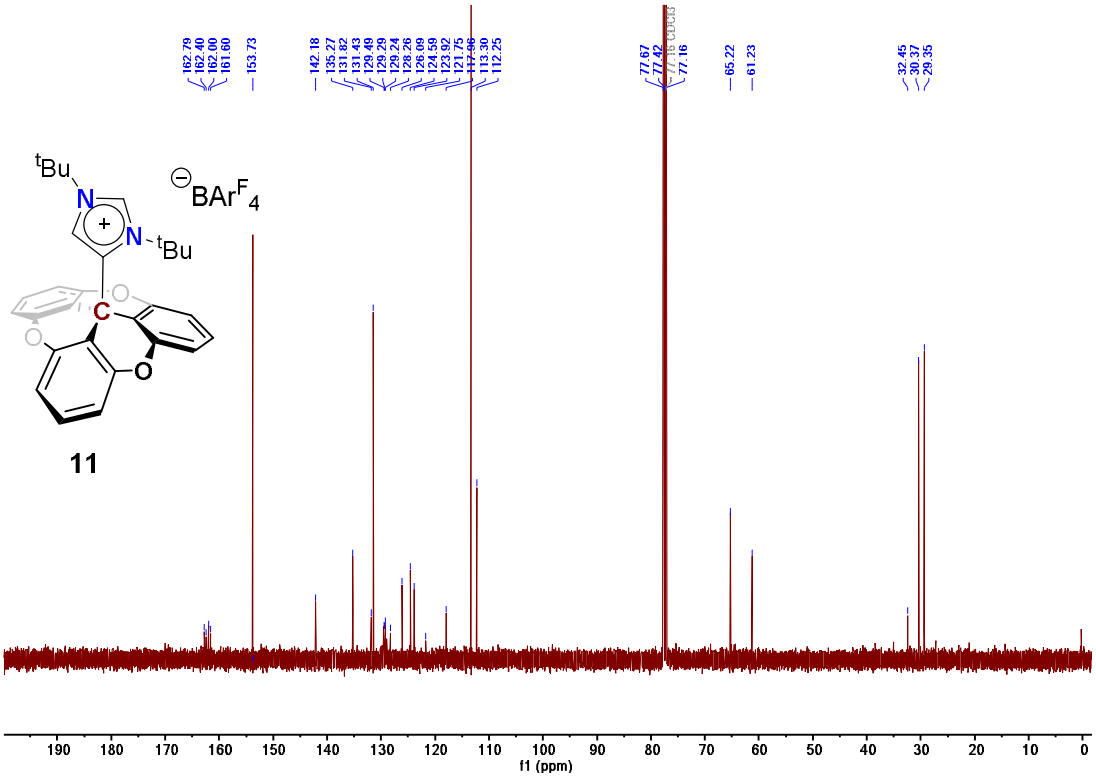

Figure S91: ^{13}C NMR spectrum of 11 in $CDCl_3$

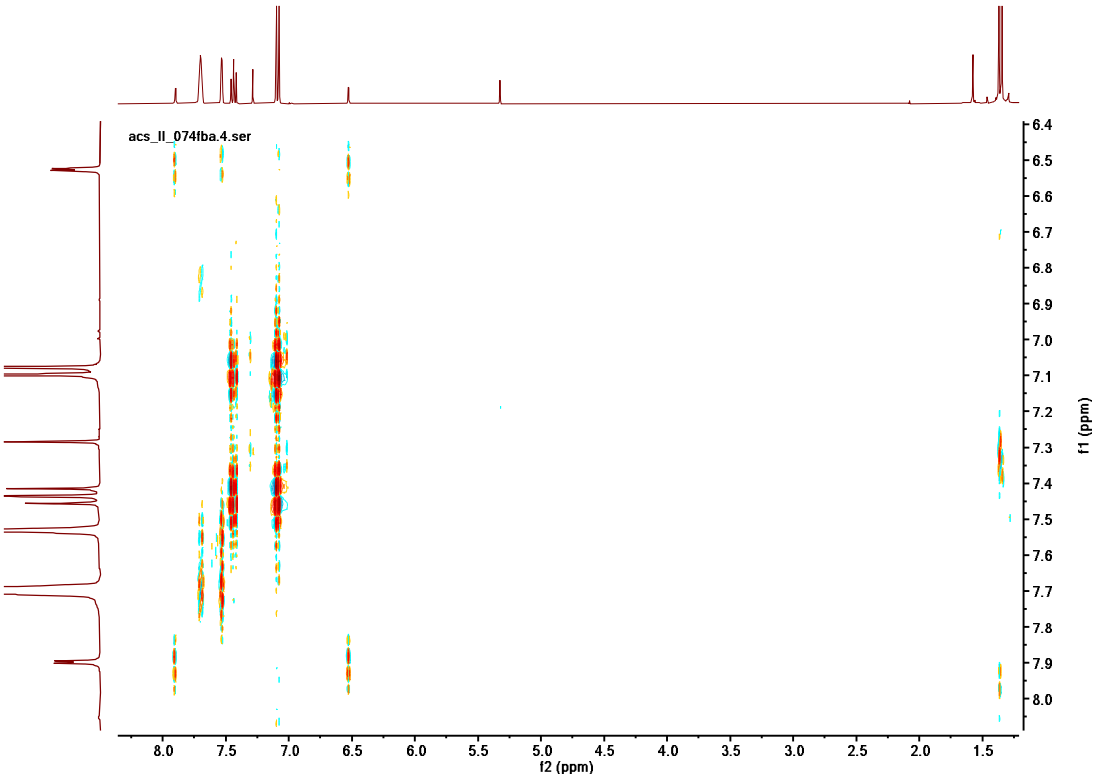

Figure S92: ^{1}H-^{1}H COSY spectrum of 11 in $CDCl_3$

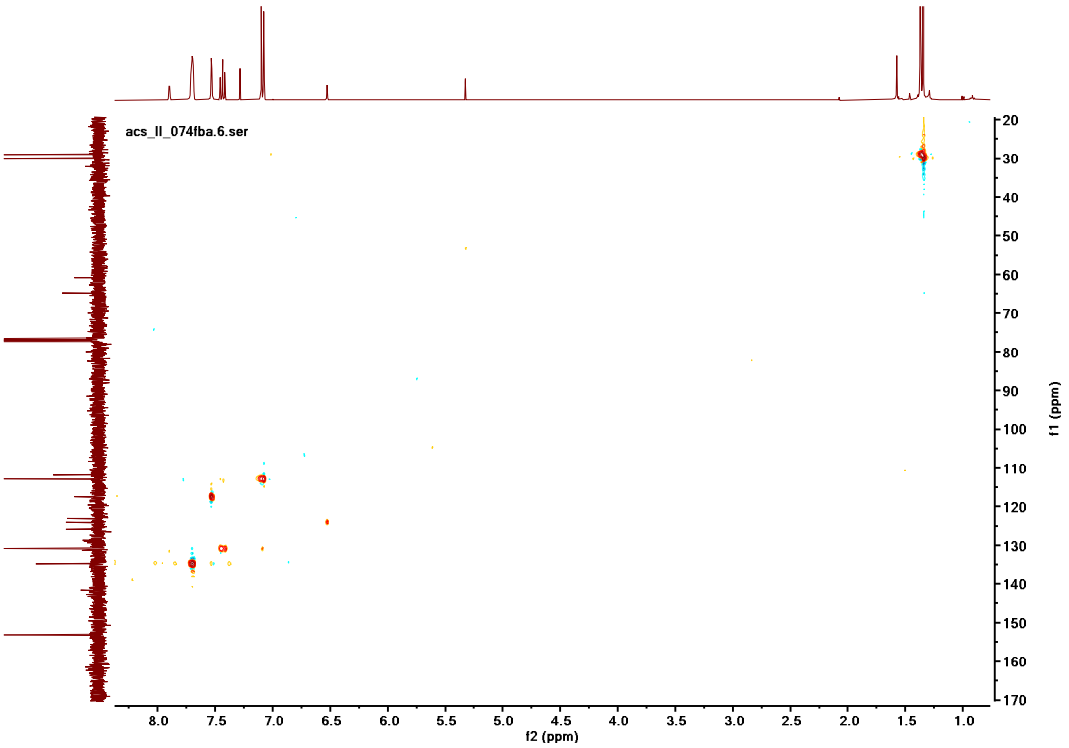

Figure S93: ^{1}H-^{13}C HSQC spectrum of 11 in $CDCl_3$

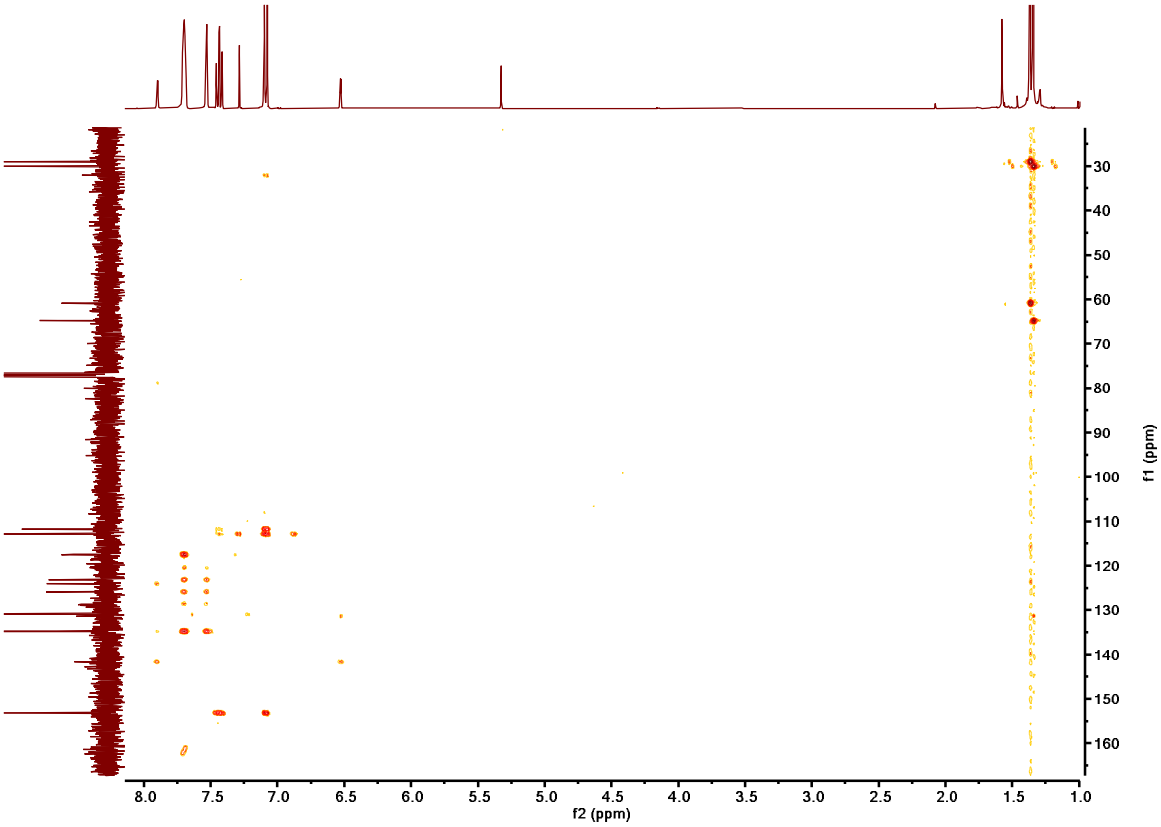

Figure S94: ^{1}H-^{13}C HMBC spectrum of 11 in $CDCl_3$

II. 9b. Reaction of I*t*Bu with 1-[BAr^F_4] in Toluene at -78 °C:

A cooled toluene solution (2 mL) of I^{t}Bu (9 mg, 0.05 mmol was added slowly to a stirred toluene solution (2 mL) of **1-BAr^F_4** (57 mg, 0.05 mmol) at –78 °C. The color of the solution changed from orange to pale yellow. The resulting suspension was stirred for another 30 min. After that, the solvent was removed under vacuum, and the residue was washed three-times with *n*-pentane (3 x 4 mL). The resulting off white solid was dried under vacuum. The crude NMR shows the mixture of C2-adduct (**11′**) and imidazolium salt (**12**) in the 3:2 ratio. The recrystallization in several solvents performed however the cleavage of the adduct is noted. Like the C4-adduct, the column purification with neutral alumina was attempted however here also cleavage of the adduct is noted. Later, the crude reaction mixture was analysed for the formation C2-adduct (**11′**).

NOTE- This compound contains non-separable imidazolium BAr^F_4 salt. In ^{1}H NMR the imidazolium salt protons are showed with an asterisk (*)

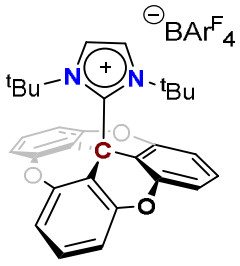

11'

Off white solid, 69% (NMR yield);

^{1}H NMR (500 MHz, $CDCl_3$) = δ 7.68 (p, *J* = 2.3 Hz, 8H), 7.53 (s, 4H), 7.39 (t, *J* = 8.3 Hz, 3H), 7.23 (d, *J* = 1.8 Hz, 2H), 7.06 (d, *J* = 8.3 Hz, 6H), 1.53 (s, 18H).

^{13}C NMR (126 MHz, $CDCl_3$) = δ 161.73 (dd, *J* = 99.8, 49.9 Hz), 152.34, 134.80, 129.86, 129.39 – 128.42 (m), 128.26, 127.79, 125.33, 123.45, 121.28, 120.38, 117.56 (d, *J* = 4.1 Hz), 111.40, 110.62, 61.08, 50.52, 29.31.

^{19}F NMR (376 MHz, $CDCl_3$) δ = -62.37.

^{11}B NMR (160 MHz, D_2O) δ = -6.65.

HRMS (ESI) m/z: [M^+] Calcd. for $C_{30}H_{29}N_2O_3$ 465.2172; 465.2170.

(Imidazolium salt (**12[BAr^F_4]**): **^{1}H NMR (400 MHz, $CDCl_3$) δ** = 8.03 (s, 1H), 7.67 (dd, *J* = 5.2, 2.6 Hz, 8H), 7.52 (s, 4H), 7.23 (d, *J* = 1.8 Hz, 2H), 1.54 (s, 18H))

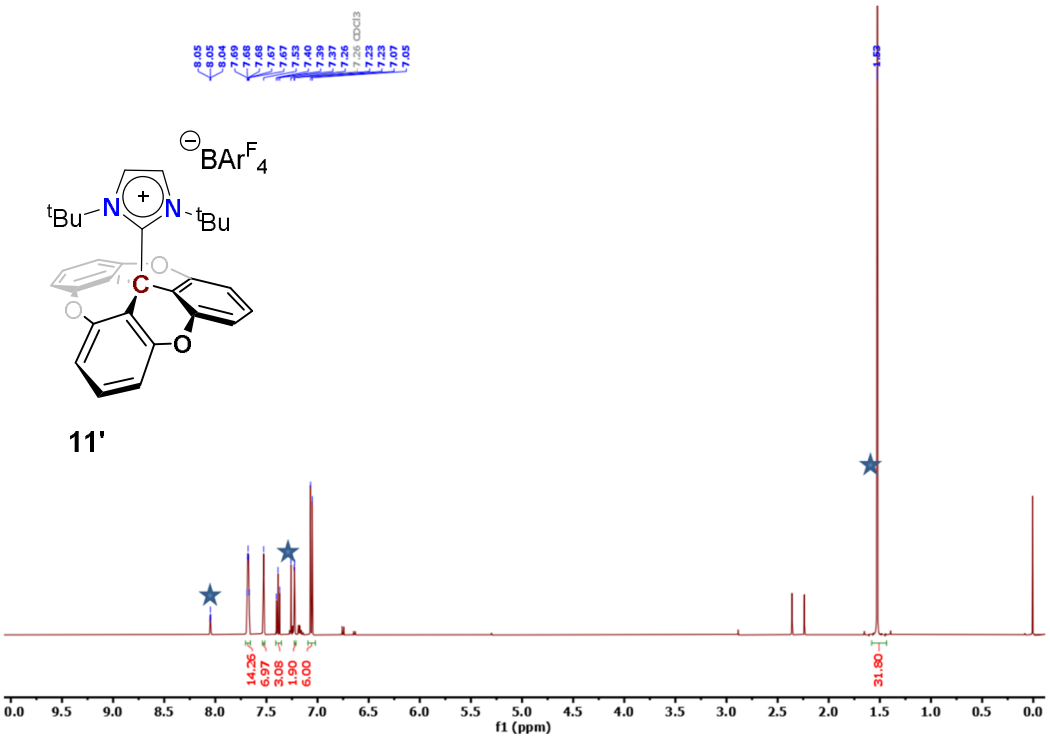

Figure S95: ^{1}H NMR spectrum of 11′ in $CDCl_3$ (*peaks belongs to imidazolium salt)

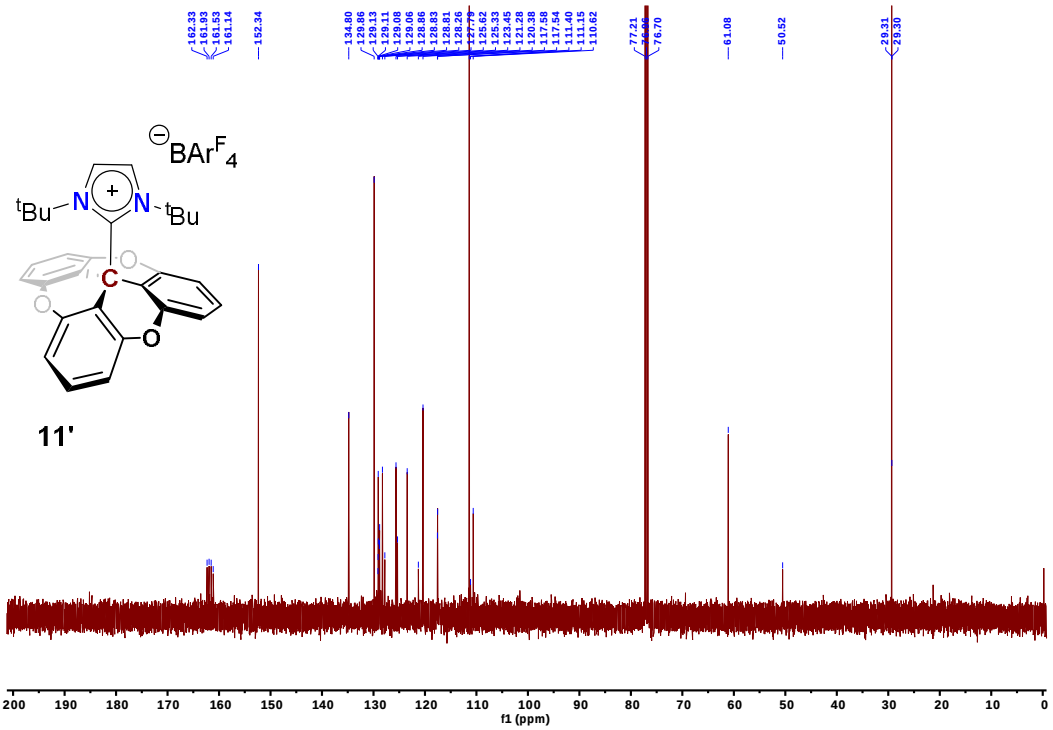

Figure S96: ^{13}C NMR spectrum of 11′ in $CDCl_3$

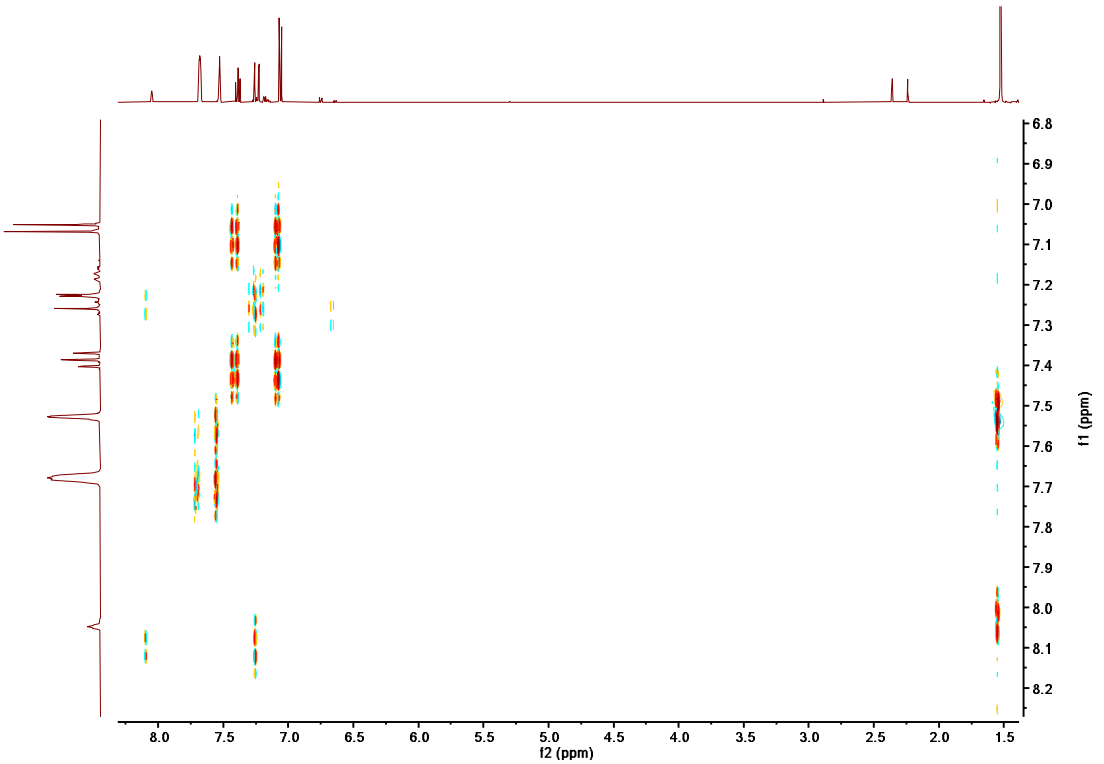

Figure S97: ^{1}H-^{1}H COSY spectrum of 11′ in $CDCl_3$

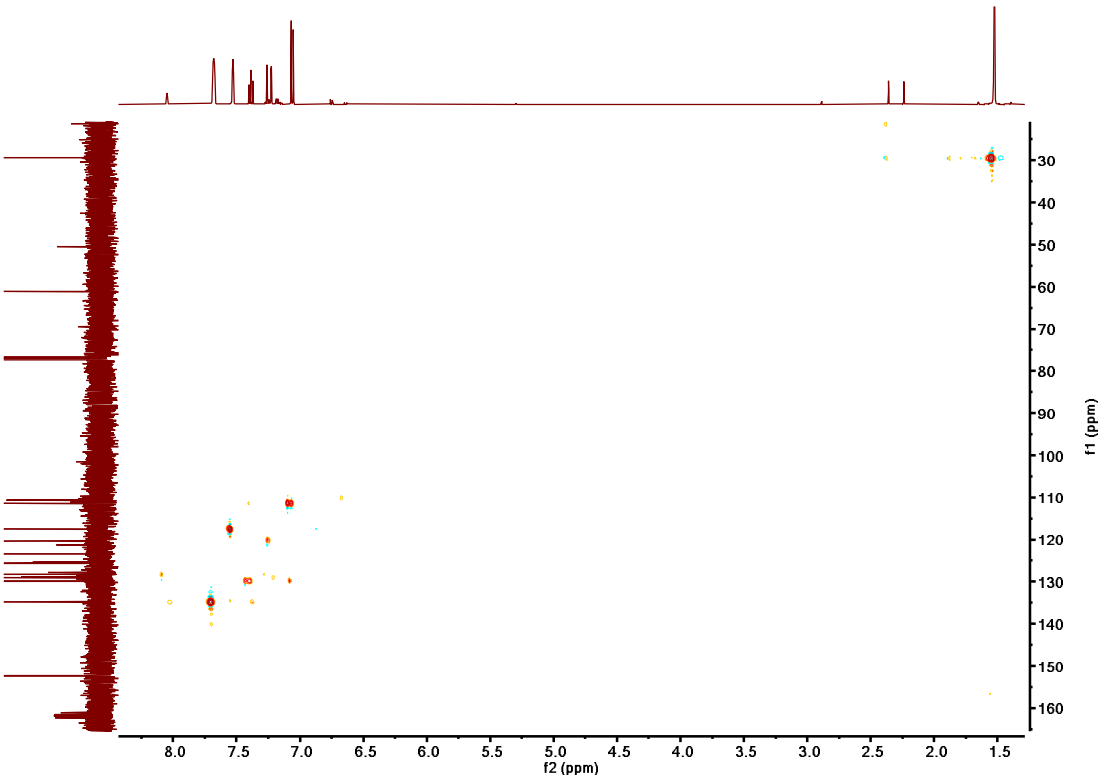

Figure S98: ^{1}H-^{13}C HSQC spectrum of 11′ in $CDCl_3$

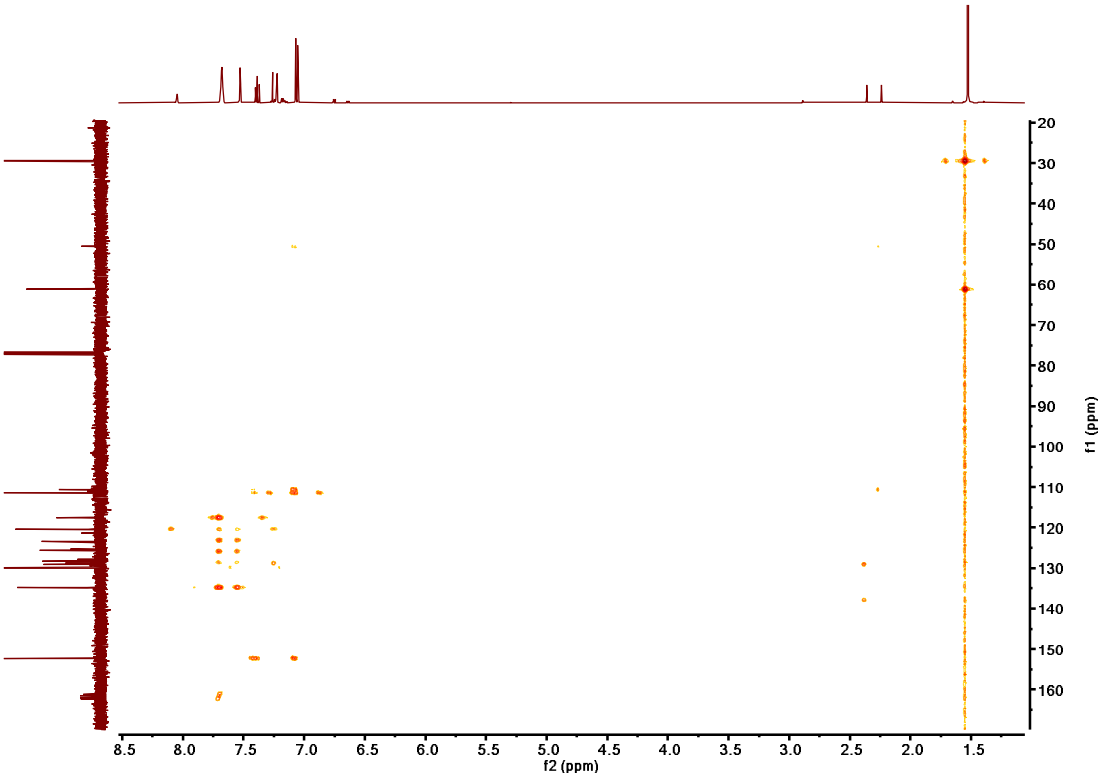

Figure S99: ^{1}H-^{13}C HMBC spectrum of 11′ in $CDCl_3$

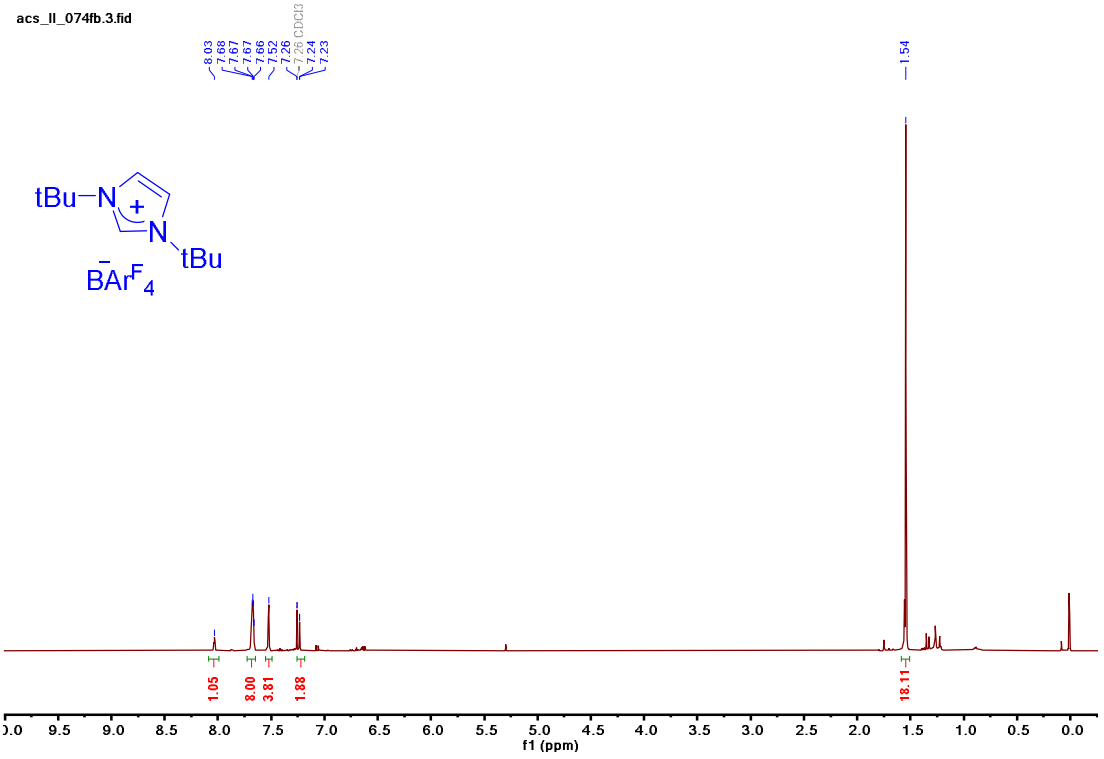

Figure S100: ^{1}H NMR spectrum for imidazolium [BAr^{F}_{4}] salt (12)

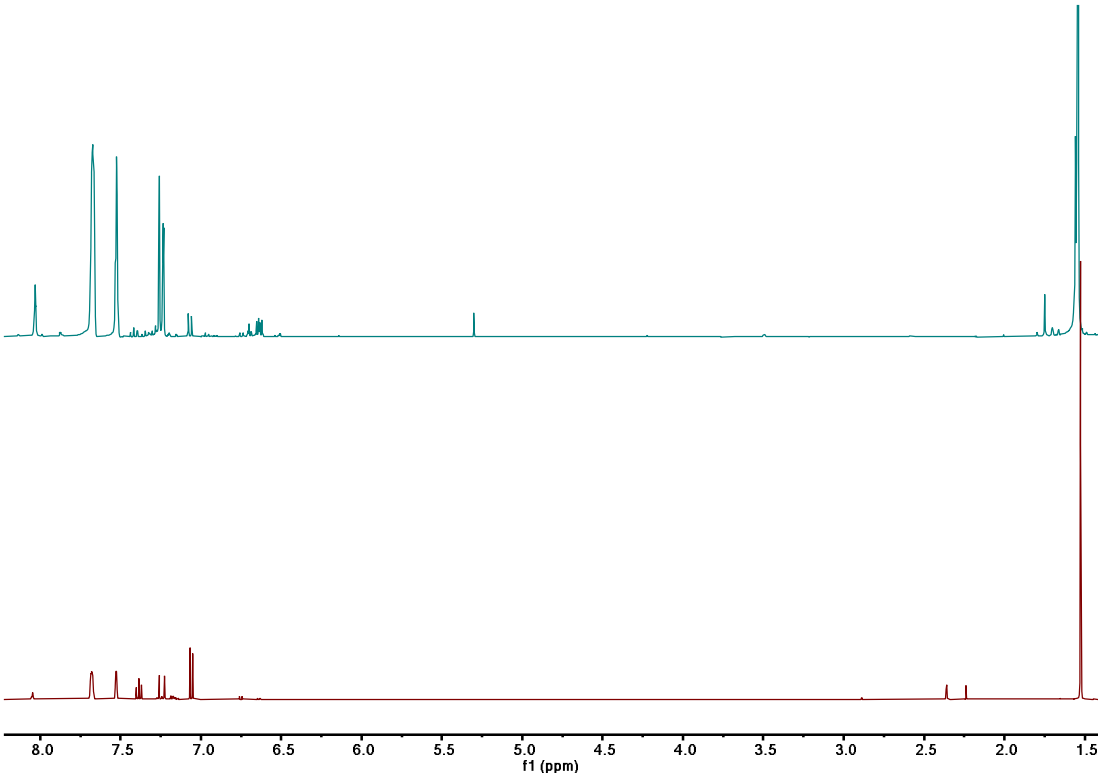

Figure S101: Stacked ^{1}H NMR spectrum for imidazolium [BAr$^{F}_{4}$] with C2-adduct (11′)

II.9c. The reaction of I^{t}Bu with 1-BF$_4$ in CH$_3$CN at room temperature:

An acetonitrile solution (1 mL) of I^{t}Bu (**10**, 18 mg, 0.1 mmol) was added slowly to a stirred acetonitrile solution (1mL) of **1-BF$_4$** (37.2 mg, 0.1 mmol) at room temperature. The color of the solution changed from yellow to green, and then to brown. The resulting suspension was stirred for another 10 min and green solid precipitated out in the reaction mixture (see below Figure S79). After that, the solvent was removed under vacuum, and the residue was washed three-times with n-pentane (3 x 4 mL). The resulting green solid was dried under vacuum (yield: 33 mg, 98%).

Figure S79 indicates the crude ^{1}H NMR spectrum for the reaction which indicates the formation of TOTA-H and TOTA-dimers. The TOTA-dimers are not soluble in acetonitrile which crash out in solution.

TOTA-dimer: **^{1}H NMR (500 MHz, CDCl$_3$) δ** = 7.26 (t, *J* = 8.2 Hz, 6H), 6.64 (d, *J* = 8.2 Hz, 12H).

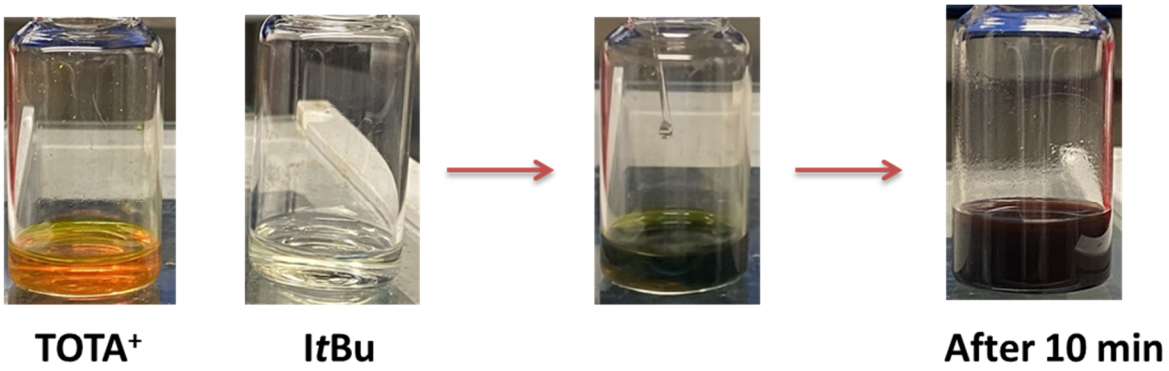

Figure S102: Colour change of reaction of I^{t}Bu with 1-BAr$^F_4$ in CH_3CN

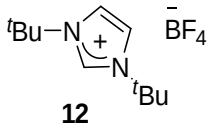

12

1,3-di-*tert*-butyl-1*H*-3λ^4-imidazole tetrafluoroborate (**12**):[10]

^{1}H NMR (400 MHz, $CDCl_3$) δ = 8.82 (t, *J* = 1.8 Hz, 1H), 7.48 (d, *J* = 1.8 Hz, 2H), 1.71 (s, 18H).

^{13}C NMR (101 MHz, $CDCl_3$) δ = 132.38, 120.42, 61.17, 30.12.

^{19}F NMR (376 MHz, $CDCl_3$) δ = -151.25.

^{11}B NMR (160 MHz, $CDCl_3$) δ = -0.96 (d, *J* = 1.0 Hz).

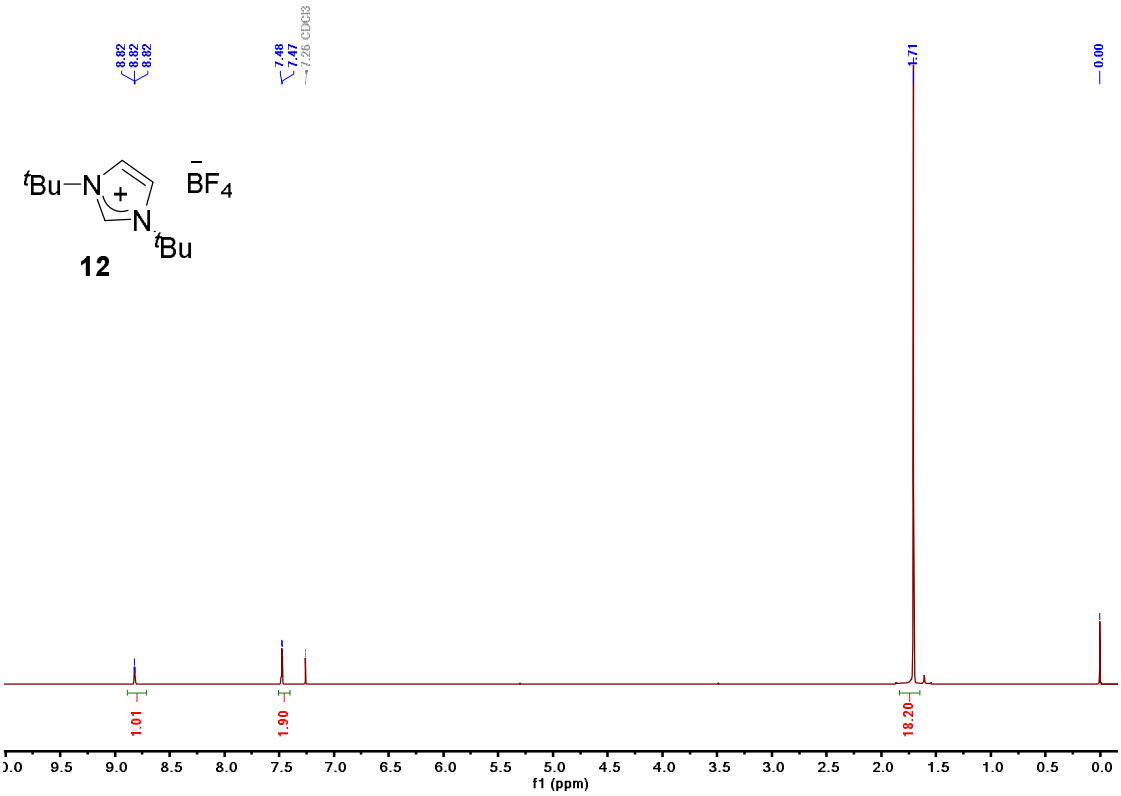

Figure S103: ^{1}H NMR spectrum of 12[BF_4] in $CDCl_3$

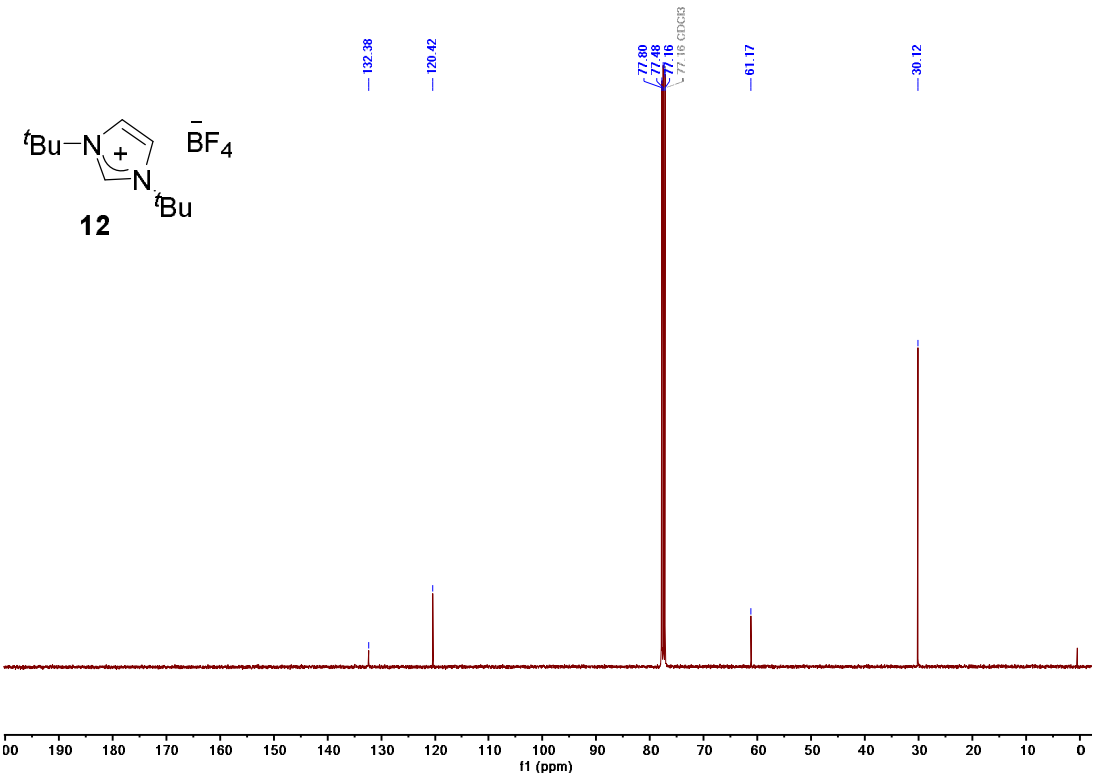

Figure S104: ^{1}H NMR spectrum of 12[BF_4] in $CDCl_3$

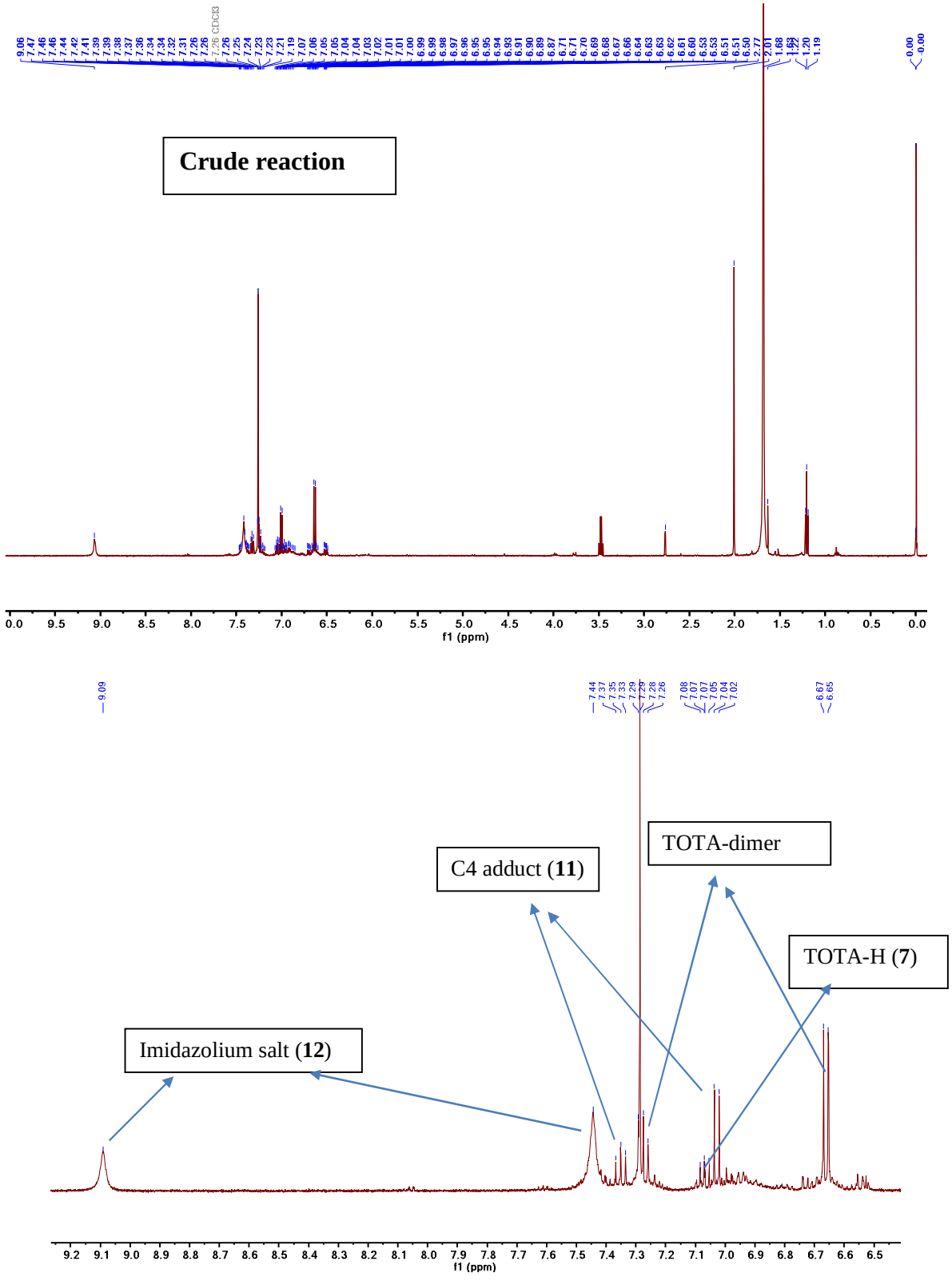

Figure S105: Crude reaction mixture of CH_3CN of analysis

II.9d. Experimental EPR spectrum of TOTA radical:

Procedure: The solid TOTA-dimer isolated from the reaction between I^{t}Bu and **1-BF$_4$** is a light green solid insoluble in the most organic solvent. HRMS analysis shows only the monomeric peak at m/z = 285. A solution of TOTA-dimer in anhydrous m-xylene ($1x10^{-4}$ M) was prepared in glovebox for EPR spectroscopy analysis. The EPR spectrum was measured at 360 K. The TOTA radical formation from its dimer is observed at 340 K and above. At 360 K a well resolved TOTA radicals signal noted. The data matches with previously reported work.[11, 12]

Simulation parameters are Sim 1 (TOTA radical): 6 x 0.91 G + 3 x 3.28 G; Linewidth: 0.42 G; g = 2.005

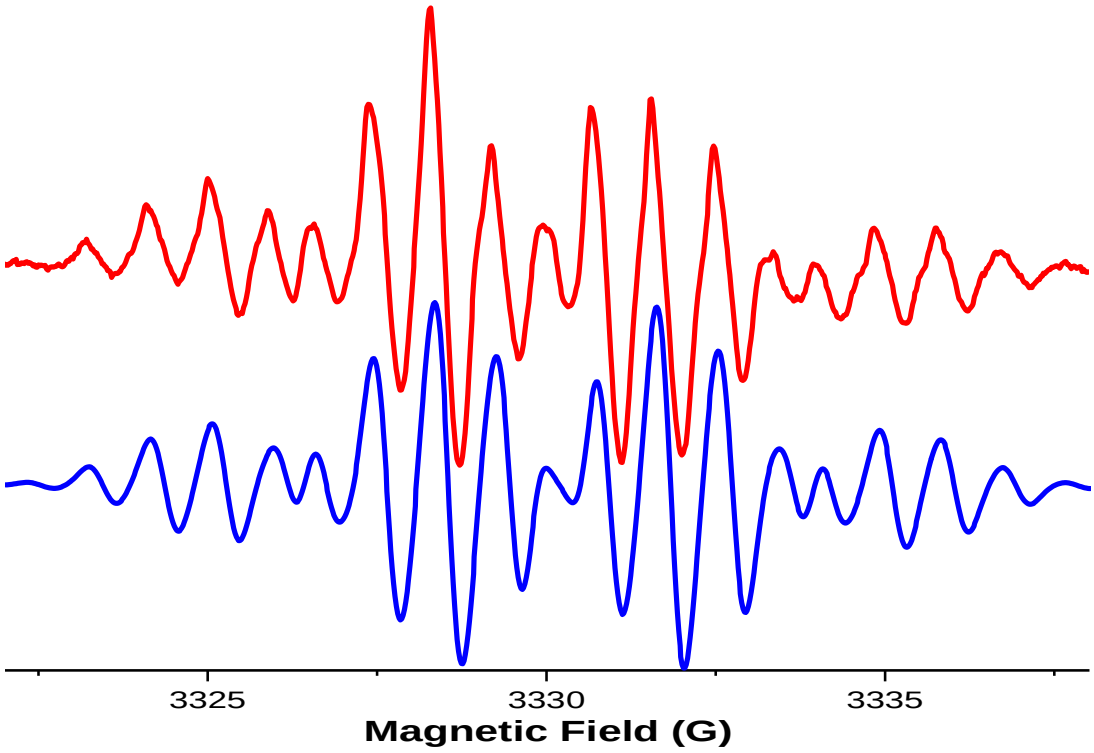

Figure S106: Experimental (red lines) and simulated (blue lines) EPR spectra of the TOTA radical in m-xylene at 360 K (g = 2.0025, 6 x 0.91 G + 3 x 3.28 G; Linewidth: 0.42 G)

II.9e UV-vis spectra analysis:

Absorption spectra were recorded on a ThermoScientific Evolution 220 UV-Visible spectrophotometer at 25 ˚C in analytical-grade solvents (con. 10-4 M). All UV samples for spectroscopy were prepared under an inert atmosphere in a Mbraun Labmaster glovebox maintained at less than 1 ppm O_2. A 3 mL gas-tight cuvette (Quartz Cuvette Self Masking Screw Cap) was used for anaerobic acquisition of spectra.

Significant changes are observed in the UV-vis spectra of the reaction mixture of I^{t}Bu and 1-[BF_4] consistent with the color changed observed.

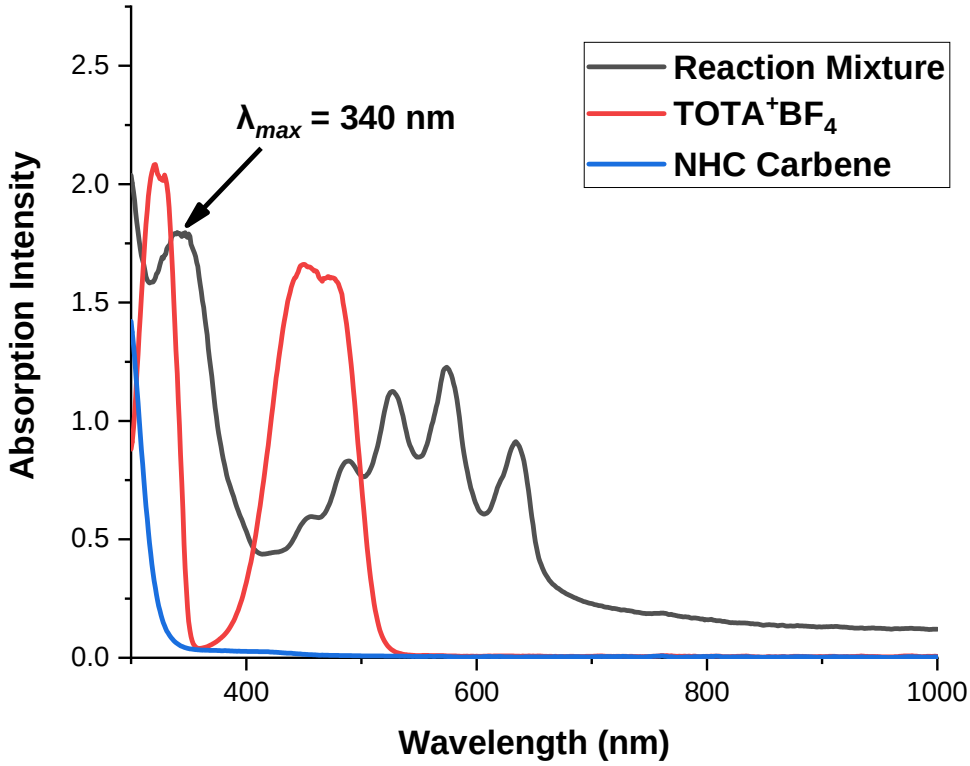

Figure S107: The UV-vis spectra of the reaction mixture of 1-[BF_4] and 10 (NHC) in acetonitrile (1 x 10^{-4} M).

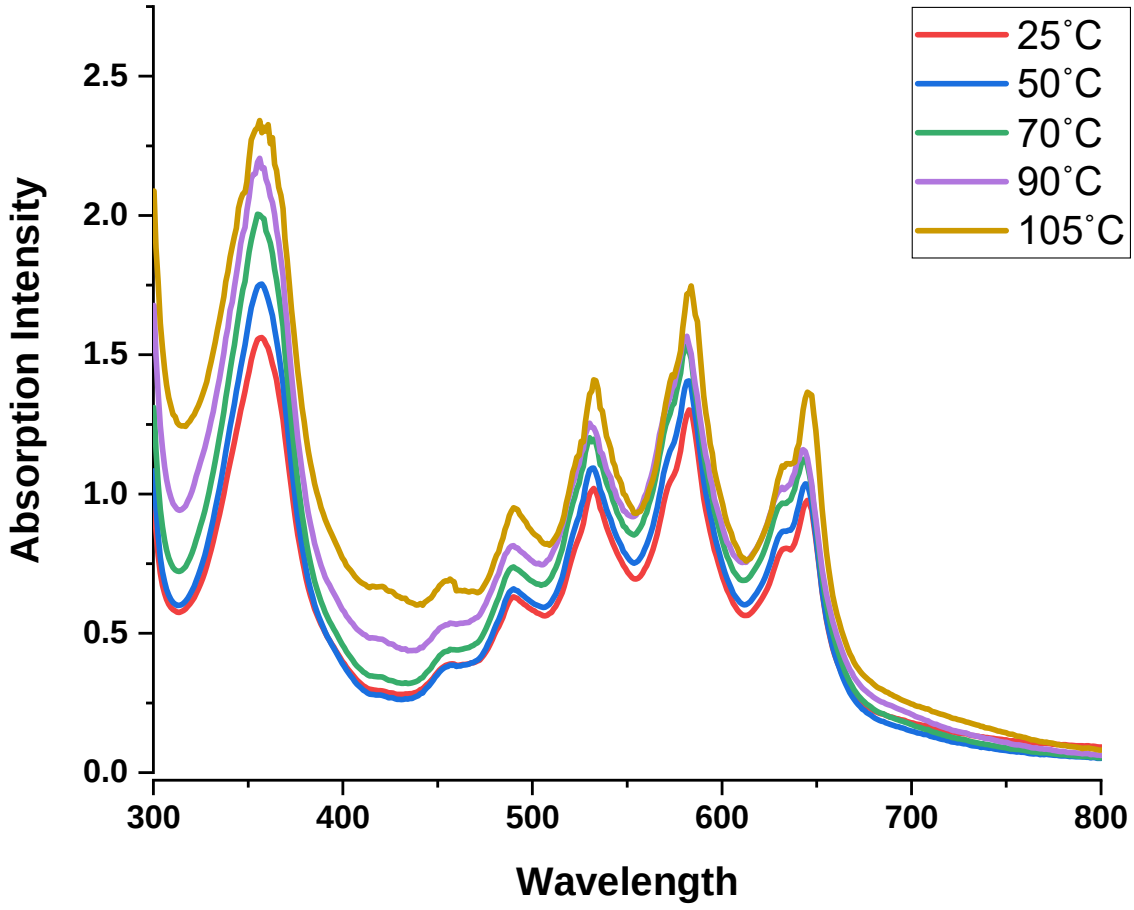

Figure S108: Variable temperature experiment of TOTA-dimer.

III. Single crystal X-ray Diffraction

Single-crystal X-ray diffraction data were collected on either a Bruker Kappa APEX II CCD diffractometer using Mo Kα radiation (λ = 0.71073Å) radiation, or a Bruker AXS single-crystal system equipped with a Excillum METALJET liquid gallium X-ray source, kappa goniometer, Oxford 800 series cryostream set from 273K to 100 K, and Photon III detector. Image collection, data reduction, and scaling were performed with Bruker AXS APEX3 software. The resolution of the solid-state structure was accomplished using the SHELXS-97 and SHELXT program.[13] The refinement was performed with the SHELXL program[14] and the structure solution and the refinement were achieved with the PLATON and Olex2 softwares.[15],[16] All atoms – except hydrogens – were refined anisotropically. The position of the hydrogen atoms was determined using residual electronic densities, which are calculated by a Fourier difference. A final weighting step was performed, followed by multiples loops of refinement.

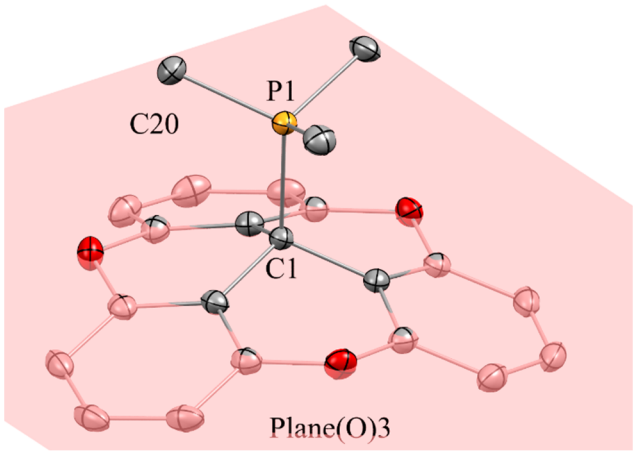

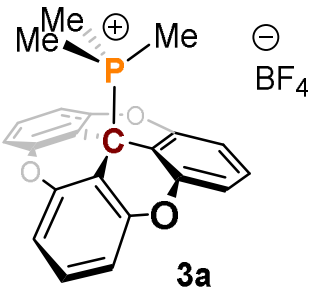

Bond	Lenght (Å)
C1-P1	1.864(1)
C1-Plane(O)$_3$	0.624
Angle	**Degree (°)**
C1P1C20^Plane(O)$_3$	89.99

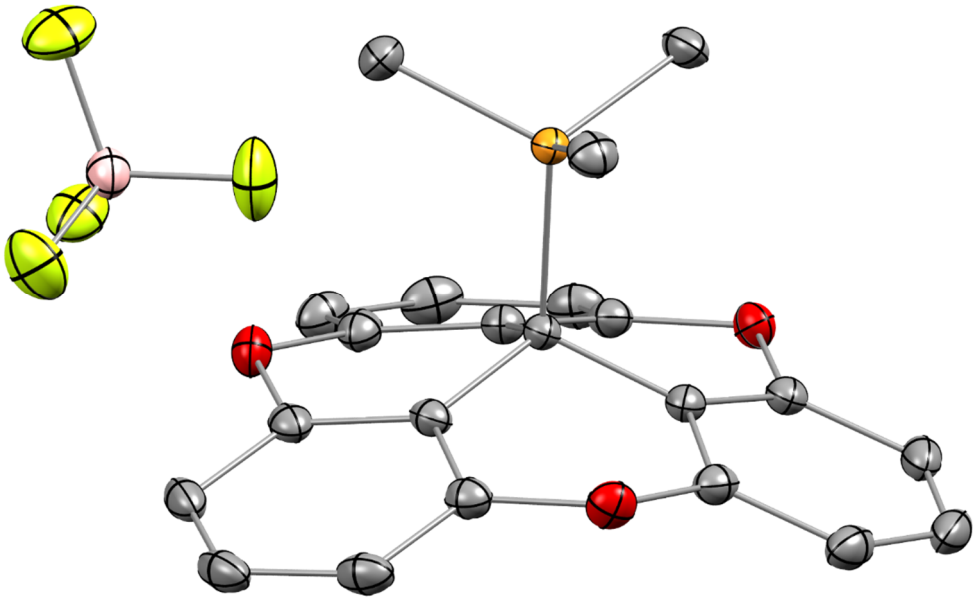

Figure S109: ORTEP and measurement table of **3a** (for clarity hydrogen atoms and solvents molecules have been omitted)

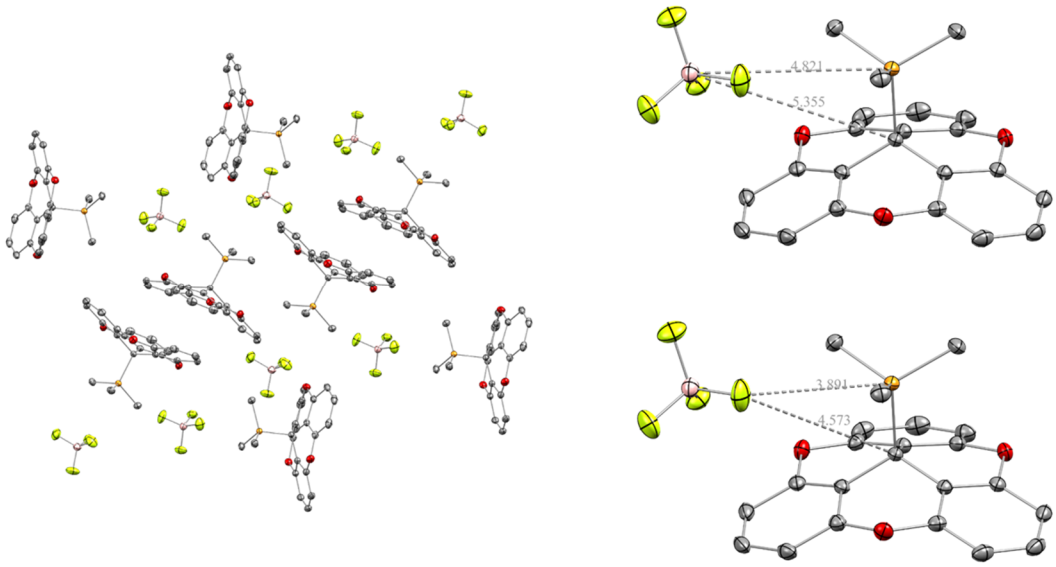

Figure S110: Crystal packing of **3a;** the BF_4^- counterions and its distance measurement from phosphonium center and carbenium center form (for clarity hydrogen atoms and solvents molecules have been omitted)

Table S2 Crystal data and structure refinement for 3a.

Identification code	3a
CCDC	**2035924**
Empirical formula	$C_{23}H_{20}BCl_2F_4O_3P$
Formula weight	533.07
Temperature/K	293(2)
Crystal system	monoclinic
Space group	$P2_1/c$
a/Å	10.0710(3)
b/Å	18.5524(4)
c/Å	13.0354(4)
α/°	90
β/°	111.106(3)
γ/°	90
Volume/Å^3	2272.16(12)
Z	4
ρ_{calc}g/cm^3	1.558
μ/mm^{-1}	0.414
F(000)	1088.0

Crystal size/mm^3	0.36 × 0.3 × 0.18
Radiation	MoKα (λ = 0.71073)
2Θ range for data collection/°	4.004 to 65.472
Index ranges	-15 ≤ h ≤ 15, -26 ≤ k ≤ 27, -19 ≤ l ≤ 18
Reflections collected	72082
Independent reflections	8024 [R_{int} = 0.0535, R_{sigma} = 0.0337]
Data/restraints/parameters	8024/0/338
Goodness-of-fit on F^2	1.023
Final R indexes [I>=2σ (I)]	R_1 = 0.0393, wR_2 = 0.0902
Final R indexes [all data]	R_1 = 0.0580, wR_2 = 0.0987
Largest diff. peak/hole / e Å^{-3}	0.44/-0.27

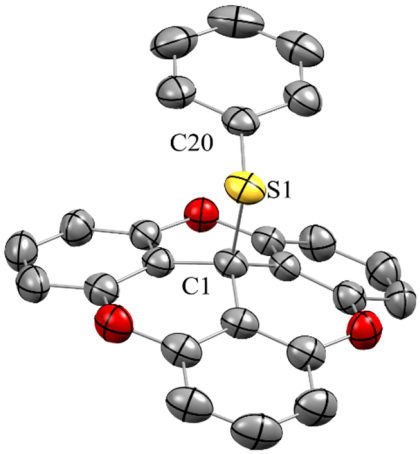

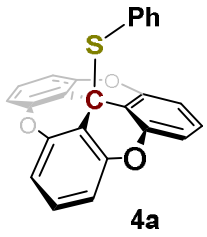

4a

Bond	lenght (Å)
C1-S1	1.902(2)
S1-C20	1.771(2)
C1-Plane(O)$_3$	0.621
Angle	**Degree (°)**
C1P1C20^Plane(O)$_3$	89.64
C1S1C20	100.99(9)

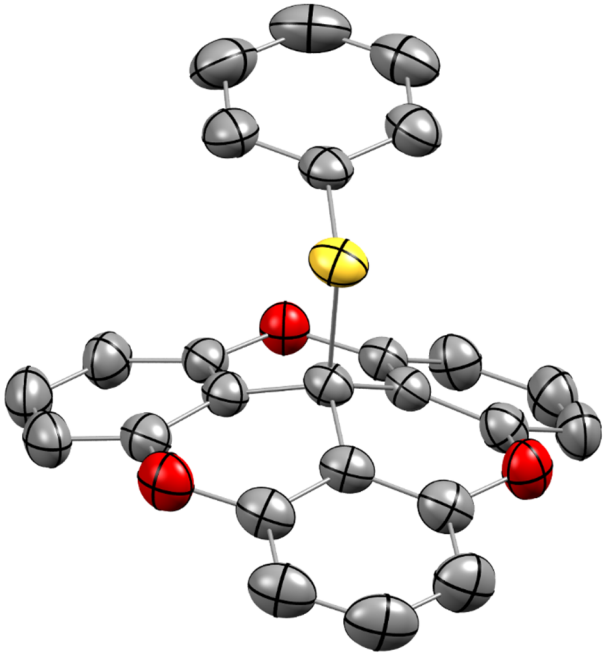

Figure S111: ORTEP and measurement table of **4a** (for clarity hydrogen atoms have been omitted).

Table S3 Crystal data and structure refinement for 4a.

Identification code	**4a**
CCDC	**2035921**
Empirical formula	$C_{25}H_{14}O_3S$
Formula weight	394.42
Temperature/K	273.15
Crystal system	monoclinic
Space group	$P2_1/m$
a/Å	7.5851(7)
b/Å	43.318(3)
c/Å	8.5930(8)
α/°	90
β/°	100.325(2)
γ/°	90
Volume/Å^3	2777.7(4)
Z	6
ρ_{calc}g/cm^3	1.415
μ/mm^{-1}	0.200
F(000)	1224.0

Crystal size/mm^3	1 × 0.58 × 0.08
Radiation	MoKα (λ = 0.71073)
2Θ range for data collection/°	1.88 to 51.504
Index ranges	-9 ≤ h ≤ 9, -41 ≤ k ≤ 52, -10 ≤ l ≤ 10
Reflections collected	19541
Independent reflections	5359 [R_{int} = 0.0322, R_{sigma} = 0.0346]
Data/restraints/parameters	5359/156/523
Goodness-of-fit on F^2	1.041
Final R indexes [I>=2σ (I)]	R_1 = 0.0425, wR_2 = 0.0939
Final R indexes [all data]	R_1 = 0.0652, wR_2 = 0.1028
Largest diff. peak/hole / e Å^{-3}	0.17/-0.15

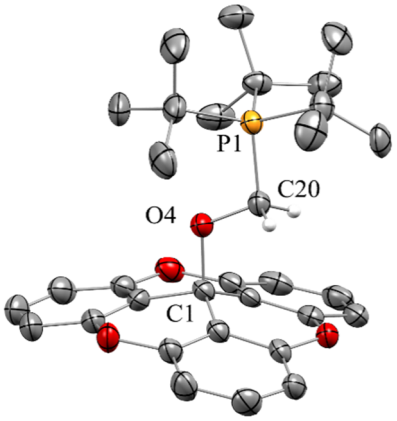

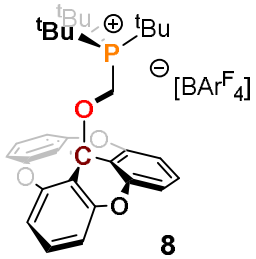

8

Bond	**Lenght (Å)**
C1-O4	1.513(4)
O4-C20	1.410(5)
C20-P1	1.825(4)
C1-Plane(O)$_3$	0.567
Angle	**Degree (°)**
C1O4C20	114.4(3)
O4C20P1	108.8(3)
C1O4C20^Plane(O)$_3$	89.69

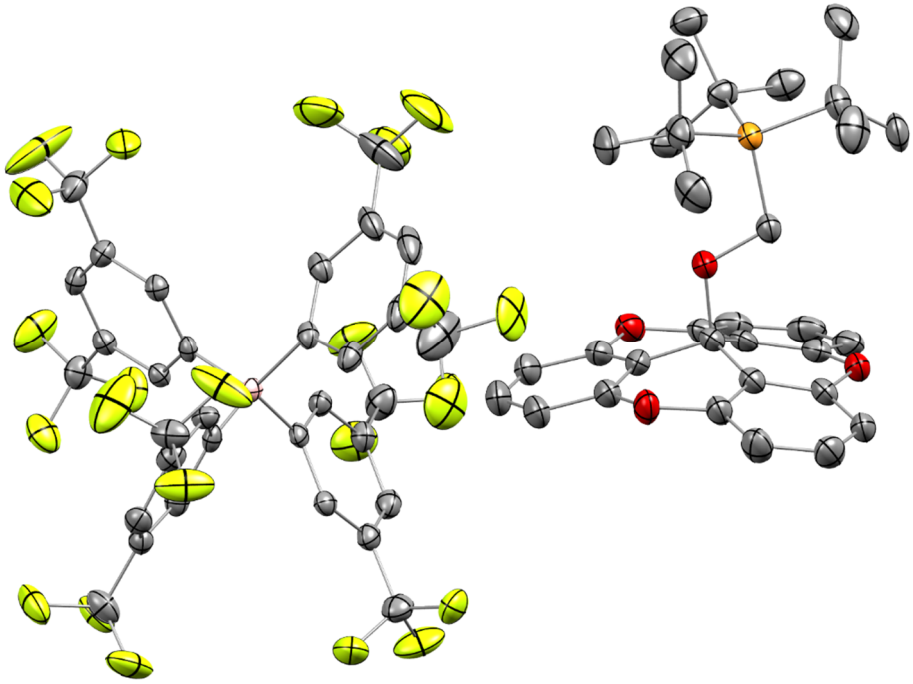

Figure S112: ORTEP and measurement table of **6** (for clarity the hydrogen atoms have been omitted)

Table S4 Crystal data and structure refinement for 8.

Identification code	**8**
CCDC	**2035922**
Empirical formula	$C_{64}H_{50}BF_{24}O_4P$
Formula weight	1380.82
Temperature/K	100.0
Crystal system	monoclinic
Space group	$P2_1/c$
a/Å	19.5960(13)
b/Å	18.3533(13)
c/Å	18.1720(13)
α/°	90
β/°	108.476(4)
γ/°	90
Volume/Å^3	6198.7(8)
Z	4
ρ_{calc}g/cm^3	1.480
μ/mm^{-1}	0.165
F(000)	2808.0
Crystal size/mm^3	0.956 × 0.8 × 0.277

Radiation	MoKα (λ = 0.71073)
2Θ range for data collection/°	2.192 to 51.362
Index ranges	-18 ≤ h ≤ 23, -22 ≤ k ≤ 21, -22 ≤ l ≤ 21
Reflections collected	51790
Independent reflections	11729 [R_{int} = 0.0714, R_{sigma} = 0.0630]
Data/restraints/parameters	11729/1416/996
Goodness-of-fit on F^2	1.070
Final R indexes [I>=2σ (I)]	R_1 = 0.0828, wR_2 = 0.1955
Final R indexes [all data]	R_1 = 0.1158, wR_2 = 0.2159
Largest diff. peak/hole / e Å^{-3}	0.73/-0.48

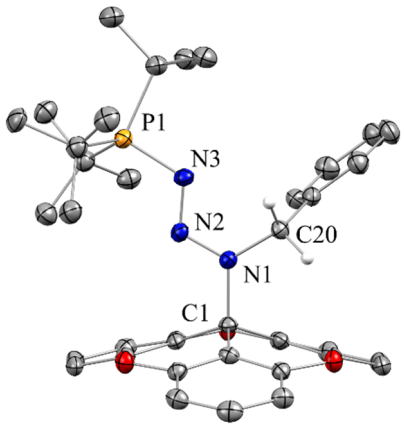

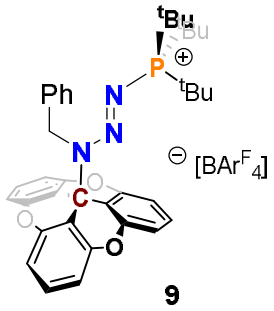

9

Bond	**Lenght (Å)**
C1-N1	1.524(4)
N1-N2	1.310(3)
N2-N3	1.299(3)
N1-C20	1.467(3)
N3-P1	1.680(3)
C1-Plane(O)$_3$	0.609(0)
Angle	**Degree (°)**
C20N1N2	121.5(2)
N1N2N3	112.9(2)
N2N3NP1	116.0(2)
C1N1N2C20^Plane(O)$_3$e	88.17(0)

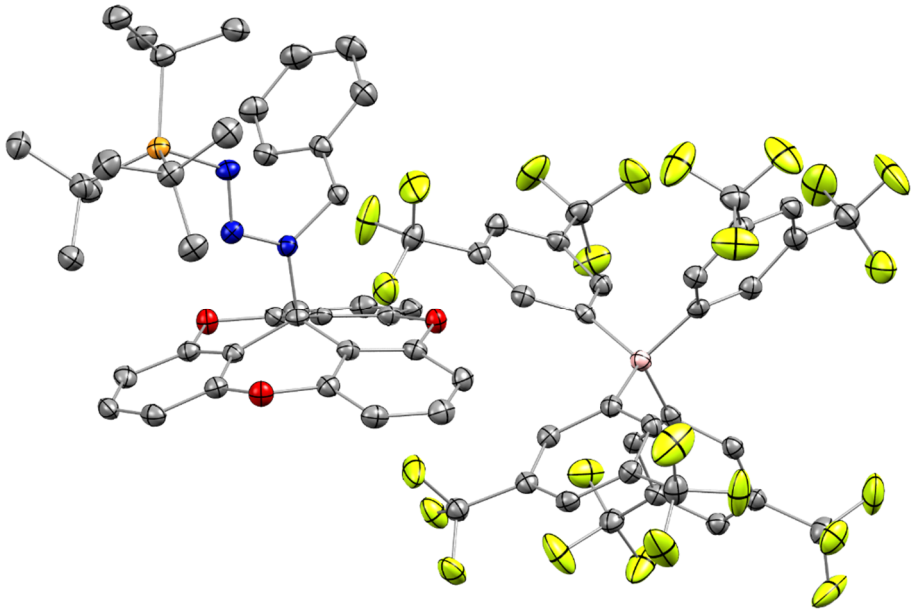

Figure S113: ORTEP and measurement table of **9** (for clarity solvent molecules and hydrogen atoms are omitted).

Table S5 Crystal data and structure refinement for 9.

Identification code	**9**
CCDC	**2035925**
Empirical formula	$C_{70.5}H_{56}BClF_{24}N_3O_3P$
Formula weight	1526.41
Temperature/K	103.85
Crystal system	triclinic
Space group	P-1
a/Å	13.1828(13)
b/Å	17.1020(16)
c/Å	17.4082(17)
α/°	114.902(3)
β/°	105.306(3)
γ/°	96.778(3)
Volume/Å^3	3313.7(6)
Z	2
ρ_{calc}g/cm^3	1.530
μ/mm^{-1}	0.201
F(000)	1554.0
Crystal size/mm^3	0.462 × 0.345 × 0.222
Radiation	MoKα (λ = 0.71073)

2Θ range for data collection/°	2.72 to 52.044
Index ranges	$-16 \leq h \leq 15$, $-21 \leq k \leq 21$, $-21 \leq l \leq 21$
Reflections collected	45023
Independent reflections	12828 [R_{int} = 0.0512, R_{sigma} = 0.0581]
Data/restraints/parameters	12828/0/956
Goodness-of-fit on F^2	1.050
Final R indexes [I>=2σ (I)]	R_1 = 0.0523, wR_2 = 0.1338
Final R indexes [all data]	R_1 = 0.0772, wR_2 = 0.1532
Largest diff. peak/hole / e $Å^{-3}$	0.35/-0.43

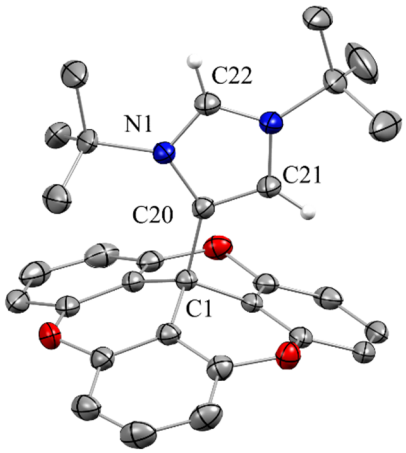

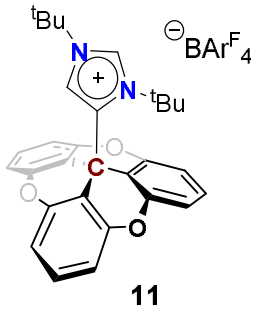

11

Bond	**Lenght (Å)**
C1-C20	1.565(3)
C20-C21	1.361(3)
C20-N1	1.419(2)
C1-Plane$(O)_3$	0.718
Angle	**Degree (°)**
C1C20C21N1^Plane$(O)_3$	85.26

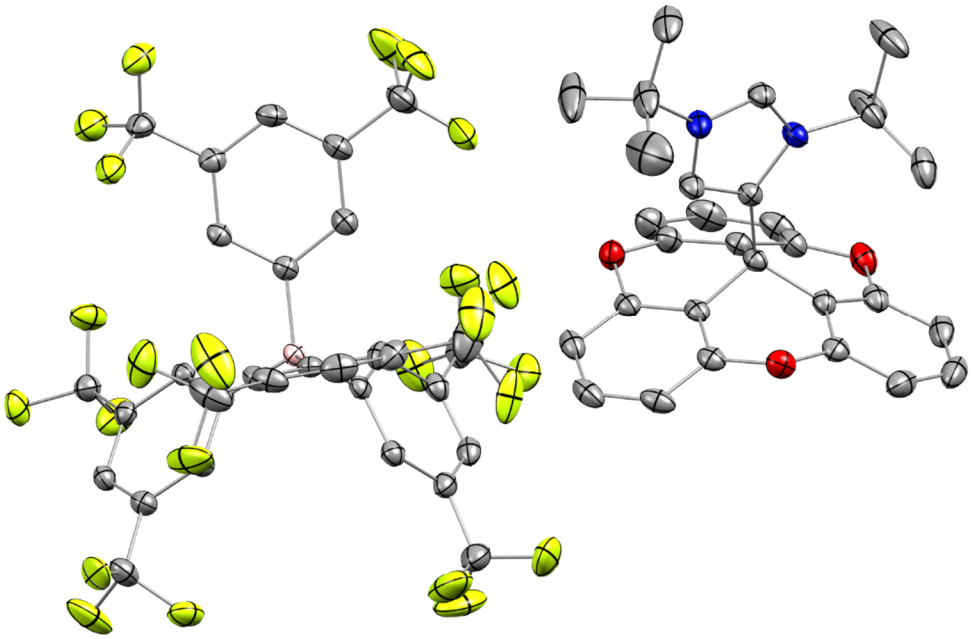

Figure S114: ORTEP and measurement table of **11** (for clarity hydrogen atoms have been omitted).

Table S6 Crystal data and structure refinement for 11.

Identification code	**11**
CCDC	**2035923**
Empirical formula	$C_{62}H_{41}BF_{24}N_2O_3$
Formula weight	1328.78
Temperature/K	100.0
Crystal system	triclinic
Space group	P-1
a/Å	13.4502(6)
b/Å	15.5304(7)
c/Å	16.0826(7)
α/°	106.612(2)
β/°	101.5130(10)
γ/°	105.3750(10)
Volume/Å^3	2962.9(2)
Z	2
ρ_{calc}g/cm^3	1.489
μ/mm^{-1}	0.143

F(000)	1344.0
Crystal size/mm^3	0.437 × 0.42 × 0.319
Radiation	MoKα (λ = 0.71073)
2Θ range for data collection/°	2.768 to 54.946
Index ranges	-16 ≤ h ≤ 16, -19 ≤ k ≤ 19, -20 ≤ l ≤ 20
Reflections collected	65798
Independent reflections	12267 [R_{int} = 0.0324, R_{sigma} = 0.0264]
Data/restraints/parameters	12267/1686/1059
Goodness-of-fit on F^2	1.044
Final R indexes [I>=2σ (I)]	R_1 = 0.0442, wR_2 = 0.1084
Final R indexes [all data]	R_1 = 0.0571, wR_2 = 0.1179
Largest diff. peak/hole / e Å^{-3}	0.61/-0.37

IV. Computational Details

The initial density functional theory (DFT)[17,18] calculations were done on a full-atom scale using a variation of hybrid and pure functionals for comparison (Table S8). Then long-range corrected version[19] of the hybrid 1993 Becke three-parameter exchange functional[20,21,22] and the Lee–Yang–Parr non-local correlation functional[23] (UCAM-B3LYP) was chosen as the functional of choice. The internal triple-ζ quality basis set 6-311G(d,p) was applied on all atoms. The resultant geometry optimized models were found to be minima in the potential energy surface by lack of imaginary vibrations after frequency calculations. Transition state models were obtained by performing optimization calculations (opt=TS) from an initial guess. The resultant models were found to be maxima by performing intrinsic reaction coordinate (IRC) calculations and by the presence of a single imaginary frequency corresponding to the expected bond formation/breaking in the initial guess. Solvated models were calculated with the polarizable continuum model (PCM) using the integral equation formalism variant (IEFPCM) as the SCRF method, using acetonitrile as solvent. All calculations were implemented in the Gaussian 09,[24] revision D.01 software installed in the Ocelote computer cluster allocated at the University of Arizona High Performance Computing (HPC) center. XYZ and output files for the correspondent models can be provided upon request.

The frontier molecular orbitals of $TOTA^+$ were plotted using the cubegen utility in G09. The lowest occupied molecular orbital (LUMO) is shown across the π-system, however a significant contribution by the central carbon could be observed (33%). Thus, it is predicted that in the presence of a Lewis base, $TOTA^+$ will act as a sigma-acceptor, with the central atom being the most electrophilic atom.

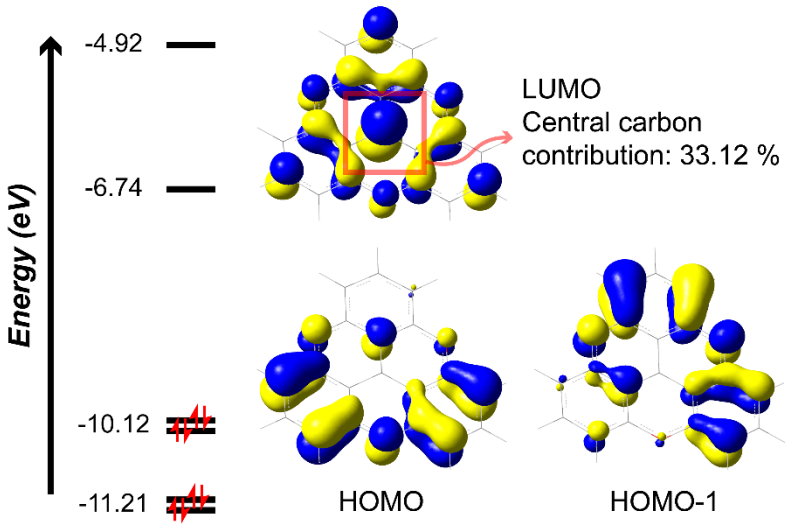

Figure S115. Frontier molecular orbitals for the DFT model of $TOTA^+$. Surfaces were plotted at a 0.04 isovalue. Contribution of the central carbon was extracted from the normalized wavefunction of the LUMO.

The modelled structures were studied using different functionals implemented in Gaussian 09 (**Table S8**). For each functional, the respective model was geometry-optimized, followed by frequency calculations. To better model non-covalent interactions, functionals with defined empirical dispersion functions were selected, requested by the keyword EmpiricalDispersion=GD3 in the Gaussian 09 input file. The resultant energies for each model were averaged and then compared to determine the difference between the mean and a given functional. For individual models of $TOTA^+$ and PR_3 (R = Me, Ph, ^{t}Bu), the functional closer to the calculated mean was found to be CAM-B3LYP (**Table S9**).

Table S8. Resultant energies for the calculated models of $TOTA^+$ and PR_3 (R = Me, Ph, or ^{t}Bu) using different functionals.

		Energy (Hartrees)		
Functional	***TOTA***	***PMe_3***	***PPh_3***	***$P(t\text{-}Bu)_3$***
CAM-B3LYP	-954.6714649	-461.0665345	-1036.088152	-814.7505980
B97D	-954.4371662	-461.0588728	-1035.942000	-814.7034861
PBE0	-954.0632726	-460.8564788	-1035.520631	-814.3149589
M06L	-955.0226191	-461.1126833	-1036.367706	-814.9463145
wB97XD	-954.7946532	-461.0996541	-1036.220825	-814.8869771
B3LYP	-955.1300557	-461.1636813	-1036.522648	-815.0825183

Average	*-954.6865386*	*-461.0596508*	*-1036.110327*	*-814.7808088*

Table S9. Difference in energy between the DFT calculated models and the averaged energy from the functionals used. Functional with the lowest energy value is highlighted in yellow. Energy shown in Hartrees.

	ΔE (Calculated - Average)			
Functional	***TOTA***	***PMe_3***	***PPh_3***	***$P(t\text{-}Bu)_3$***
CAM-B3LYP	**-0.0151**	0.007	**-0.0222**	**-0.0302**
B97D	-0.2494	**-0.001**	-0.1683	-0.0773
PBE0	-0.6233	-0.203	-0.5897	-0.4658
M06L	0.3361	0.053	0.2574	0.1655
wB97XD	0.1081	0.040	0.1105	0.1062
B3LYP	0.4435	0.104	0.4123	0.3017

To further determine the suitability of this functional for further DFT studies, the FLP/Lewis adduct formation reaction was similarly compared. In this chemical reaction, the energy of the reactants was obtained by adding the enthalpy of formation of $TOTA^+$ and the respective phosphines under different functionals (*Net* $E_{(Reactants)}$, **Table S10**). The stabilization energy of the adduct/FLP formation was obtained by subtracting *Net* $E_{(Reactants)}$ and the corresponding energy of $[TOTA\text{-}PR_3]^+$ ($\Delta E_{(Products\ -\ Reactants)}$, **Table S10**), then averaged for descriptive statistical analysis. Then mean was subtracted with the energy of the reaction using different functionals. The values with the lowest energy difference are highlighted below. The hybrid functional PBE0 (also known as PBE1PBE) showed the lowest energy difference in the modelled reaction using PMe_3 and $P(t\text{-}Bu)_3$, followed by CAM-B3LYP. For the reaction using PPh_3, CAM-B3LYP showed the closest value to the calculated mean. The small variation in the calculated energies using CAM-B3LYP and the averaged values of all the functionals used, both in individual models and in a chemical reaction, allowed use to select this functional for further DFT calculations, this, to decrease the expense of computing time.

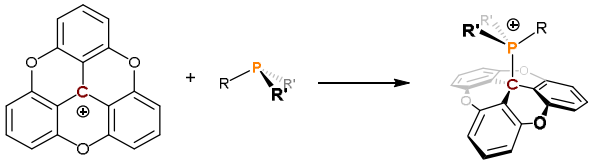

Table S10. Comparison of the calculated energies for the respective models for the stable Lewis addict/FLP chemical reaction.

R	Functional	Reactants		Net $E_{(Reactants)}$	Product $[TOTA–PR_3]^+$	$\Delta E_{(Products - Reactants)}$	Average - ΔE
		$TOTA^+$	PR_3				
Methyl	CAM-B3LYP	-954.6714649	-461.0665345	-1415.7379994	-1415.7751120	-0.0371126	0.006827
	B97D	-954.4371662	-461.0588728	-1415.4960390	-1415.5173945	-0.0213555	-0.008930
	PBE0	-954.0632726	-460.8564788	-1414.9197514	-1414.9565447	-0.0367933	**0.006508**
	M06L	-955.0226191	-461.1126833	-1416.1353024	-1416.1526683	-0.0173659	-0.012920
	wB97XD	-954.7946532	-461.0996541	-1415.8943073	-1415.9331080	-0.0388007	0.008515
					Average	***-0.0302856***	
Tert-Butyl	CAM-B3LYP	-954.6714649	-814.7505980	-1769.4220629	-1769.4502378	-0.0281749	-0.001720
	B97D	-954.4371662	-814.7034861	-1769.1406523	-1769.1688404	-0.0281881	-0.001707
	PBE0	-954.0632726	-814.3149589	-1768.3782315	-1768.4072556	-0.0290241	**-0.000871**
	M06L	-955.0226191	-814.9463145	-1769.9689336	-1770.0007181	-0.0317845	0.001889
	wB97XD	-954.7946532	-814.8869771	-1769.6816303	-1769.7139350	-0.0323047	0.002409
					Average	***-0.0298953***	
Phenyl	CAM-B3LYP	-954.6714649	-1036.0881520	-1990.7596169	-1990.7942185	-0.0346016	**-0.000478**
	B97D	-954.4371662	-1035.9420000	-1990.3791662	-1990.4110494	-0.0318832	-0.003196
	PBE0	-954.0632726	-1035.5206311	-1989.5839037	-1989.6228741	-0.0389704	0.003891
	M06L	-955.0226191	-1036.3677060	-1991.3903251	-1991.4160944	-0.0257693	-0.009310
	wB97XD	-954.7946532	-1036.2208250	-1991.0154782	-1991.0596509	-0.0441727	0.009093
					Average	***-0.0350794***	

A. $[TOTA\text{-}PR_3]^+$ Models

The formation of frustrated Lewis pairs or covalent adducts was studied by comparing the dissociation energy correspondent to the DFT models of the individual reactants, or products. The functional, basis set, solvation models, and type of calculations were set constant, thus only comparing the resultant energy of the models.

Table S11. DFT calculated energies for the models stable Lewis adducts or FLPs. All optimization and frequency calculations were done using the CAM-B3LYP functional, 6-311G(d,p) basis set, using the polarizable continuum model SCRF=(solvent=acetonitrile) and the Grime D3 empirical dispersion damping functions. *Energy corresponds to the optimized structure lower in energy (See Figures **S116** and **S117**).

Model	Energy (Kcal.mol^{-1})

PR_3	Phosphine	Reactants ($TOTA^+ + PR_3$)	Product $[TOTA\text{-}PR_3]^+$	ΔE
PMe_3	-289321.2151	-888414.9270	-888438.3698	-23.4428
$PPhMe_2$	-409592.6898	-1008686.4017	-1008712.6373	-26.2356
$P(^nPr)_3$	-437277.8281	-1036371.5400	-1036404.2814	-32.7414
$P(^nBu)_3$	-511272.1338	-1110365.8457	-1110388.5865	-22.7409
PPh_2Me	-529873.7873	-1128967.4992	-1128983.9945	-16.4953
PPh_3	-650149.5940	-1249243.3059	-1249256.1731*	-12.8672
$P(^tBu)_3$	-511258.0542	-1110351.7662	-1110363.6071*	-11.8409

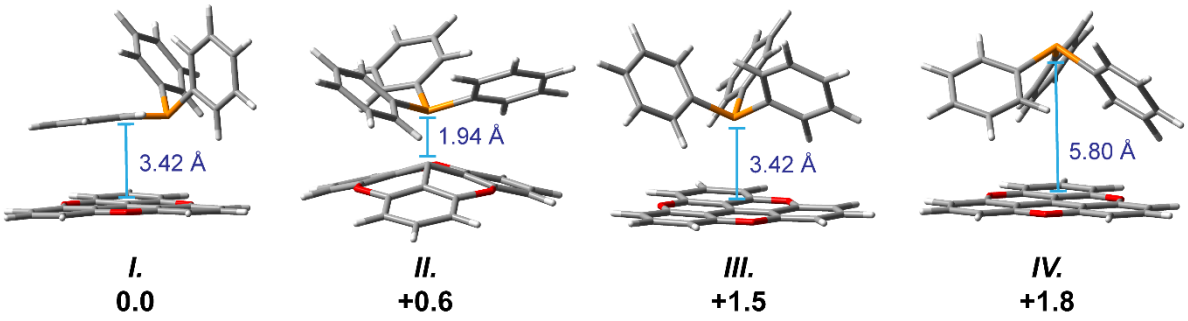

Figure S116. Geometry optimization calculations of different $[TOTA\text{-}PPh_3]^+$ conformers were studied to gain insight on the experimental results found via VT-NMR. For the $[TOTA\text{-}PPh_3]^+$ adduct, the conformations studied consist of (I) π-stacking interaction between $TOTA^+$ and a phenyl group of PPh_3 with no C^+-P interaction, (II) direct C^+-P interaction forming a covalent Lewis adduct, (III) the lone pair of PPh_3 pointing in the direction of the C^+ center in TOTA+, and (IV) the lone pair of PPh_3 pointing in the opposite direction of the C^+ center in TOTA+.

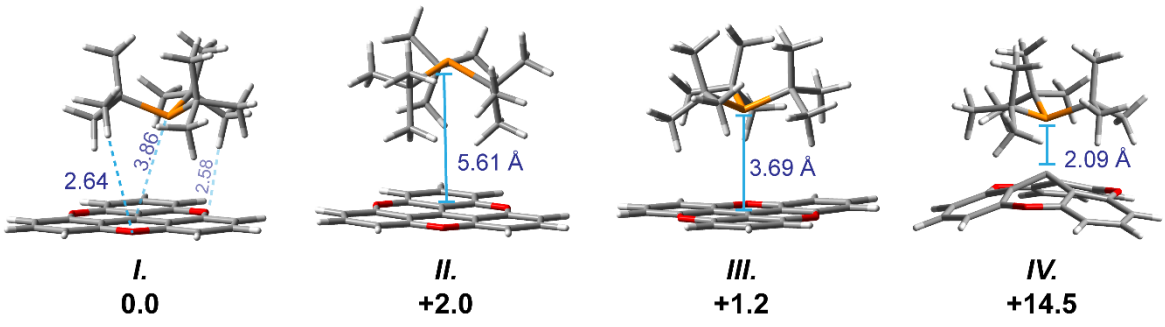

Figure S117. Geometry optimization calculations of different $[TOTA\text{-}P(^tBu)_3]^+$ conformers were studied to gain insight on the experimental results found via VT-NMR. For the $[TOTA\text{-}P(^tBu)_3]^+$ adduct, the conformations studied consist of (I) $P(^tBu)_3$ off-

center, lone pair of phosphine is pointing towards TOTA$^+$ but not to the central C$^+$ atom, (II) the lone pair of P(^{t}Bu)$_3$ pointing in the opposite direction of the C$^+$ center in TOTA$^+$, (III) the lone pair of P(^{t}Bu)$_3$ pointing in the direction of the C$^+$ center in TOTA$^+$, and (IV) direct C$^+$-P interaction forming a covalent Lewis adduct.

Table S12. Selected bond lengths of the DFT calculated Lewis adducts or FLPs models. *Bond lengths correspond to the optimized structure lower in energy (See Figures **S114** and **S115**).

	Distances (Å)			
Model	**P-R (Reactants)**	**P-R (Products)***	**P-C$_{TOTA}$ (DFT)**	**P-C$_{TOTA}$ (Experimental)**
PMe_3	1.863, 1.863, 1.863	1.800, 1.800, 1.800	1.870	1.864(1)
$PPhMe_2$	1.847, 1.847, 1.847	1.797, 1.797, 1.791	1.887	-
$P(nPr)_3$	1.862, 1.857, 1.857	1.815, 1.815, 1.815	1.891	-
$P(^nBu)_3$	1.857, 1.857, 1.861	1.819, 1.820, 1.821	1.891	-
PPh_2Me	1.844, 1.842, 1.846	1.801, 1.802, 1.797	1.910	-
PPh_3	1.843, 1.843, 1.843	1.841, 1.837, 1.842	3.804	-
$P(^tBu)_3$	1.923, 1.923, 1.923	1.923, 1.920, 1.921	3.860	-

B. Activation of (SPh)$_2$

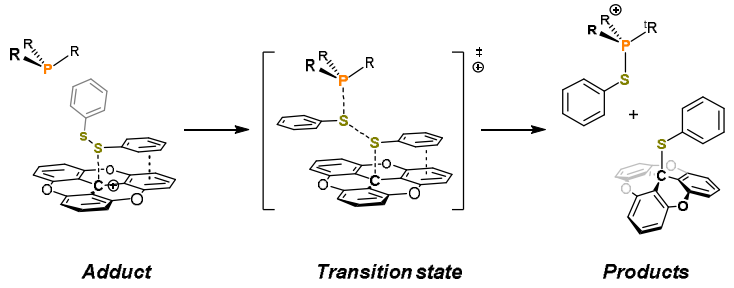

Table S13. Selected bond lengths of the DFT calculated models. *Experimental S-C$_{TOTA}$ bond distance obtained from the single crystal X-ray diffraction data.

Model	**P-R Distances (Å)**	**S-C$_{TOTA}$ Distance (Å)**	**S-S Distance (Å)**	**P-S Distance (Å)**
$(SPh)_2$	-	-	2.057	-
Adduct TOTA$^+$ + $(SPh)_2$ + PMe_3	1.846, 1.846, 1.845	3.568	2.058	3.859
Adduct TOTA$^+$ + $(SPh)_2$ + $P(^tBu)_3$	1.819, 1.921, 1.920	3.430	2.064	3.970
Adduct TOTA$^+$ + $(SPh)_2$ + PPh_3	1.859, 1.839, 1.836	3.185	2.076	3.627
Transition State [TOTA-$(SPh)_2$-PMe_3]$^+$	1.835, 1.835, 1.836	3.135	2.294	2.631
Transition State [TOTA-$(SPh)_2$-$P(^tBu)_3$]$^+$	1.946, 1.942, 1.942	3.159	2.712	2.405
Transition State [TOTA-$(SPh)_2$-PPh_3]$^+$	1.82, 1.82, 1.82	2.80	2.50	2.50
Products TOTA-SPh + [PhS-PMe3]$^+$	1.795, 1.796, 1.795	1.904 (*vs.* 1.902(2))*	3.62	2.090

Products TOTA-SPh + $[PhS\text{-}P(^tBu)_3]^+$	1.907, 1.896, 1.903	1.90	3.63	2.118
Products TOTA-SPh + $[PhS\text{-}PPh_3]^+$	1.80, 1.80, 1.180	1.905	3.581	2.099

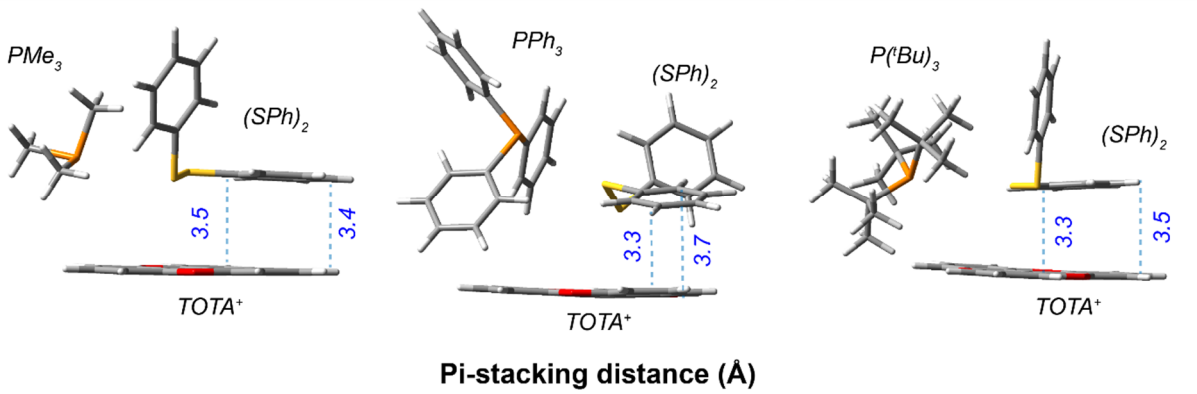

Figure S118. DFT calculated models for the TOTA + $(SPh)_2$ + PR_3 (R = Me, Ph, or ^{t}Bu) adducts. Pi-stacking is depicted in these models correspondant to the TOTA-$(SPh)_2$ adduct formation prior to cleavage of the disulfide bond in $(SPh)_2$.

C. NHC Adducts

Table S14. Selected bond lengths of the calculated DFT $[NHC\text{-}TOTA]^+$ adducts.

Model	C_{NHC}-C_{TOTA} Distance (Å)	
	DFT	Experimental
C2 Adduct	1.63	-
C4 Adduct	1.57	1.565(3)

Table S15. Calculated electron affinity energy for $TOTA^+$ and Ionization potential for I^{t}Bu using CAM-B3LYP functional and 6-311G(d,p) basis set with acetonitrile as PCM.

Compound	Energy (Hartrees)	Ionization Potential (eV)	Electron Affinity (eV)
$TOTA^+$	-955.1300557		-7.41
$TOTA^\bullet$	-954.8576357		
I^{t}Bu	-540.5241418	5.59	
$[I^tBu]^+$	-540.3185576		
Ph_3C^+	-732.6052956		-4.65[a]
$Ph_3C^\bullet$	-732.7760166		

[a] The reported value for this compound is -4.93 eV, in chlorobenzene at the SCRF/M06-2X/6-311+G(d,p) level of theory.[25]

V. References

1 B. W. Laursen, F. C. Krebs, M. F. Nielsen, K. Bechgaard, and J. B. Christensen, N. Harrit, *J. Am. Chem. Soc.* 1998, **120**, 12255-12263.

2 J. C. Martin, and R. G. Smith, *J. Am. Chem. Soc*. 1964, **86**, 2252–2256.0

3 R. Löw, T. Rusch, T. Moje, F. Röhricht, O. M. Magnussen, and R. Herges, *Beilstein J. Org. Chem.* 2019, **15**, 1815–1821.

4 a) T.J. Herrington, A. J. W. Thom, A. J. P. White, and A. E. Ashley, *Dalton Trans.*, 2012, **41**, 9019-9022; b) M. A.Beckett, G. C.Strickland, J. R.Holland, and K. S. Varma, *Polymer*, 1996, **37**, 4629-4631.

5 L. Rocchigiani, G. Ciancaleoni, C. Zuccaccia, and A. Macchioni, *J. Am. Chem. Soc*. 2014, **136**, 112 – 115.

6 M. A. Dureen, G. C. Welche, T. M. Gilbert, and D. W. Stephan, *Inorg. Chem.* 2009, **48**, 9910–9917.

7 L. C. Forfar, M. Green, M. F. Haddow, S. Hussein, J. M. Lynam, J. M. Slattery, and C. A. Russell, *Dalton Trans*., 2015, **44**, 110–118.

8 H. Ohmori, H. Maeda, K. Konomoto, K. Sakai, and M. Masui, *Chem . Pharm . Bull* . 1987, **35**, 4473 -4481.

9 P. Huszthy, K. Lempert, and G. Simig *J. Chem. Soc., Perkin Trans. 2*, 1985, 1351-1354.

10 Z. Dong, C. Pezzato, A. Sienkiewicz, R. Scopelliti, F. Fadaei-Tirani, and K. Severin, *Chem. Sci*., 2020,**11**, 7615-7618.

11 M. J. Sabacky, C. S. Johnson, R. G. Smith, H. S. Gutowsky, and J. C. Martin, *J. Am. Chem. Soc*. 1967, **89**, 2054–2058

12 E. Müller, A. Moosmayer, A. Rieker, and K. Scheffler, *Tetrahedron Lett*., 1967, **39**, 3877-3880.

13 G. M. Sheldrick *Acta Cryst.* 2008, **A64**, 112-122.

14 G. M. Sheldrick, *Acta Cryst.* 2015, **C71**, 3-8.

15 A. L. Spek, *J. Appl. Cryst.* 2003, **36**, 7-13.

16 O. V. Dolomanov, L. J. Bourhis, R. J. Gildea, J. A. K. Howard and H. Puschmann *J. Appl. Cryst.* 2009, **42**, 339-341.

17 J. D. Patterson, Density-Functional Theory of Atoms and Molecules, Oxford University Press, Oxford, 1989.

18 P. Hohenberg, and W. Kohn, *Phys. Rev.*, 1964, **136**, B864–B871

19 T. Yanai, D. P. Tew, and N. C. Handy, *Chem. Phys. Lett.*, 2004, **393**, 51–57

20 A. D. Becke, *J. Chem. Phys.*, 1993, **98**, 1372–1377.

21 A. D. Becke, *J. Chem. Phys.*, 1993, **98**, 5648–5652.

22 A. D. Becke, *Phys. Rev. A*, 1988, **38**, 3098–3100

23 C. Lee, W. Yang, and R. G. Parr, *Phys. Rev. B*, 1988, **37**, 785–789.

24 M. J. Frisch, G. W. Trucks, H. B. Schlegel, G. E. Scuseria, M. A. Robb, J. R. Cheeseman, G. Scalmani, V. Barone, B. Mennucci, G. A. Petersson, H. Nakatsuji, M. Caricato, X. Li, H. P. Hratchian, A. F. Izmaylov, J. Bloino, G. Zheng, J. L. Sonnenberg, M. Hada, M. Ehara, K. Toyota, R. Fukuda, J. Hasegawa, M. Ishida, T.

Nakajima, Y. Honda, O. Kitao, H. Nakai, T. Vreven, J. A. Montgomery, Jr., J. E. Peralta, F. Ogliaro, M. Bearpark, J. J. Heyd, E. Brothers, K. N. Kudin, V. N. Staroverov, R. Kobayashi, J. Normand, K. Raghavachari, A. Rendell, J. C. Burant, S. S. Iyengar, J. Tomasi, M. Cossi, N. Rega, J. M. Millam, M. Klene, J. E. Knox, J. B. Cross, V. Bakken, C. Adamo, J. Jaramillo, R. Gomperts, R. E. Stratmann, O. Yazyev, A. J. Austin, R. Cammi, C. Pomelli, J. W. Ochterski, R. L. Martin, K. Morokuma, V. G. Zakrzewski, G. A. Voth, P. Salvador, J. J. Dannenberg, S. Dapprich, A. D. Daniels, Ö. Farkas, J. B. Foresman, J. V. Ortiz, J. Cioslowski, and D. J. Fox, *Gaussian 09* (Gaussian, Inc., Wallingford CT, 2009).

25 A. Merk, H. Großekappenberg, M. Schmidtmann, M.-P. Luecke, C. Lorent, M. Driess, M. Oestreich, H. F. T. Klare, T. Müller *Angew. Chem. Int. Ed*. 2018, **57**, 15267 –15271.